

Universität Stuttgart

**Auslandsorientierter Studiengang
Wasserwirtschaft
Master of Science Program
Water Resources Engineering and
Management - WAREM**

Independent Study:

Saturation Determination for Multiphase Systems in Porous Medium Using Light Transmission Method

submitted by :

Alexandru-Bogdan Tatomir

Date : **December 05, 2007**

Supervisor : **Dr. rer.nat. Insa Neuweiler
Dr.-Ing. Arne Färber**

Institut für Wasserbau
Lehrstuhl für Hydromechanik und Hydrosystemmodellierung
Prof. Dr.-Ing. Rainer Helmig
Pfaffenwaldring 61
70569 Stuttgart

ACKNOWLEDGEMENTS

After bringing to an end this independent study which necessitated a considerable amount of work, I would like to thank the German Federal Ministry of Education and Research which awarded me the IPSWaT scholarship and implicitly gave me the opportunity to perform and complete this work.

I express my sincere gratitude to my supervisor, Dr.ret.nat Insa Neuweiler, for her unflinching support and fruitful discussions.

In the same time I am thankful to Dr. Arne Färber who came with very innovative ideas especially regarding the laboratory part. I wish him all the best in his new career.

I have furthermore to express my gratitude to Veronica Heiss for her comments, suggestions and help both with the numerical and laboratory part. I had the great opportunity to learn a lot while working with her and her experience was of capital importance for bringing this study to the end.

Last but not least, I want to thank my family and my friends (Cezar, Beatrice, Mirel, Dagmar) for their moral support during all this time.

“Gratitude is not only the greatest of virtues, but the parent of all the others” (Cicero)

Author's Statement

I hereby certify that I have prepared this master's thesis independently, and that only those sources, aids and advisors that are duly noted herein have been used and / or consulted.

Signature _____ Date _____

Table of Contents

1.	Introduction	3
2.	Theoretical Concepts	5
2.1.	Non-intrusive methods for saturation determination	5
2.2.	Light Transmission Method	6
2.3.	Physical considerations	7
2.3.1.	Beer Lambert Law	7
2.3.2.	Fresnel's Law	8
2.4.	Technique Limitations	9
2.5.	Color Theory Considerations	10
2.5.1.	RGB Color Model	10
2.5.2.	Numerical Representations of RGB Color Model	11
2.5.3.	HSV Color Space	11
2.5.4.	HSL Color Space	12
2.6.	Color Conversions	14
2.6.1.	Converting from RGB to HSL	14
2.6.2.	Expressing HUE in the range [0,1]	15
2.6.3.	Gray	16
2.6.4.	Intensity	16
2.6.5.	Hue	16
2.7.	Camera Parameters	17
2.7.1.	WB Mode	17
2.7.2.	Shutter	17
2.7.3.	F-No	17
2.7.4.	Shutter Speed / Exposure Time	18
3.	Experimental Methodology	19
3.1.	The Setup	19
3.2.	Photo Camera	19
3.3.	Chamber Construction	21
3.4.	DNAPL (Dense Non-Aqueous Phase Liquid)	21
3.5.	Glass Beads Characteristics	22
4.	The Experiments	23
4.1.	Filling procedures	24
4.2.	Porosity determination	24
4.3.	Bulk density determination	25
4.4.	Volumetric fluid content of the experiments	25
5.	Results and Discussion	26
5.1.	Picture interpretation	26
5.2.	Variation of the Color attribute with the F-number	29
5.3.	100 Percent DNAPL Saturation	31
5.3.1.	Variation of Color attribute with F-Number for 100% DNAPL saturation	31
5.3.2.	Variation of Color Attribute with DNAPL Saturation	32
5.4.	HUE	34
5.4.1.	Variation of Hue color attribute as a function of F-number for a given DNAPL saturation and different exposure times	35
5.4.2.	Variation of Hue color attribute with DNAPL saturation	38
5.5.	Saturation Color Attribute	40
5.5.1.	Variation of Saturation color attribute as a function of F-number for a given DNAPL saturation and different exposure times	40
5.5.2.	Variation of Saturation color attribute with DNAPL saturation	43
5.6.	RED Color Attribute	45

5.6.1.	Variation of RED color attribute as a function of F-number for different DNAPL saturations.....	45
5.6.2.	Comparison between RED color attribute as a function of F-number and the other color attributes.....	46
5.7.	Comparison of the different color attributes as function of F-number and white balance mode	48
5.8.	Variation of the color attributes (Green, Blue, Gray, Luminance, Intensity) averaged for all DNAPL saturations with the F-number and exposure time	51
5.9.	Image contrast distribution for different color attributes	54
5.10.	Green Color Attribute.....	56
5.10.1.	Variation Green color attribute - DNAPL saturation curves with F-numbers and exposure times.....	56
5.10.2.	Variation of Green color attribute with F-number plotted for different DNAPL saturations.....	59
5.11.	Blue Color Attribute.....	61
5.11.1.	Variation of BLUE color attribute with F-number plotted for different DNAPL saturation.....	61
5.11.2.	Variation of “Blue color attribute - DNAPL saturation” curves with F-numbers and exposure times.....	62
5.12.	Best Ranges for F-number and Exposure times	64
5.13.	Example of Calibration Curves	64
6.	Discussion of Error.....	66
6.1.	Experimental error.....	66
6.2.	Errors Related to Assumptions in the Conceptual Model	67
6.3.	Standard deviation.....	67
7.	Summary of Conclusions	70
8.	REFERENCES.....	71

1. Introduction

Groundwater pollution involving non-aqueous phase liquids (NAPLs) is threatening the environment and human health.

The presence of spilled DNAPLs (dense non-aqueous phase liquids), e.g. chlorinated solvents, in the subsurface causes pervasive groundwater contamination problems due to their toxicity, common use and long term persistence within the environment. In order to effectively remove DNAPL and remediate contaminated aquifer, the study of DNAPL transport in groundwater requires a good knowledge of multiphase flow in porous media.

In the multiphase flow and transport through porous systems measuring the contaminant concentrations or the saturations is one of the most important factors.

The flow processes of DNAPL infiltration into saturated soil is a highly nonlinear problem including relationships between capillary pressure, saturation and relative permeability (P_c - S - k_r relationship). The determination of this relationship is often difficult and costly.

One of the laboratory methods to quantify the liquid saturation which is analyzed and developed in this study is called light transmission method (described in subchapter 2.2).

The primary objective of this work was to develop a calibration curve for the results given by the light transmission method when quantifying the liquid saturation in 2D laboratory system containing translucent porous media (see subchapter 5.13)

Another objective was to determine which is the sensitivity of the measurements with regard to the camera parameters: shutter, exposure time and white balance; and which is the best color space to evaluate the pictures (see subchapter 5.13). The theoretical background for the color theory is given subchapter 2.5 , 2.6 and for the camera parameters in 2.7.

Additionally, as we are interested in knowing the influence of the measurement error on the interpretation, we performed in the last chapter (6) an error evaluation for the light transmission method.

Briefly, the work presented here implied several steps:

- designing the experimental part (see chapter 3)
- running the experiments (see chapter 4)
- arranging, managing the raw data (1190 elements, camera settings, physical variables) (see chapter 5)
- computing the color attributes (see chapter 5)
 - writing the computer code
 - running the programs
- arranging, managing the data for interpretation

- interpreting the data (see chapter 5)
 - building curves and tables
 - finding the pattern
 - deriving the equations
- error evaluation (see chapter 6)
- conclusions
- the writing

The present study includes some innovative elements.

2. Theoretical Concepts

In this chapter will be given all the theoretical notions one might need for understanding the light transmission method as this study implies knowledge from various disciplines: multiphase-flow hydraulics, optics, color theory, photography and programming.

The first subchapter presents the motivation for using the non-intrusive methods for liquid saturation determination in the porous media and explains the necessity to determine the saturation as one of the key unknowns for modeling multiphase-flow systems and for the validating tools of these models. Subchapter 2.2 describes the light transmission method as it is one of the best methods for saturation determination. Subchapters 2.5 and 2.6 introduce the basic concepts of color theory and subchapter 2.7 explains what the studied camera parameters are.

2.1. Non-intrusive methods for saturation determination

The testing of the flow in saturated and unsaturated porous media is narrowed by the capability to measure dependent variables in heterogeneous and/ or transient systems.

Models for multiphase flow and transport in the unsaturated and saturated zones of the subsurface environment are most often not rigorously validated both in steady state and transient flow. For instance, in transient flow, one of the less well understood and extensively studied phenomena in the porous systems is the unstable fingering of infiltration which decreases the fluid retention time in the vadose zone and leads to early arrival times of contaminants in underlying aquifers.

As it has been already mentioned in the Introduction the flow processes in multiphase porous systems constitute a highly nonlinear problem and the key variable is the saturation. Therefore, finding saturation is the major objective and especially without disturbing the porous media. For this we should concentrate especially on the non-intrusive measurement techniques.

The list of tools for non intrusive measurement of water saturation in the laboratory include: *computed tomography (CT)*, *nuclear magnetic resonance (NMR)*, *electromagnetic tomography* and *microwave attenuation*, *X Ray absorption*, *light transmission technique (LTT)*, .

Usually these methods require very specialized and very expensive equipment and have a limited spatial or temporal resolution, or are limited in size of the analyzed sample.

Most of the available non-intrusive methods involve some form of radiation: *dual-energy gamma radiation* which measures multiphase fluid contents at a point; *X-ray absorption*, *X-ray attenuation*, and *computerized tomography*.

Generally these methods exploit differences in the absorbance of electromagnetic energy between, depending on the case, liquid, gas and solid phase.

One method that does not use X rays which are ionizing radiation, but non-ionizing radio frequency signals, is *magnetic resonance imaging* (MRI). The disadvantage of the fore mentioned methods is that they cannot measure transient flow phenomena, or the time resolution is too poor. *Synchrotron X rays* allow for accurate and fast measurements of fluid contents in transient flow fields, in any soil type, but can measure only a small section of the flow field at one time because of the small beam size of 1 mm by 8 mm as described in [Darnault, 2001].

X ray absorption and *light transmission techniques* rely on the transmission of either X rays or visible light through the test system incident rays oriented normal to the slab plane.

2.2. Light Transmission Method

One of the non-destructive, non-invasive laboratory techniques currently utilized for the determination of the liquid saturation in porous media is the ***light transmission method (LTM)***. This method requires the least amount of specialized equipment and is by far the lowest cost alternative. Utilization of CCD (charged couple device) cameras in light transmission systems provides a nearly instantaneous high-density array of spatial measurements over a very large dynamic range and/or small pointwise measurements (less than 1 cm²) are typical for the other methods.

Light transmission techniques have been used in multiphase systems containing water and non-aqueous phase liquid (NAPL), in the study of fracture flow and in experiments regarding preferential flow of water.

Tidwell and Glass [1994] presented a physical model for determination of liquid saturation from light transmission containing a single empirically determined parameter. This model was based on the earlier work of Hoa [1981]. The calibration was done by mass balance to the total mass of liquid removed. The resulting water saturation profiles (saturation vs. height) compared favorably to those obtained using X-ray and gamma-ray attenuation for three sands of different textures.

As porous media must be sufficiently translucent in order to conduct a quantifiable level of light through a significant thickness of media, this essential condition rules out its use with most natural sediments in light transmission systems.

Yet, a significant number of silica sands that occur in nature and are sufficiently translucent can be purchased. Some of them have recently been defined for use in the laboratory hydrologic studies by Schroth et al. [1996].

Direct gravimetric calibration in these systems is problematic due to the different measurement scales, this representing an impeding element with regard to the use of light transmission for determination of liquid saturation

Most favorably, each gravimetric sample necessitates a sample area of few square centimeters, where each pixel of a CCD image represents a measured area of about 1 mm². With the degree of saturation dropping rapidly above the capillary fringe, the apparent change differs considerably between measurement scales. Moreover, the hydrostatic distribution of liquid is easily disturbed when cutting or coring samples from the system which increases the error associated with the gravimetric measurements.

With both the X ray and light techniques, electromagnetic energy is passed through the test media and the liquid saturation distribution integrated over the media's thickness is measured as variations in the transmitted X ray or light intensity field. The difference between the techniques lies in the frequency of the radiation used and in the physics governing the interaction that gives rise to variations in the transmitted intensity field. When using low energy X rays (below 75keV) variations in the transmitted intensity field arise from the sensitivity of X ray absorption (photoelectric absorption) to the density of the media, which is directly related to liquid saturation (i.e., increase in saturation yields a decrease in X ray transmission).

2.3. Physical considerations

There are two fundamental physical principles that describe the light absorption when passing through the porous media and the interfaces. First is Beer Lambert's law or simply Beer's law and the second is Fresnel's law. These two physical laws will be presented in the following.

2.3.1. Beer Lambert Law

As light propagates through a homogeneous medium, it is absorbed exponentially in accordance with Beer's law. For a specific wavelength of light, the measured radiant flux (herein referred to as intensity), I , transmitted through a medium of thickness l , is given by

$$I = CI_0e^{-\alpha_i l} \quad (2.1)$$

where I_0 is the measured intensity of the light source and α_i is the adsorption coefficient of the medium i . Since the intensity of diffuse light drops approximately with the square of distance and the distances from the detector to the media and the source are not necessarily the same, C is an optical geometric term that corrects for differences between points of emission and observation. For collimated light, or if the source and media are approximately the same distance from the detector, C can be omitted.

The Beer-Lambert's law can be also expressed as a function of the solute's concentration C_i :

$$I = I_0 \exp \left[\sum_i (-\alpha_i C_i l + \xi) \right] \quad (2.2)$$

In this equation ξ is a constant that accounts for absorbance by the solvent and the apparatus containing the solute

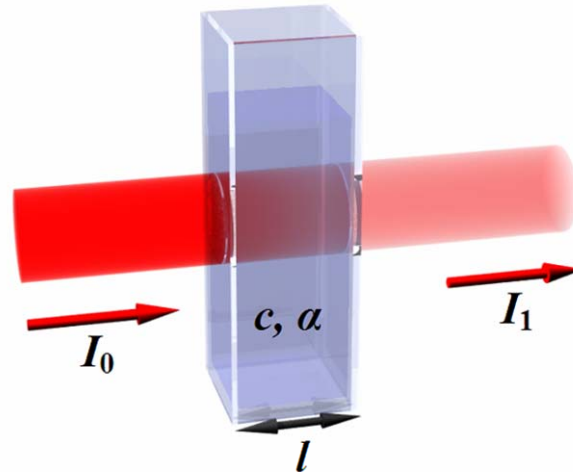


Figure 1 Diagram of Beer-Lambert absorption of a beam of light as it travels through a media of size l , α – absorption coefficient and c – concentration of the absorbing species in the material

It is important to note that α is strongly wavelength-dependent, given that most translucent media is a color other than neutral gray.

2.3.2. Fresnel's Law

A homogeneous porous media of uniform liquid content can be considered as a single phase, with an effective Beer's law adsorption coefficient representative of the bulk media. However, at the pore scale, light passes through solid, (water, and DNAPL) phase constituents, each with a separate absorption coefficient. Applying Beer's law incrementally to each phase as if it were a separate compartment encountered along a given light path is not sufficient to accurately predict the degree of transmission through the bulk media. When passing between phases of different refractive indices, the interfaces between phases refract and absorb a portion of the incident light based on the relative indices of refraction, angle of incidence, and polarization, as described by Fresnel's law. It is not important that a form of Fresnel's law is chosen to represent the interfacial loss component explicitly, but rather to recognize that an average transmittance, τ , exists when a particular wavelength light traverses any two phases (water-sand, DNAPL-sand, or DNAPL-water).

The **refractive index** (or **index of refraction**) of a medium is a measure for how much the speed of light (or other waves such as sound waves) is reduced inside the medium. For example, liquid

water has a refractive index of 1.33, which means that light travels at $1 / 1.33 = 0.75$ times the speed in air or vacuum.

By accumulating the absorptive and interfacial loss components from phase to phase over the media thickness, and by letting the index $i, i+1$ represent each interface where i is each preceding phase compartment, it follows that the combined Beer-Lambert and Fresnel law is:

$$I = CI_0 \left(\prod_i \tau_{i,i+1} \right) \exp \left(- \sum_i \alpha_i d_i \right) \quad (2.3)$$

where $\tau_{i,i+1}$ is the transmittance of the interface between compartment i and $i+1$.

$$\tau_{12} = \frac{4n_1n_2}{(n_1 + n_2)^2} \quad (2.4)$$

and n_i is refractive indices of the two phases.

In Table 1 is given a list of refractive indices and equation (2.5) describes how the transmittance is calculated between sand and water.

$$\tau_{sw} = \frac{4 \cdot 1.333 \cdot 1.6}{(1.333 + 1.6)^2} = 0.9917 \quad (2.5)$$

Table 1 List of refractive indices

Refractive indices list (n_i)	
Vacuum	1
Air @ STP	1.0002926
Water Ice	1.31
Liquid Water (20°C)	1.332986
Teflon	1.35 - 1.38
Glycerol	1.4729
Oil Vegetable	1.47
Sand	1.6

Table 2 Light transmission factor

Light transmission factor (τ_{ij})	
oil water	0.9976106
sand water	0.99006861
sand oil	0.99820688

2.4. Technique Limitations

In [Glass 1994] to improve the image contrast in the determination of the liquid saturation they used a contrast enhancing agent. In light transmission method using a different dye color will produce different image contrasts because the light intensity is governed by the differences in the refractive indices of the water-DNAPL interfaces.

Another condition for applying light transmission method is that the media has to be translucent and thus the thickness of the media is limited (on the order of centimeters for most cases).

As will be later shown (subchapter 5.3) confusing results can be obtained for the extremes (0% water saturation) due to lack of water-DNAPL interfaces.

2.5. Color Theory Considerations

Images produced with the light transmission method require to be interpreted. In order to obtain a very good interpretation and to build a robust and easy to use method we compared different color spaces and conversions. There are different formats in which the color observed in the pictures can be expressed; the most common are red, green and blue (RGB) and hue, saturation and intensity (HSI). In this chapter there are presented the principal color models and the conversions from the RGB color space to HSI, HSV, Gray and Intensity.

2.5.1. RGB Color Model

The RGB color model is an additive model that combines red, green, and blue in multiple ways to reproduce other colors (Figure 2). The name as well as the abbreviation ‘RGB’ of the model result from the three primary colors, red, green, and blue and the technological development of cathode ray tubes and their ability to display color instead of a monochrome phosphorescence (including grey scaling) such as black and white film and television imaging.

These three colors should not be confused with the primary pigments of red, blue, and yellow, known in the art world as ‘primary colors’, as the latter combine based on reflection and absorption of photons whereas RGB depends on emission of photons from (in the case of a Cathode ray tube display) a compound excited to a higher energy state by impact with an electron beam.

Within the RGB color model itself ‘red’, ‘green’ and ‘blue’ are not exactly determined (spectroscopically), where consequently the results of mixing them remain unspecified as exact (but relative, and averaged by the human eye).

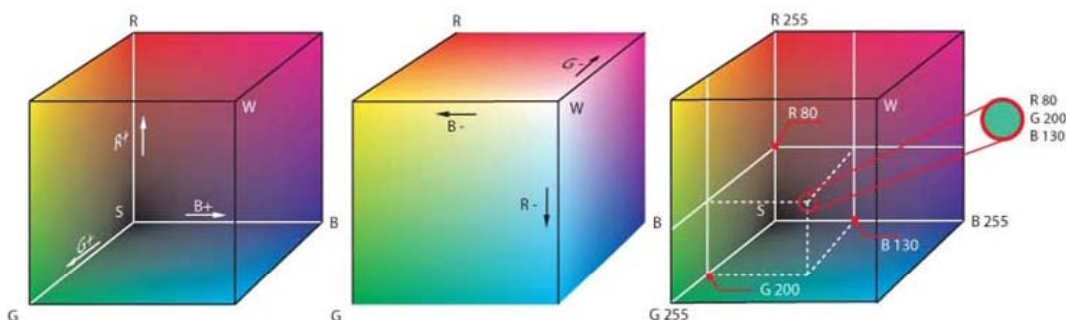


Figure 2 : The RGB-Cube

2.5.2. Numerical Representations of RGB Color Model

A color in the RGB color model can be described by indicating how much of each of the red, green and blue color is included. Each can vary between the minimum (no color) and maximum (full intensity). If all the colors are at minimum the result is black. If all the colors at maximum, the result is white. A confusing aspect of the RGB color model is that these colors may be written in several different ways, which are:

- Color science talks about colors in the range 0.0 (minimum) to 1.0 (maximum). Most color formulae take these values. For instance, full intensity red is 1.0, 0.0, 0.0
- The color values may be written as percentages, from 0% (minimum) to 100% (maximum). To convert from the range 0.0 to 1.0. Full intensity red is 100%, 0%, 0%.
- The color values may be written as numbers in the range 0 to 255, simply by multiplying the range 0.0 to 1.0 by 255. This is commonly found in computer science, where programmers have found it convenient to store each color value in one 8-bit byte. This convention has become so widespread that many writers now consider the range 0 to 255 authoritative and do not give a context for their values. Full intensity red is 255,0,0 (Figure 3)
- The same range, 0 to 255, is sometimes written in hexadecimal, sometimes with a prefix (e.g. #). Because hexadecimal numbers in this range can be written with a fixed two digit format, the full intensity red #ff, #00, #00 might be contracted to #ff0000. This convention is used in web colors and is also considered by some writers to be authoritative

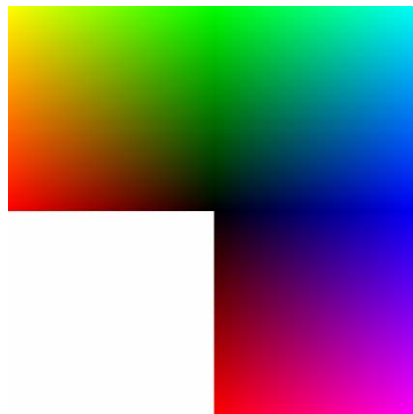


Figure 3: The three “fully saturated” faces of the RGB cube. On the left and bottom: maximum red=255, on the top: maximum green = 255; on the right: maximum blue = 255; center: red=green=blue=0

2.5.3. HSV Color Space

The HSV (Hue, Saturation, Value) model, also known as HSB (Hue, Saturation, Brightness), defines a color space in terms of three constituent components:

- Hue: describes the pure color or the color type (i.e. red, blue, yellow). It ranges from 0 – 360 in most applications or from 0 – 100% in others. Represents the color attribute that describes the pure color.
- Saturation: corresponds to the degree to which the color is diluted with white or the “intensity” of the color. It ranges from 0 – 100%. 0 means no color, i.e., a shade of grey between black and white. 100 means intense color.
- Value or brightness: corresponds to the gray value. It ranges from 0-100% or in some applications from 0 to 255. 0 is always black. Depending on the saturation, 100 may be white or a more or less saturated color.

The HSV model is a nonlinear transformation of the RGB color space. The definition of the HSV color model is not device independent but is only defined relative to RGB intensities.

One suggestive visualization method of the HSV model is the cone (Figure 4). The hue is depicted as a three-dimensional conical formation of the color wheel; the saturation is represented as the distance from the center of a circular cross section of the cone, and the value is the distance from the pointed end of the cone.

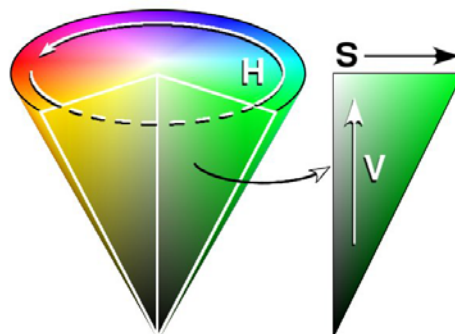


Figure 4: HSV color space as a conical object

2.5.4. HSL Color Space

The HSL color space, also called HLS or HSI, stands for Hue, Saturation, Lightness (also Luminance or Luminosity)/ Intensity.

While HSV (Hue, Saturation, Value) can be viewed graphically as a color cone or hexcone (Figure 4, Figure 7), HSL can be drawn as a double cone, HSL can be drawn as a double cone (Figure 5) or double hexcone as well as a sphere (Figure 6). Both systems are non-linear deformations of the RGB color cube.

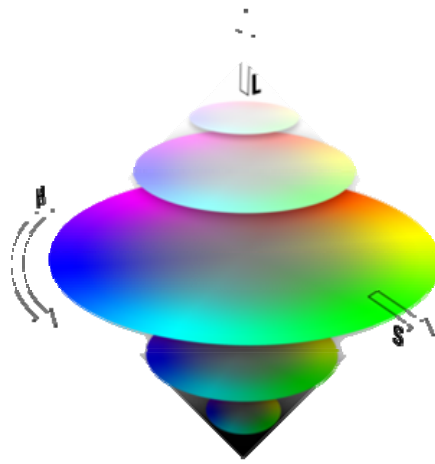


Figure 5 Double cone, or double hexcone

The two apexes of the HSL double hexcone correspond to black and white. The angular parameter of the HSL double hexcone corresponds to hue, distance from the axis corresponds to saturation and distance along the black/white axis corresponds to lightness.

HSL does not define colors exactly because, like RGB is not an absolute color space. Since the color of RGB depends on the exact shade of red, blue and green (“primaries”) used, so HSL, which is a simple transformation of RGB, also depends on the primaries. Strictly speaking, it is not a color space but a color model.

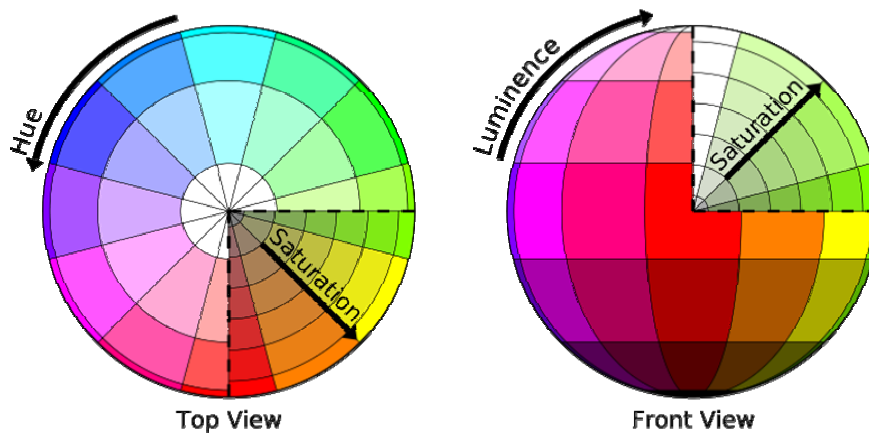


Figure 6: HSI representation as a sphere

The advantage of the HSI and HSV format is that it treats color roughly the same way that humans perceive and interpret color [Wilson, 1998]. Therefore, if the human eye is able to see differences in color and intensity for different fluid contents, these differences can be quantified using the HSI or HSV format.

2.6. Color Conversions

2.6.1. Converting from RGB to HSL

Matlab is a numerical computing environment and programming language.

Our pictures have a dimension of 2560x1920 pixels are represented as three dimensional matrixes, each dimension for each color attribute (red, green, blue) or after conversion: hue, saturation, intensity or value.

The Matlab “H=RGB2HSL(M) build in function converts an RGB color map to an HSL color map. Each map is a matrix with any possible number of rows, exactly three columns, and elements in the interval 0 to 1. The columns of the input matrix, M, represent intensity of red, blue and green, respectively. The columns of the resulting output matrix, H, represent hue, saturation and color luminance, respectively.

In the conversion of RGB to HSI color space, the (R, G, B) values must be expressed as numbers from 0 to 1. For this, let MAX equal the greatest of the (R, G, B) values, and MIN equal the least of those values. The formula can then be written as

$$MAX = MAX(R, G, B)$$

$$H = \begin{cases} \text{undefined} & \text{if } MAX = MIN \\ 60^\circ \times \frac{G - B}{MAX - MIN} + 0^\circ, & \text{if } MAX = R \text{ and } G \geq B \\ 60^\circ \times \frac{G - B}{MAX - MIN} + 0^\circ, & \text{if } MAX = R \text{ and } G < B \\ 60^\circ \times \frac{B - R}{MAX - MIN} + 120^\circ, & \text{if } MAX = G \\ 60^\circ \times \frac{R - G}{MAX - MIN} + 240^\circ, & \text{if } MAX = B \end{cases} \quad (2.6)$$

$$S = \begin{cases} 0 & \text{if } L = 0 \text{ or } MAX = MIN \\ \frac{MAX - MIN}{MAX + MIN} = \frac{MAX - MIN}{2L} & \text{if } 0 < L \leq \frac{1}{2} \\ \frac{MAX - MIN}{2 - (MAX + MIN)} = \frac{MAX - MIN}{2 - 2L} & \text{if } L > \frac{1}{2} \end{cases} \quad (2.7)$$

$$L = \frac{1}{2}(MAX + MIN) \quad (2.8)$$

H is generally normalized to lie between 0 and 360°, and $H=0$ is often used when $MAX=MIN$ instead of leaving H undefined.

2.6.2. Expressing HUE in the range [0,1]

Using a percentage representation is more useful in our case, so we apply the following transformation from RGB to hue:

$$MAX = \text{maximum}(R, G, B)$$

$$MIN = \text{minimum}(R, G, B)$$

When $MAX=MIN$ then hue is undefined being an achromatic case.

$$\begin{cases} rc = \frac{MAX - R}{MAX - MIN} \\ gc = \frac{MAX - G}{MAX - MIN} \\ bc = \frac{MAX - B}{MAX - MIN} \end{cases} \quad (2.9)$$

$$H = \begin{cases} bc - gc & , \text{if } R = MAX \\ 2 + rc - bc & , \text{if } G = MAX \\ 4 + gc - rc & , \text{if } B = MAX \end{cases} \Rightarrow \begin{cases} \frac{G - B}{R - MIN} & , \text{if } R = MAX (a) \\ 2 + \frac{B - R}{G - MIN} & , \text{if } G = MAX (b) \\ 4 + \frac{R - G}{B - MIN} & , \text{if } B = MAX (c) \end{cases} \quad (2.10)$$

- (a) – resulting color between yellow and magenta
- (b) – resulting color between cyan and yellow
- (c) – resulting color between magenta and cyan

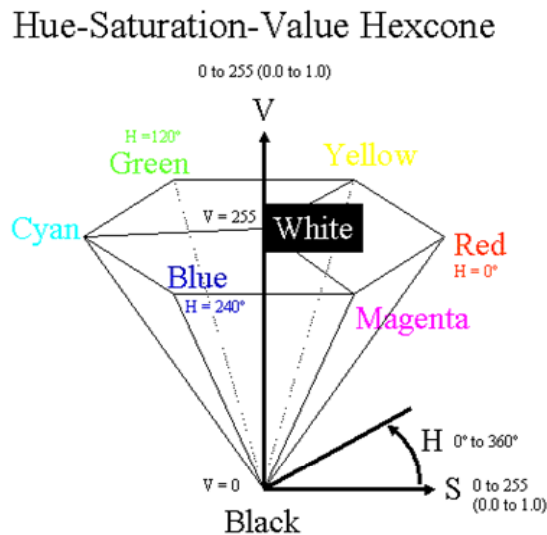


Figure 7: HSV hexcone

Converting from RGB to HSV

HSL and HSV have the same definition of hue, but the other components differ. The other two components of HSV are defined as follows:

$$S = \begin{cases} 0 & \text{if } MAX = 0 \\ 1 - \frac{MIN}{MAX} & \text{if otherwise} \end{cases} \quad (2.11)$$

$$V = MAX \quad (2.12)$$

The values obtained are in the range 0 to 1, after red, green and blue were expressed in the same range at the beginning .

2.6.3. Gray

RGB2GRAY Matlab function converts an RGB image or colormap to grayscale by eliminating the hue and saturation information while retaining the luminance.

The algorithm of *rgb2gray* function when converting RGB values to grayscale values is by forming a weighted sum of the R, G and B components:

$$0.2989 \cdot R + 0.5879 \cdot G + 0.1140 \cdot B \quad (2.13)$$

These are the same weights used by the *rgb2ntsc* function to compute the Y component.

2.6.4. Intensity

For expressing the light intensity Darnault uses the formula of Wilson, 1988 as follows

$$I = 255 \left(\frac{R + G + B}{3} \right) \text{ for } R, G, B \text{ range from 0 to 1.} \quad (2.14)$$

or:

$$I = \left(\frac{R + G + B}{3} \right) \text{ for } R, G, B \text{ range from 0 to 255.} \quad (2.15)$$

Values of *I* range from 0 to 255.

2.6.5. Hue

In order to convert RGB to HSI, hue (H) can be expressed as [Wilson,1998]

$$H = 225 \left\{ \frac{1}{360} \left[Y - \arctan \frac{2R - G - B}{\sqrt{3}(G - B)} \right] \right\} \quad (2.16)$$

Y=90 G>B, Y=270, G<B

where R, G and B are red, green, and blue intensities, respectively. The value for Y depends on the green and blue intensities. Intensity (I) is calculated as [Wilson,1998]

Values of H range from 0 to 255.

This Hue transformation was used by Darnault (1997) to determine a soil-oil-water system and in (2001) for a oil-water-air system.

2.7. Camera Parameters

For the picture interpretation obtained with the light transmission method the study of the different camera parameters is very important. Understanding the influence of these parameters on the light transmission results is one task of this study.

The adjustment of these parameters can be made both manually and automatically from the computer.

After a proper adjustment, we observed that for certain camera parameters we acquired a better quality for interpretation than for other settings.

2.7.1. WB Mode

In photography and image processing, **color balance** (gray balance, neutral balance, or white balance) refers to the adjustment to the relative amounts of red, green, and blue primary colors in an image such that neutral colors are reproduced correctly.

WB Mode stands for white balance mode. Preset WB values are: Lamp1(3000k), Fluorescent1 (4000k), Fluorescent2 (4500k), Fluorescent3 (6600k), Daylight (5300k), Cloudy (6000k), Shade (7500k)

During experiments we picked only Fluorescent1 (4000k) and Fluorescent2 (4500k)

2.7.2. Shutter

In photography, a **shutter** is a device that allows light to pass for a determined period of time, for the purpose of exposing photographic film or a light-sensitive electronic sensor to the right amount of light to create a permanent image of a view.

2.7.3. F-No

In optics, the **f-number** (sometimes called **focal ratio**, **f-ratio**, or **relative aperture**) of an optical system expresses the diameter of the entrance pupil in terms of the effective focal length of the lens. It is the quantitative measure of lens speed, an important concept in photography.

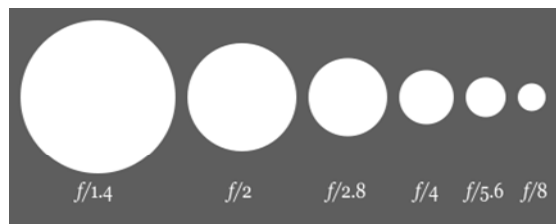


Figure 8 Diagram of decreasing apertures, that is, increasing f-numbers, in one-stop increments; each aperture has half the light gathering area of the previous one. The actual size of the aperture will depend on the focal length of the lens

The f-number $f/\#$, often notated as N , is given by :

$$f/\# = N = \frac{f}{D} \quad (2.17)$$

where f is the focal length, and D is the diameter of the entrance pupil. By convention, " $f/\#$ " is treated as a single symbol, and specific values of $f/\#$ are written by replacing the number sign with the value. For example, if the focal length is 16 times the pupil diameter, the f-number is $f/16$, or $N = 16$. The greater the f-number, the less light per unit area reaches the image plane of the system.

The literal interpretation of the f/N notation for f-number N is as an arithmetic expression for the effective aperture diameter (input pupil diameter), the focal length divided by the f-number: $D = f/N$.

2.7.4. Shutter Speed / Exposure Time

In photography, **shutter speed** is the time for which the shutter is held open during the taking of a photograph to allow light to reach the film or image sensor (in a digital camera).

In combination with variation of the lens aperture, the shutter speed regulates how much light the camera will record. For a given exposure, a fast shutter speed demands a larger aperture or more light to avoid under-exposure, just as a slow shutter speed is offset by a very small aperture to avoid over-exposure. Long shutter speeds are often used in low light conditions, such as at night. Shutter speed is measured in seconds. A typical shutter speed for photographs taken in sunlight is 1/125th of a second. In addition to its effect on exposure, shutter speed changes the way movement appears in the picture. Very short shutter speeds are used to freeze fast-moving subjects. Very long shutter speeds are used to intentionally blur a moving subject.

A standardized scale was adopted for shutter speed.

The general camera settings can be configured in the camera control window or the [Shooting Setup/ Camera Setup] dialog box.

Shutter speeds are arranged so that one stop in the shutter speed scale corresponds to one stop in the aperture scale. Opening up a lens by one stop allows twice as much light to fall on the film in a given period of time, therefore to have the same exposure, you must have a shutter speed twice as fast (shutter open half as long).

3. Experimental Methodology

3.1. The Setup

The experimental chamber is placed between a diffuse light source and a digital camera that takes the pictures that will be later analyzed. The diffuse light source in our experiments is built in a wood illumination box. Six 230V/50Hz fluorescent lamps with tubular shape from the company Rigionox are horizontally installed in parallel in the box (Figure 9). A piece of glass with prismatic structures is put in front of the lamps. The glass acts as a diffuse plate, through which light is distributed evenly onto the front of the chamber.



Figure 9: The experimental chamber with the six fluorescent lamps in the background

3.2. Photo Camera

A 12-bit five-megapixel single reflex digital camera Olympus E-1 with a 14-54 mm F2.8-3.5 lens is used (Figure 10). Camera resolutions are between 0.03 and 0.05 mm²/pixel. (Table 6)

The digital camera can be remotely controlled with a computer.

The shutter time and the f-number of the camera are modified from picture to picture through the computer program of the camera: Olympus Studio.

The other parameters of the camera, e.g. are set manually (focal length) or with the computer program (ISO speed, Flash mode) and kept identically in all experiments.

Illumination box, chamber and digital camera including its stand are all fixed on a table.

Therefore, the relative positions of all three elements are assumed to be constant.

The whole system is overlaid by a thick black polyethylene curtain, and hereby external light does not influence the digital camera. Since the area of the illumination box is larger than that of

the chamber, the extra space around the chamber is also covered with a textile curtain so that only transmitted light through the chamber is determined and so that the camera is focused on the chamber itself at the widest zoom of the lens. By these ways errors resulting from light reflection and scattering are minimized.

The light bank and CCD camera were allowed to reach temperature equilibrium before starting the experiment (minimum 30 min).



Figure 10: Olympus E-1 Digital Camera



Figure 11: The whole experiment setup: illumination box, slab chamber, camera stand, digital camera, inner and exterior curtains

3.3. Chamber Construction

The chamber is constructed of two plates of hydrophilic safety glass (8mm thick each) from the company Südwest Glas. The sealing between the spacer and the glass are done with silicon sealant. The internal thickness of the chamber is 10 mm thick. An exterior frame of steel is clamped by a total of 11 M16 screws to the outside of the glass plates at the both sides and bottom to avoid leakage.

The effective visible area of the chamber is about 350 mm wide by 190 mm high. The exterior frame's dimensions are 377 mm long and 200 mm high.

The weight of the empty chamber is about 10 kg.

A bigger chamber constructed similarly as the small one is used to run the transient flow experiments. The thickness of the safety glass of the bigger chamber is the same 10mm by 600 mm wide by 400 mm high.

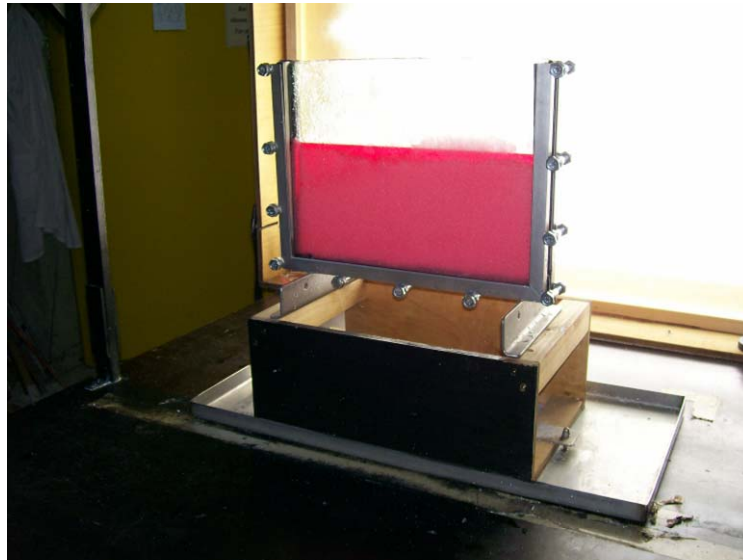


Figure 12: The small slab chamber filled

3.4. DNAPL (Dense Non-Aqueous Phase Liquid)

The DNAPL is called *diethyl phthalate* and is produced by Merck Schuchardt OHG.

Synonyms for it are : ethyl phthalate, DEP, Phthalic acid diethyl ester.

The chemical formula is $C_6H_4(COOC_2H_5)_2$.

The physical and chemical properties are extracted from the Safety Data Sheets.

Table 3 Physical and chemical properties

Form	liquid	
Color	colorless	
pH value (20°C)	7	
Viscosity dynamic (20°C)	13	mPa·s
Vapor pressure (20°C)	0.002	hPa
(100°C)	0.825	hPa
Relative vapor density	7.66	
Density (20°C)	1.12 g/cm ³	
Solubility in water (20°C)	insoluble	
log Pow (20°C)	2.35	

The DNAPL and the glass beads contaminated with it must be disposed of in compliance with the national regulations.

After running our experiments we disposed the DNAPL into the sewage system going to the institutes waste water treatment plant. The contaminated glass beads were disposed in a sealed barrel which will be disposed later according to regulations.

The DNAPL is immiscible with water. We performed an experiment to see how fast the DNAPL separates from water after the two were stirred in a beaker. Only 10 – 20 seconds after stirring one could clearly see a separation front. After 1 – 2 minutes the DNAPL is almost entirely separated.

Dyestuff

For clearly pointing out the wetting phase (water) and the non-wetting phase (pollutant) we colored the DNAPL using a red dyestuff.

The name of the dyestuff is *Oil Red O* and in the DNAPL it has been used in a concentration of 0.4 mg/l.

3.5. Glass Beads Characteristics

The calibration experiments were conducted with glass sand “Silibeads” ordered from Sigmund Linder GmbH (Table 4). The size range of the glass beads used in the experiments is 0.3125 – 0.5 mm. For this grains size corresponds a roundness value higher than 95%.

Table 4 Sieve analysis of glass beads from Sigmund Linder GmbH

Glass Beads [mm]		Size range [mm]		Cumulative percent	Roundness	Bulk density [g/cm ³]
0.25 - 0.50	>0.50	0%	>95%	1.51		
	>0.40	30%				
	>0.35	80%				
	>0.30	90%				
	>0.25	99%				
	>0.20	100%				
	<0.20	0%				

4. The Experiments

We performed a set of nine experiments taking 1193 pictures with a resolution of 2560 x 1920 pixels (Table 5). All experiments were conducted at the room temperature.

In the column “Exposure times” of Table 5 are shown the values of the *exposure time* (camera parameter) investigated. First we set a fixed *exposure time* and we took one picture with each F-number for the entire range of F-numbers and after we changed the camera setting to the next value of *exposure time* and again took pictures for each F-number.

During all laboratory experiments a constant distance from the camera to the slab chamber of 74 cm was kept.

Table 5: List and characteristics of the experiments

	Date	Experiment		No of pictures	No of Exposure Times	Exposure times	Filling Procedure	Focal length [mm]
		DNAPL	water					
1a	18.05.2007	0%	100%	224	12	1/6, 1/5, 1/4, 1/3, 1/2, 1/1 for 4000k and 4500k	Dripping Sand	28
1b	20.02.2007	0%	100%	50	11	1/50, 1/25, 1/10, 1/5, 1/4, 1/3, 1/2, 1, 1.6, 2, 3.2	Dripping Sand	29
2	15.03.2007	30%	70%	111	10	1/6, 1/5, 1/4, 1/2, 1/1 for 4000k and 4500k	Mixing	29
3	19.03.2007	50%	50%	135	12	1/6, 1/5, 1/4, 1/3, 1/2, 1/1 for 4000k and 4500k	Mixing	29
4	16.03.2007	70%	30%	119	12	1/6, 1/5, 1/4, 1/3, 1/2, 1/1 for 4000k and 4500k	Mixing	31
5	18.05.2007	90%	10%	226	12	1/6, 1/5, 1/4, 1/3, 1/2, 1/1 for 4000k and 4500k	Mixing	28
6	19.05.2007	100%	0%	217	12	1/6, 1/5, 1/4, 1/3, 1/2, 1/1 for 4000k and 4500k	Mixing	29
7a	22.02.2007	100%	0%	81	7	1/8, 1/6, 1/5, 1/3, 1, 1.3, 2	Dripping Sand	32
7b	23.02.2007	100%	0%	30	2	1/4, 1/5 for 4000k	Dripping Sand	32
TOTAL				1193				

Instead of using compartments with known quantities of oil and water [Darnault, 2001], we used the same slab chamber each time for each value of DNAPL-water content.

4.1. Filling procedures

For filling in the sand chamber, many procedures were considered and tested. The main problems that arise are air entrapment and creation of heterogeneities. The best two procedures developed are described below.

Procedure 1 : Dripping sand

For 0% DNAPL and 100% water, and for 100% DNAPL and 0% water, the slab chamber was filled by dripping sand into water through a funnel at a low pouring speed and constantly moving the funnel through the whole length of the chamber for avoiding air entrapment. Another measure to prevent air entrapment is keeping the funnel approximately 2-3 centimeters above the water level so that the glass beads do not enter the fluid with high velocities.

Procedure 2 : Mixing

The second procedure was used for the rest of the experiments: 30, 50, 70, 90, 100 % DNAPL saturation by mixing the exact amounts of water, oil and sand in a beaker and loading the mixture in the slab chamber. After the chamber is loaded one sees that the color is not uniformly distributed and that there are slight spatial differences due to DNAPL and water ganglia formation. For removing these non-uniformities and creating a more homogeneous aspect a steel rod is being used. It has been observed that the non-uniformities can be diminished by moving the steel rod upwards and downwards and pressing it towards lateral direction. In this way the small ganglia formations are broken and a homogeneous aspect is obtained.

Only static flow experiments were performed with the slab chamber.

4.2. Porosity determination

Porosity of the sand has been calculated by measuring the water volume which was added to an initial mass of glass sand until saturation.

The water at a room temperature of 20°C has a density of 0.9982 g/cm³.

$$\rho_w = 0.9982 \text{ g / cm}^3$$

$$\rho_w = \frac{M_{\text{water}}}{V_{\text{water}}}$$

$$V_{\text{water}} = V_{\text{pores}}$$

$$n = \frac{V_{\text{pores}}}{V_{\text{total}}}$$

V_{total} – is measured in a graded cylinder

where M_{water} – the measured mass of water; V_{water} – the measured volume of water.

The water weight is measured with an electronic balance with a precision of 0.01 grams.

The same determination procedure was done four times to avoid and diminish errors. The final sand porosity was 38.4%.

With this value we calculated the different saturations.

4.3. Bulk density determination

For the determination of the bulk density we used a 500 ml cylindrical glass. We measured a mass of 765.47 g for the sand volume of 500 ml.

$$\rho_{bulk} = \frac{M_{sand}}{V_{sand}} = \frac{765.47g}{500cm^3} = 1.53094g/cm^3$$

4.4. Volumetric fluid content of the experiments

For each DNAPL saturation we prepared a total volume (sand – water – DNAPL) of 800ml. For example for 0% and 30% DNAPL saturation the afferent calculations look :

0% DNAPL– 100% Water Saturation

We prepared a total volume of 800 ml experiment.

$$V_{liquid} = n \cdot V_{total} = 0.384 \cdot 800 = 306.907cm^3$$

$$V_{sand} = (1 - n) \cdot V_{total} = (1 - 0.384) \cdot 800 = 493.093cm^3$$

$$V_{water} = V_{liquid} = 306.907cm^3$$

30% DNAPL– 70% Water Saturation

We prepared a total volume of 800 ml experiment.

$$V_{liquid} = n \cdot V_{total} = 0.384 \cdot 800 = 306.907cm^3$$

$$V_{sand} = (1 - n) \cdot V_{total} = (1 - 0.384) \cdot 800 = 493.093cm^3$$

$$V_{water} = V_{liquid} \cdot 0.70 = 306.907 \cdot 0.70 = 214.8349cm^3$$

$$V_{DNAPL} = V_{liquid} \cdot 0.30 = 306.907 \cdot 0.30 = 92.0721cm^3$$

5. Results and Discussion

Our objective is to determine a calibration curve, a methodology to derive this calibration curve, and to see which combination of camera parameters gives the best calibration curve.

As will be seen later, each color attribute has a non-linear variation with regard to the camera parameters that have been investigated: *F-number*, *Exposure time* and *White balance*. Thus, firstly we will understand the way color attributes vary with camera parameters and afterwards we will pick up the ones (*color attributes* and *camera parameters*) that give the best calibration curve.

We have three sets of variables: the nine *color attributes* (red, green, blue, hue, saturation, value, luminance, intensity and gray) that will be compared; the three *camera parameters* that have been already mentioned; and the six *liquid saturations* (0, 30, 50, 70, 90, 100%). In order to make our work easier we show first which color attributes cannot be used or are bad for interpretation and consequently eliminated from the following graphics. Therefore sections 5.4, 5.5 and 5.6 come to show that *hue*, *saturation*, *red* and *value* are not good color attributes for building a calibration curve.

Section 5.3 explains why we use as a highest value the 90% DNAPL saturation and not 100%.

In the following sections (5.7 and 5.8) the color attributes are compared to each other as they vary with regard to F-number and white balance. The purpose is to determine the color attribute that has the widest range (of color units) for the whole spectrum of DNAPL saturations.

The best two color attributes are analyzed separately in sections 5.11 and 5.12.

Subchapter 5.13 presents the final results of this work in the shape of a table, where for each color attribute and for each exposure time one could pick a range of F-numbers in order to get the very best calibration curve corresponding to that color attribute. In subchapter 5.14 there are given examples of the best calibration curves.

As a final comment this study answered to two questions “which is the best color attribute” and “which are the best camera settings”. For the first question one could clearly agree that one color attribute is better than the other but for the second question the answer is that there are more combinations of camera settings.

5.1. Picture interpretation

This subchapter presents the methodology of interpreting the pictures.

The nine sets of pictures from the nine experiments have been interpreted separately. We used Matlab to analyze each set of pictures. The dimension of all pictures taken is 2560 x 1920 pixels (Figure 13).

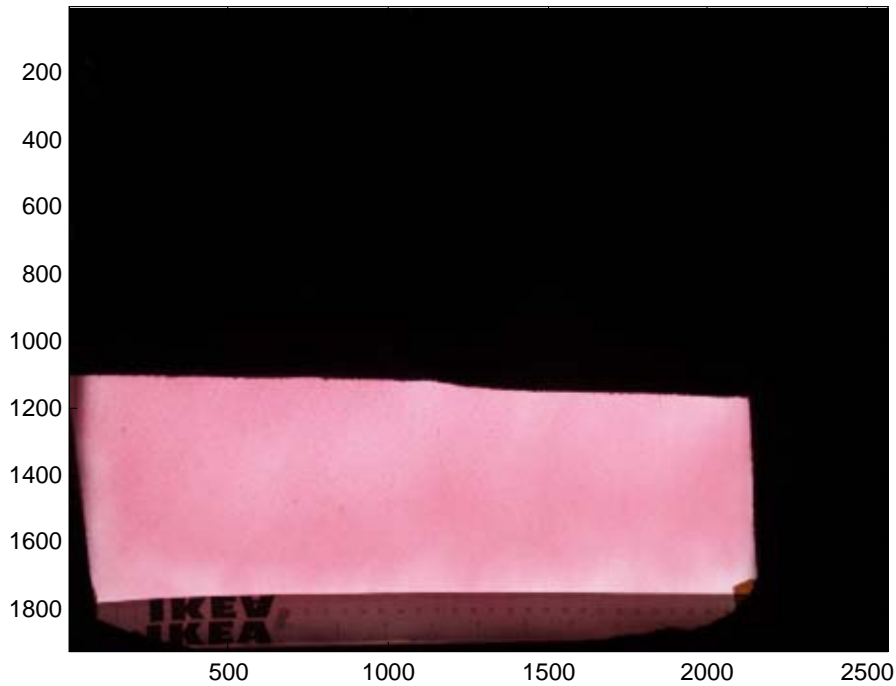


Figure 13: Picture of 2560x1920 pixels for 30% DNAPL saturation F-Number - F/5, Exposure Time - 1/6 sec.

When interpreting the pictures, the first step is to eliminate the black area from each picture. Also, the edge effects at the margins of the domain had to be removed.

A further step was to carefully examine the pictures and chose the areas with minimal heterogeneity for obtaining a representative average. This operation has been performed numerically, by making more cuts and comparing the results afterwards, and also visually. The conclusion is that *we can rely on human eye* when choosing the representative areas.

An example where both edge influences and non-uniform color distribution can be seen is shown in Figure 14. Figure 14 also shows how the first picture cut could be made when electing a representative picture area for averaging.

The camera resolution and the picture cuts that have been used for each experiment individually are depicted in Table 6. A scale has been placed on the experimental slab chamber in order to determine the resolution.

The X and Y cuts are expressed in pixels and related to the initial picture. (i.e. X cut 500:1750 and Y 1200:1600 means that from the original picture that has 2560 pixels on X axis and 1920 on Y axis we chose the area between 500 and 1750 on X and 1200 and 1600 on Y). The origin of the coordinate system in Matlab is the upper left corner. The X values increase from left to right and the Y values increase from top to bottom. (See Figure 13)

For each experiment we determined the following color attributes: *red, green, blue, gray, hue, saturation, value, luminance, intensity* and for each of this attributes it has been determined the mean value, the maximum and the minimum, and the standard deviation.

For each set of pictures the average computing time on a 1.8 GHz Intel Pentium M processor with 512 MB of RAM was about 6 hours.

Table 6: Camera resolution, X and Y picture cuts for each experiment

Experiment	1a	1b	2	3	4	5	6	7a	7b
Saturation	0%	0%	30%	50%	70%	90%	100%	100%	100%
Number of Pictures Taken	224	50	111	135	119	226	217	81	30
X Cut [pixel]	500:1750	500:1750	500:1750	500:1750	500:1750	500:1750	500:1750	500:1750	500:1750
Y Cut [pixel]	1300:1600	1200:1600	1200:1600	1200:1600	1200:1600	1200:1600	1200:1600	1200:1600	1200:1600
Resolution [pixels/mm ²]	33.64	33.64	33.64	31.36	36	20.25	32.49	40.96	40.96
Resolution [mm ² /pixels]	0.02972	0.02972	0.02972	0.03189	0.02778	0.04938	0.03078	0.02441	0.02441



Figure 14: Example for seeing the edge effects and heterogeneity

The images were interpreted with regard to more parameters:

- Color-Attribute – F-Number variation for given
 - Exposure times
 - white balance numbers
 - DNAPL saturations
- Comparison between Color-Attribute – F-Numbers for given
 - Exposure times
 - White balance
 - DNAPL saturations
- Color-Attribute – Exposure Time variation for given
 - F-Numbers
 - DNAPL saturations
- Color-Attribute –DNAPL saturation for given
 - F-Numbers
 - Exposure times
 - White balance

To compute the values of the color attributes when interpreting the pictures a computer program was written based on the color formulas.

5.2. Variation of the Color attribute with the F-number

In order to understand how the camera parameter *F-number* influences our results for each experiment we plotted the variation of the color attribute with the F-number for different exposure times and a given DNAPL saturation. The graphics of the variation of *red*, *green* and *blue* color attributes with F-numbers for all DNAPL saturations can be found in the Appendix 1; for the *hue* in Figure 22 to Figure 27 and *saturation* in Figure 29 to Figure 35.

Important remark: When reading the graphics is not important to compare the values pointwise. The graphics should be regarded from their sensitivity and how the curves succeed with regard to the camera parameters.

Each “color attribute – F-number” curve behaves differently than the other ones. We looked for a pattern in the variation of the curves in order to understand how F-number, exposure time and white balance camera parameters influence the color value.

As a general self-evident remark we ascertained that curves with different white balance number and with different exposure times have the same profile meaning that the same results can be obtained with different camera settings.



Figure 15: Variation in the color of the pictures (before being interpreted) by the increase of F-Number for constant exposure time (ET) 1/5 seconds and constant WB4000k. The pictures are taken from the 30% DNAPL saturation experiment.

In Figure 15 is being observed that by increasing the F-number the picture is getting darker. The same effect is happening for decreasing exposure times.

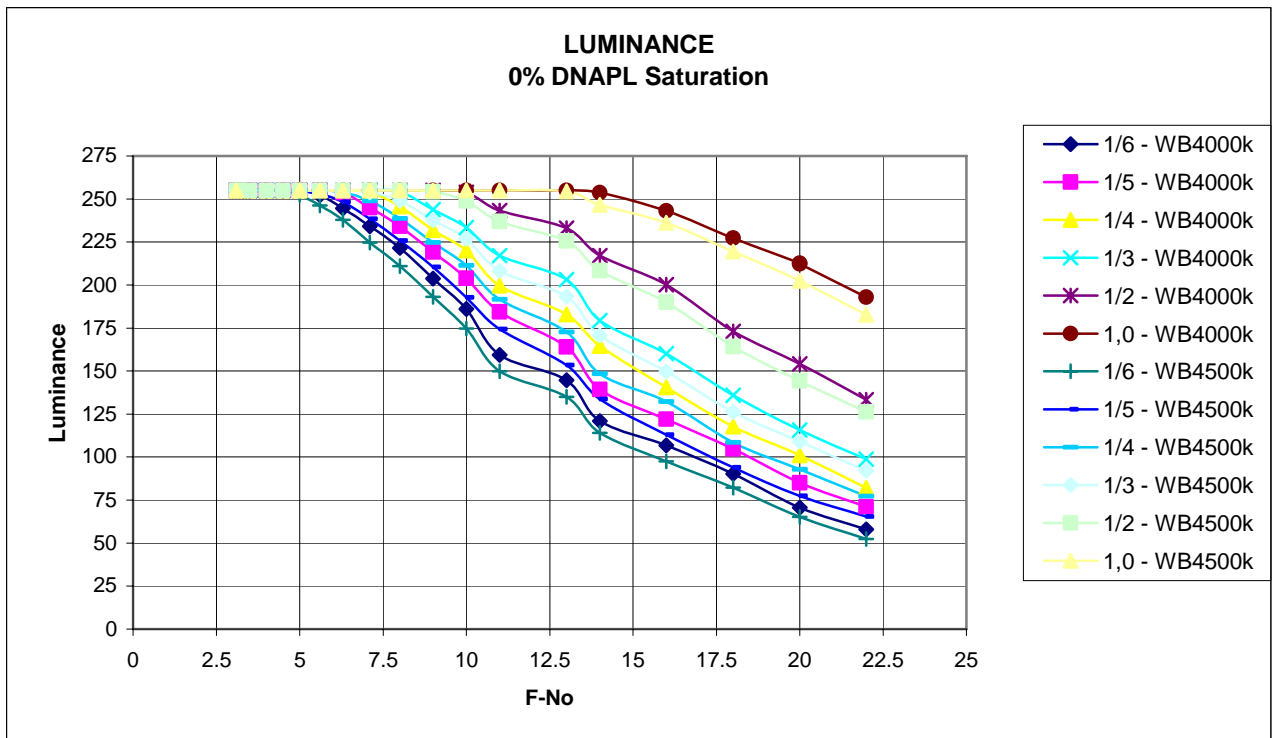


Figure 16: Variation of Luminance color attribute – F-number for 0% DNAPL saturation and different exposure times and white balance values

By examining the graphics of the variation of color attribute with the F-Number for a 0% DNAPL saturation we can determine the inferior limit for the F-numbers. F-numbers smaller than 4.5 result in the same color value of 255. White color value is (255,255,255), this is the reason for which for F-numbers smaller than 4,5 with a minimum time exposure of 1/6 seconds in all color attribute curves we will get for the color value 255.(Figure 16)

The upper limit is calculated on the Color (Mean)-F-Number graphic for 90% saturation. When the change between color values of two successive F-numbers is smaller than 5 color units (approx. 2% of 255, the maximum value for color attribute) the reading is starting to become difficult.

In this sense, reasonable limits of F-numbers for different exposure times to be used when building a calibration curve are given in Table 7.

Table 7: F-numbers good to be used in picture interpretation

Expo sure time	Red		Green		Blue		Gray		Luminance		Intensity	
	F-No Min	F-No Max										
1/6	4.5	22	4.5	10	4.5	10	4.5	22	4.5	22	4.5	22
1/5	5	22	5	10	5	10	5	22	5	22	5	22
1/4	5.6	22	5.6	10	5.6	10	5.6	22	5.6	22	5.6	22
1/3	6.3	22	6.3	14	6.3	14	6.3	22	6.3	22	6.3	22
1/2	8	22	8	14	8	18	8	22	8	22	8	22
1,0	11	22	11	18	11	22	11	22	11	22	11	22

5.3. 100 Percent DNAPL Saturation

In the experiments it has been observed that for 100 percent DNAPL saturation the color attribute curves behave different than it would have been expected. In this subchapter the discrepancies are shown that appear when using the 100% DNAPL saturation curve (sections 5.3.1 and 5.3.2) and the explanation for the causes of these discrepancies are given.

5.3.1. Variation of Color attribute with F-Number for 100% DNAPL saturation

In Figure 17 it is plotted the variation of the Red Color attribute with the F-number for different saturations of DNAPL. One observation that we can make is that by increasing DNAPL saturation the curves succeed one under the other. This behavior is valid for all color attributes except *hue* and *saturation*. Normally we would expect the 100% curve to be situated under the 90% DNAPL saturation curve. The 100% DNAPL saturation curve has a totally different

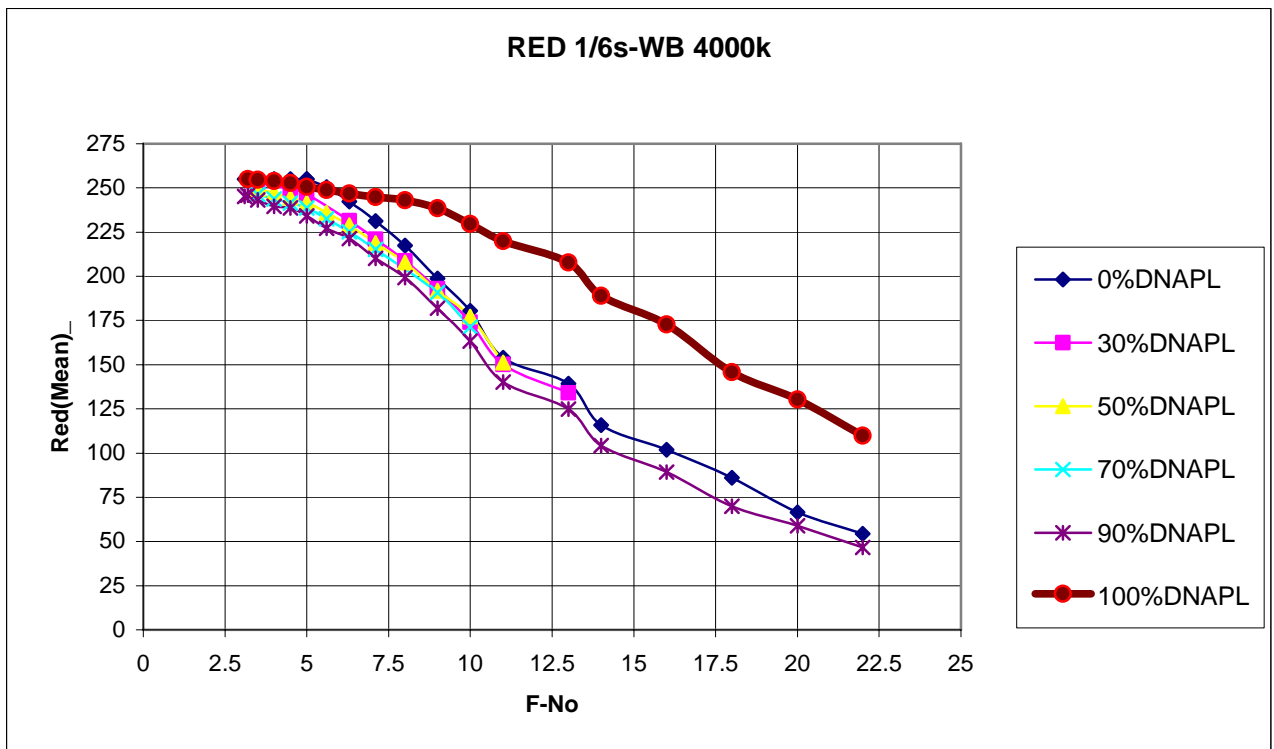


Figure 17: Red – F-No curves for 0, 30, 50, 70, 90% and 100% DNAPL saturation, for 1/6 seconds exposure time and white balance WB4000k showing the different behavior for the 100% DNAPL saturation curve

In the other “Color attribute – F-number” graphics the 100% DNAPL saturation curves keep also the same distinct behavior.

5.3.2. Variation of Color Attribute with DNAPL Saturation

Figure 18 shows the variation of *green* color attribute with the DNAPL saturation. The expected behavior of the curve, plotted using the values from 0 to 90 % DNAPL saturation, is displayed with red color and the real curve with blue.

For the other color attributes we get the same discrepancies between the expected and the real color values of 100% DNAPL saturation.

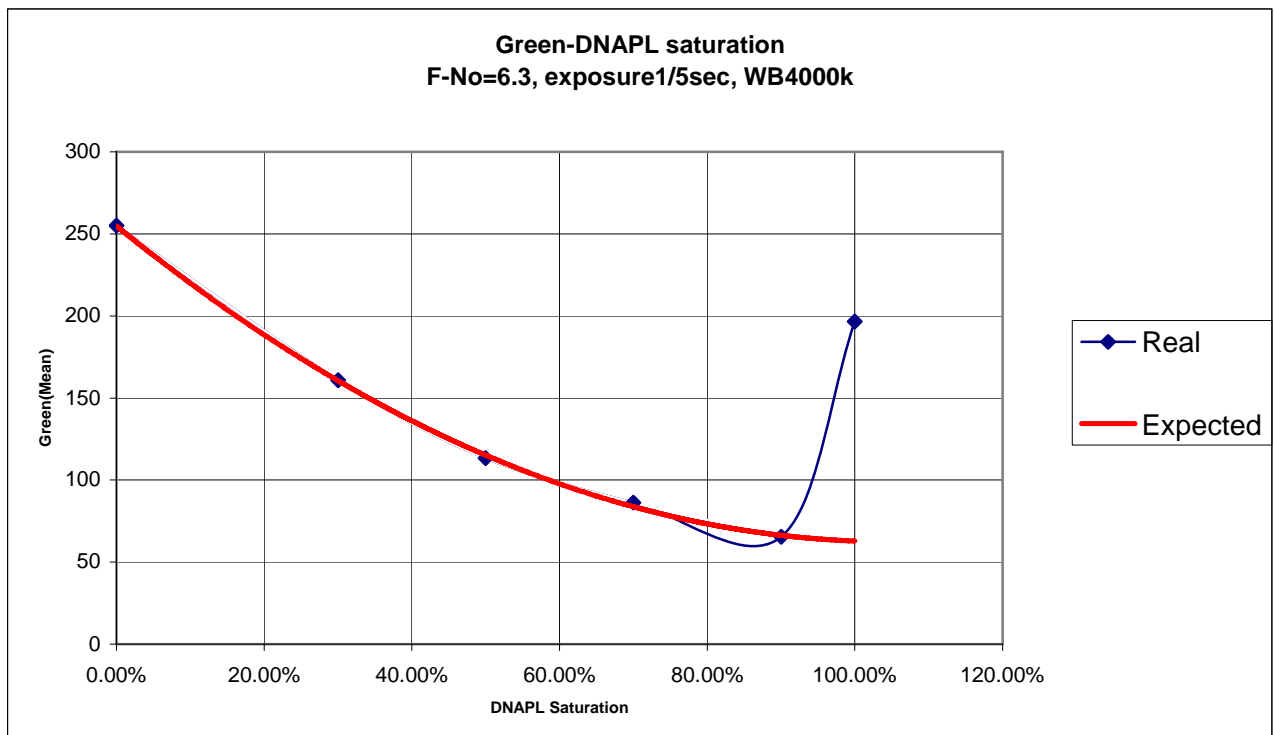


Figure 18: Variation of Green color attribute with DNAPL saturation for F-number 6.3 at an exposure time of 1/5 seconds and white balance WB4000k

In order to be sure that this is not due to experimental error a second experiment has been conducted for 100% DNAPL saturation. The filling procedure used was mixing DNAPL and sand (Table 5). After interpreting the pictures in Matlab a very similar behavior was obtained for both “Color attribute – F-number” and “Color attribute – DNAPL saturation” curves as when using the dripping sand filling procedure.

With the second experiment the two filling procedures could be compared.

When light passes through the porous media two phenomenons occur. First, light rays change direction when crossing the interfaces and second, light reflects partially from the surface with a different refractive index.

We assume a porous media idealized as uniform cubic particles of width d_s . As water is the wetting fluid and DNAPL the non-wetting fluid, a fine layer of water always covers the sand (Figure 19).

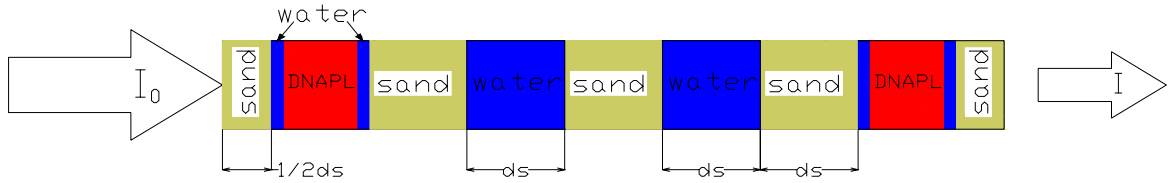


Figure 19: Physically based model for multiphase system: Uniform pore size. Pores filled with water and DNAPL

Constructing the physical model of the two fluid phase system it will be graphically represented like in Figure 19. We have pores fully filled with water and with DNAPL. The pores filled with DNAPL do not come in contact with the sand due to the fine water layer and this results in the lack of sand – DNAPL transmission factor from the equation (5.1). We make the assumption that the thickness of the water layer is very small and it will not be considered in the exponential part of the equation.

With these assumptions, from Beer (2.1) and Fresnel's laws (2.3) the light intensity for the system is derived:

$$I = CI_0 \tau_{sw}^{2kS} \tau_{wD}^{2k(1-S)} \exp(-k\alpha_s d_s - k\alpha_w d_s S - k\alpha_D d_s (1-S)) \quad (5.1)$$

I_0 – measured intensity of the light source

τ_{sw} – transmission factor sand-water

τ_{wD} – transmission factor water-DNAPL

k – average number of particles or pores across the media thickness

d_s – width of the idealized cubic particle

α_i – absorption coefficient of i (s – sand, w – water, D – DNAPL)

S – water saturation

For a DNAPL saturation that is getting close to 100%, but still having the water phase in the system (Figure 20), which is the case for our experiment number 6, the equation becomes:

$$I = CI_0 \tau_{sw}^{2k} \tau_{wD}^{2k(1-S)} \exp(-k\alpha_s d_s - k\alpha_D d_s) \quad (5.2)$$

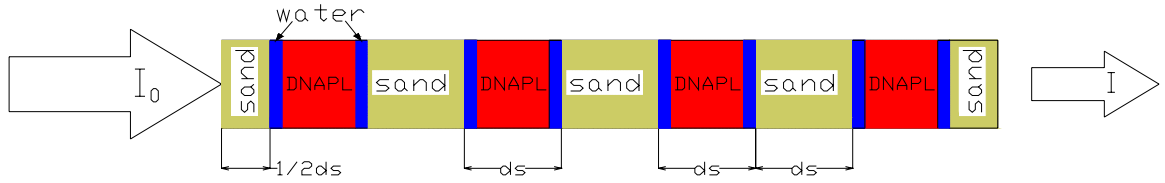


Figure 20: Physical based model for multiphase system: sand – water – DNAPL; for a water saturation close to 0%.

In the case where DNAPL saturation is 100% (Figure 21), so for a water saturation $S = 0\%$, as in the case of experiment 7a and 7b, equation (5.1) becomes:

$$I = CI_0 \tau_{sD}^{2k} \exp(-k\alpha_s d_s - k\alpha_D d_s) \quad (5.3)$$

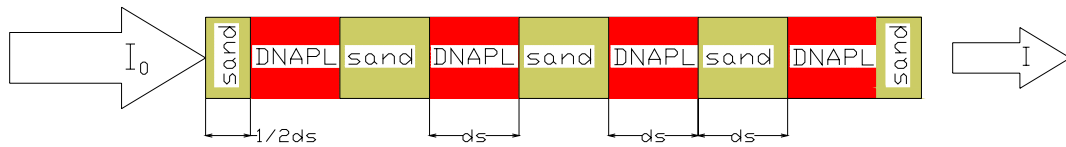


Figure 21: Physically based model for multiphase system: sand-DNAPL

Comparing equation (5.2) and (5.3) it is seen that the sand-water and water DNAPL transmission factors are missing. The lack of the water interfaces has a very strong effect leading to huge differences in the expected and obtained color attributes. For example, for Green color attribute in Figure 18, the color value for 100% DNAPL saturation is the same as the one corresponding to 17% saturation.

Remark: The 100% DNAPL saturation curves will not be included in the future graphics of this study because, as it has been shown, they have a distinct behavior and are not relevant for building of a calibration curve.

5.4. HUE Color Attribute

In this subchapter will be shown that *hue* is not a good color attribute to be used in the calibration of the light transmission method.

Important remark: For the interpretation of the graphics the size of the interval of the color attribute for the different saturations at a given F-number should be considered.

In the works of Darnault [1997, 2001], the calibration curve obtained in their experiment related hue and water content, and also intensity and total liquid content (water and oil respectively for their case). Instead of coloring the water we used colored DNAPL. Two analyses, that will be presented in this subchapter, have been performed: one showed the variation of the *hue* color

attribute as a function of F-number, the other presented the variation of the *hue* color attribute with the DNAPL saturation.

5.4.1. Variation of Hue color attribute as a function of F-number for a given DNAPL saturation and different exposure times

As can be seen from Figure 22 - Figure 27 the hue value is 0 for small F-numbers has a steep increase and remains almost constant for the rest of the F-numbers.

The *white balance* mode determines the value of the hue color attribute for the same exposure time and F-number.

Another important remark is that the behavior of the *Hue-F-No* curves is not similar in all six DNAPL saturations graphics, and it is sometimes oscillating.

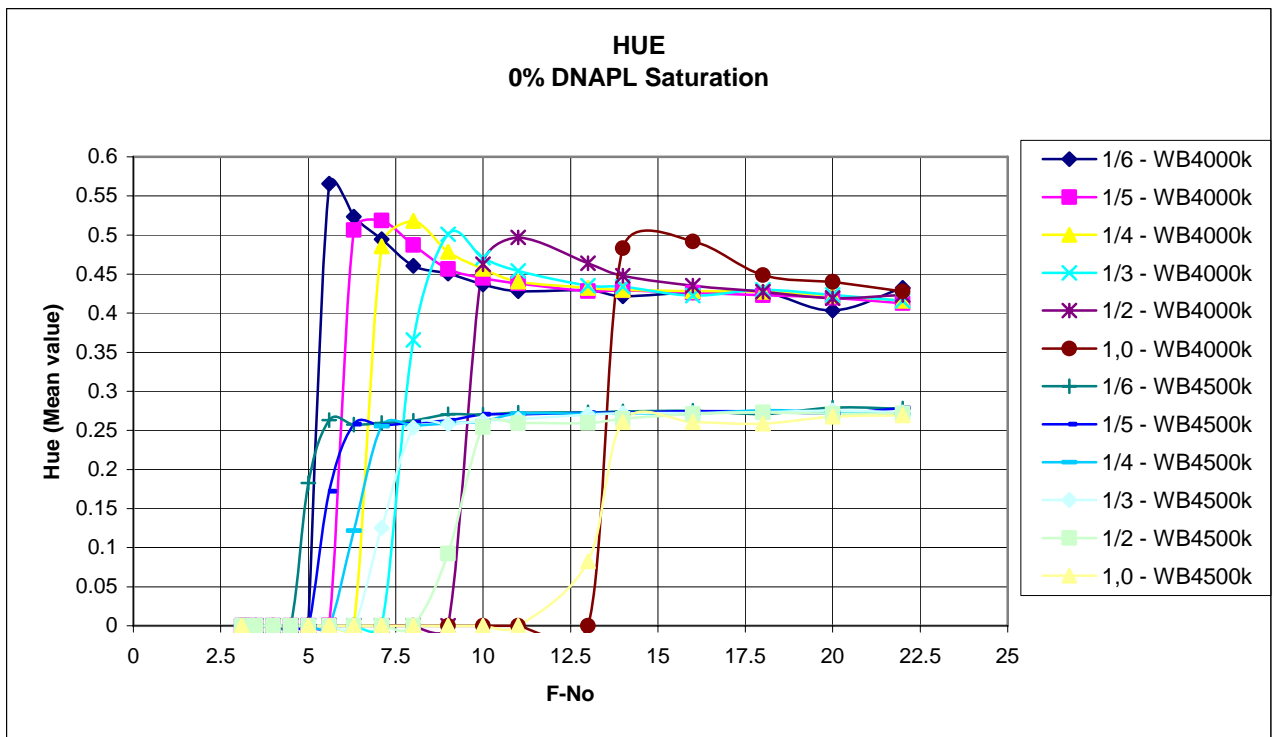


Figure 22: Variation Hue – F-Number for 0 % DNAPL saturation and different exposure times

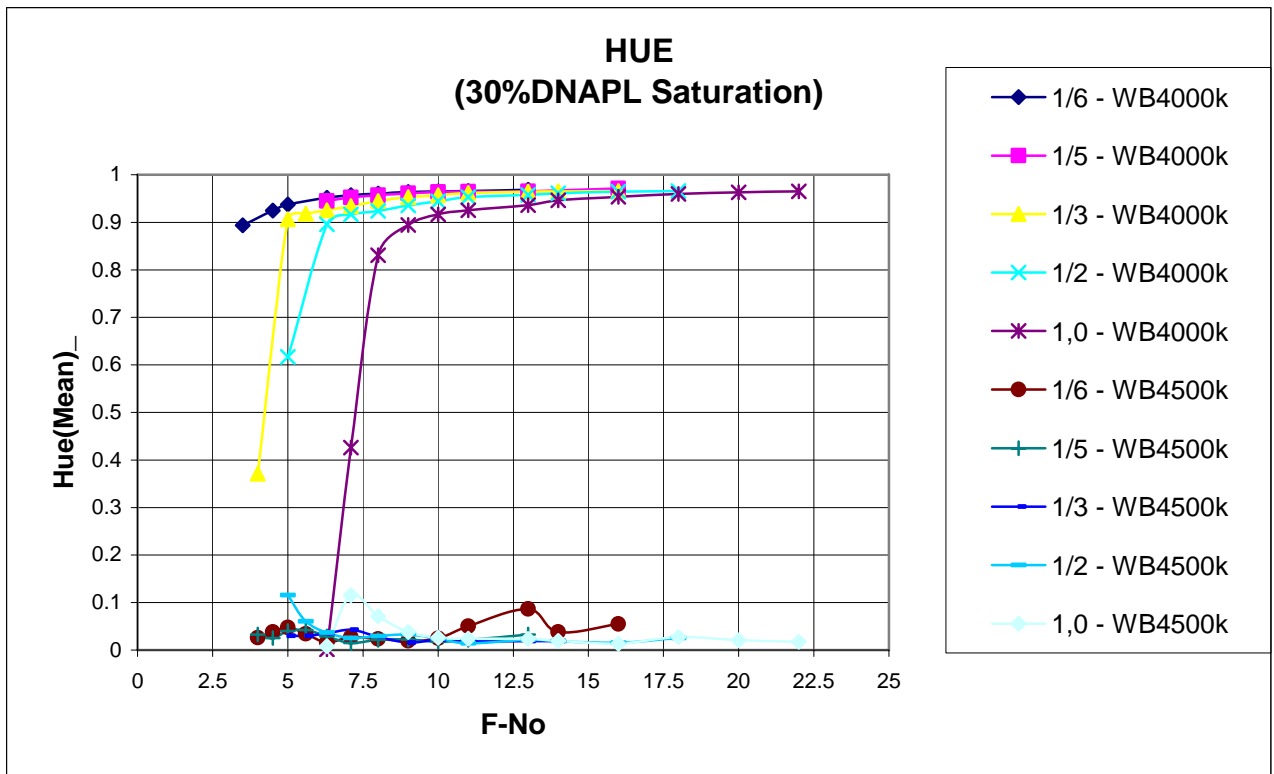


Figure 23: Variation Hue – F-Number for 30 % DNAPL saturation and different exposure times

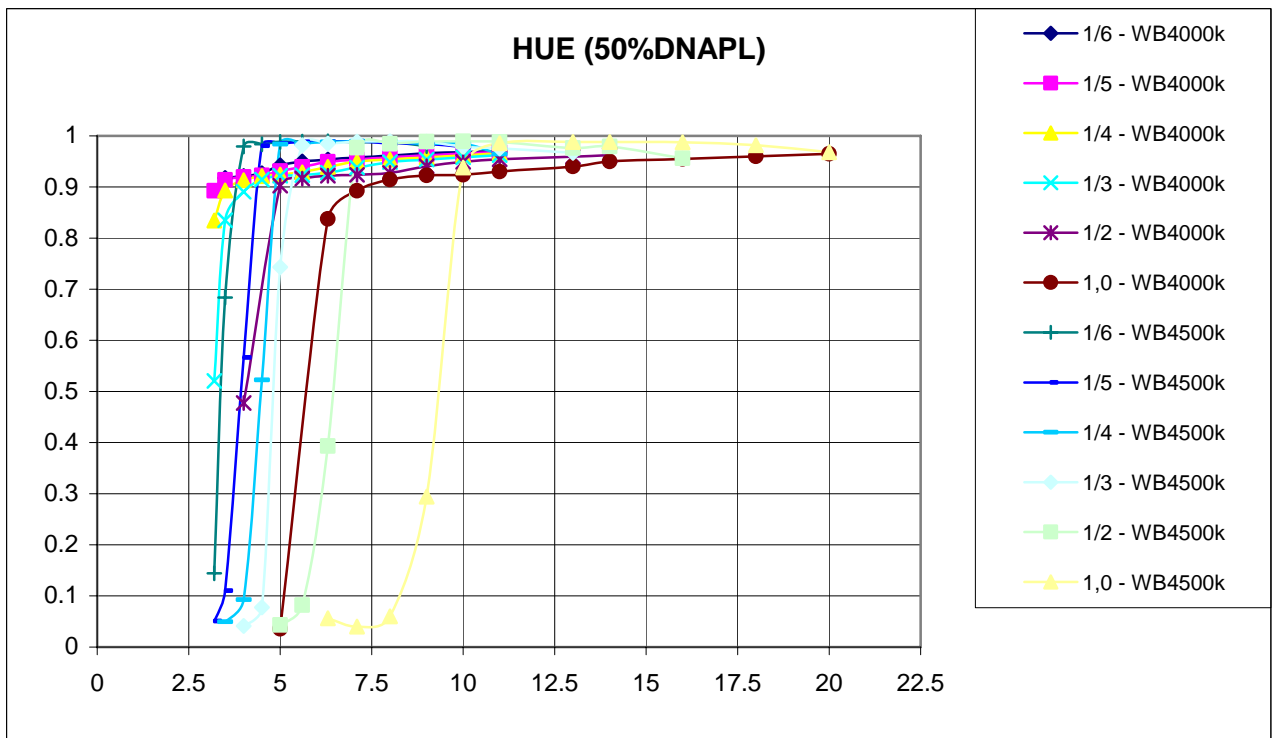


Figure 24: Variation Hue – F-Number for 50 % DNAPL saturation and different exposure times

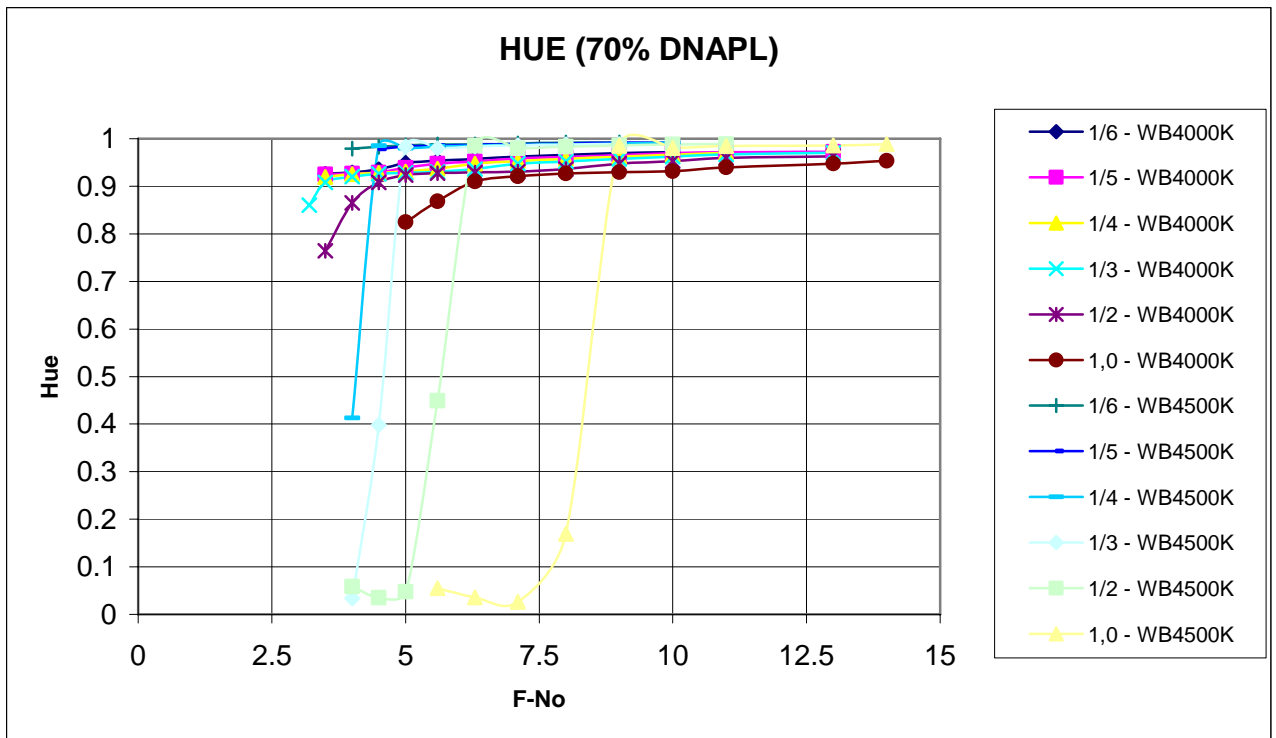


Figure 25: Variation Hue – F-Number for 70 % DNAPL saturation and different exposure times

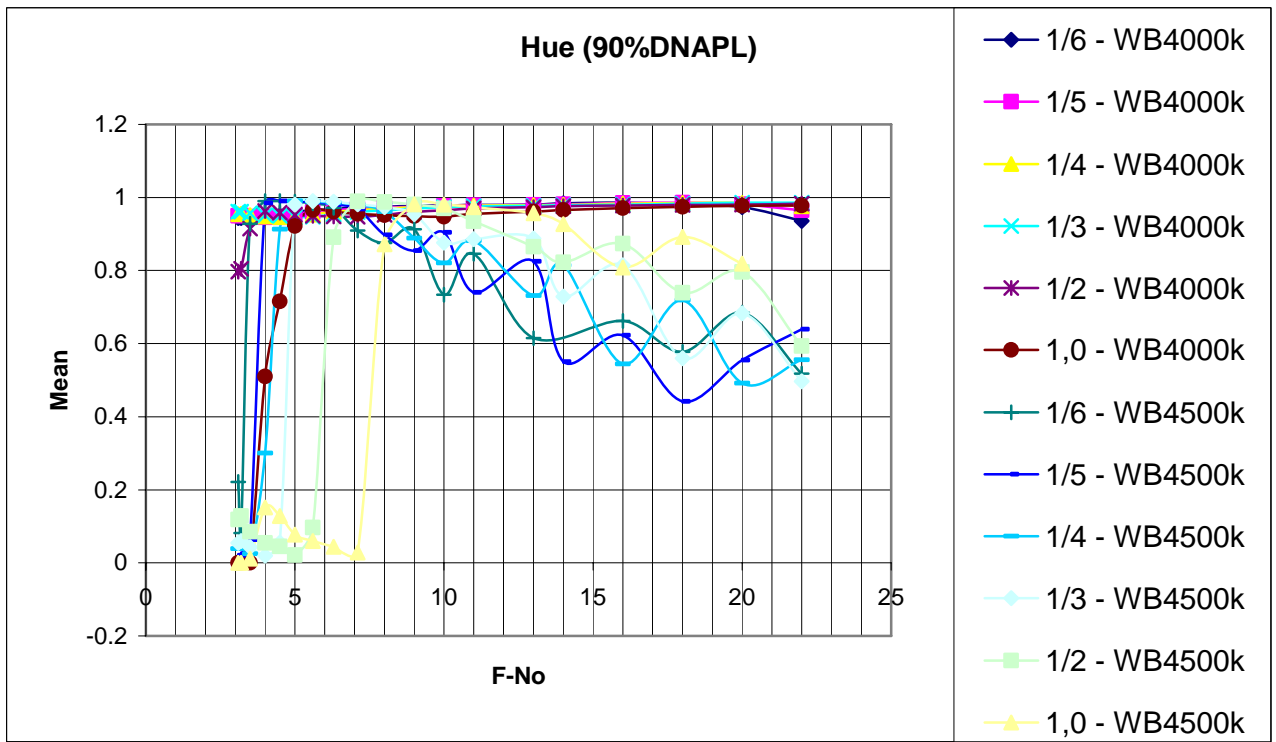


Figure 26: Variation Hue – F-Number for 90 % DNAPL saturation and different exposure times

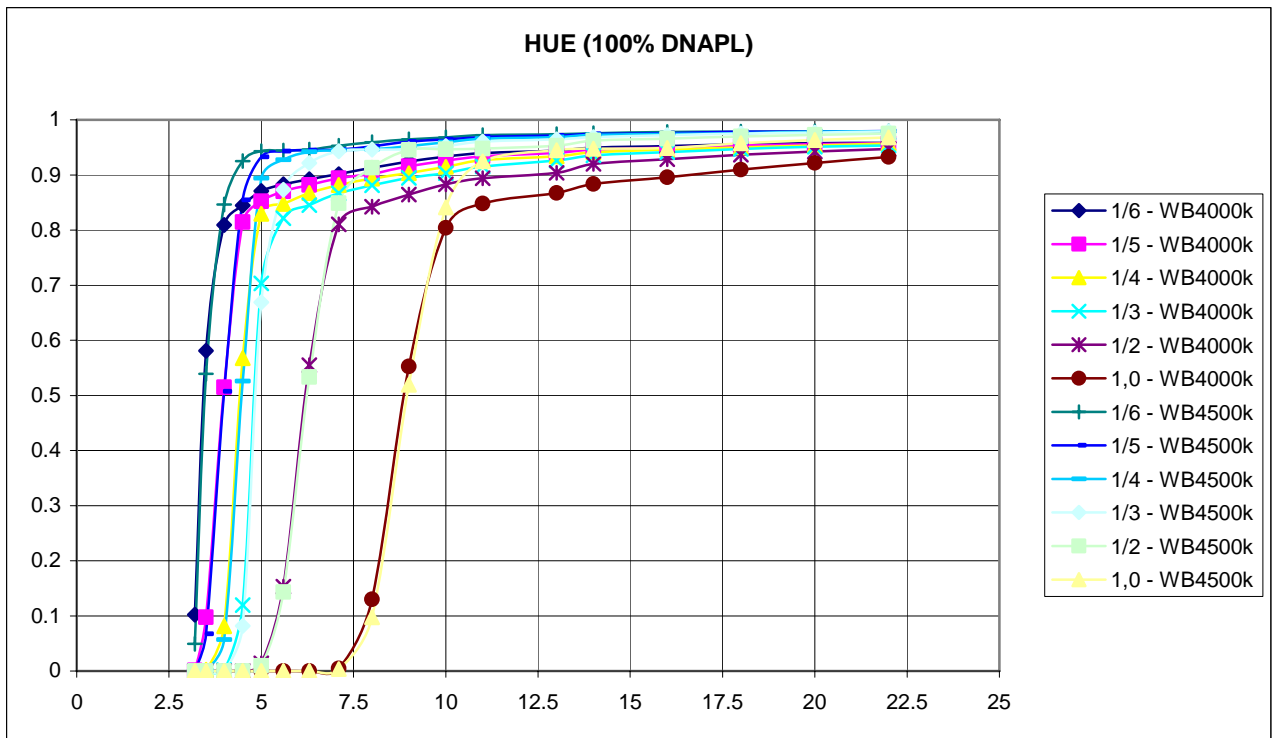


Figure 27: Variation Hue – F-Number for 100 % DNAPL saturation and different exposure times

The oscillations and the different behavior of *hue-F-No* curves have the consequence that the method is not reliable for the whole range of DNAPL saturations or other F-number exposure time configurations.

5.4.2. Variation of Hue color attribute with DNAPL saturation

In Figure 28 it is seen that the variation of the *hue* color attribute with the change in liquid saturation is very small, almost zero between 30 to 90 percent saturations. Similar profile curves are obtained for other F-numbers and exposure times. This means that for small changes in hue value there can be big changes in DNAPL saturation.

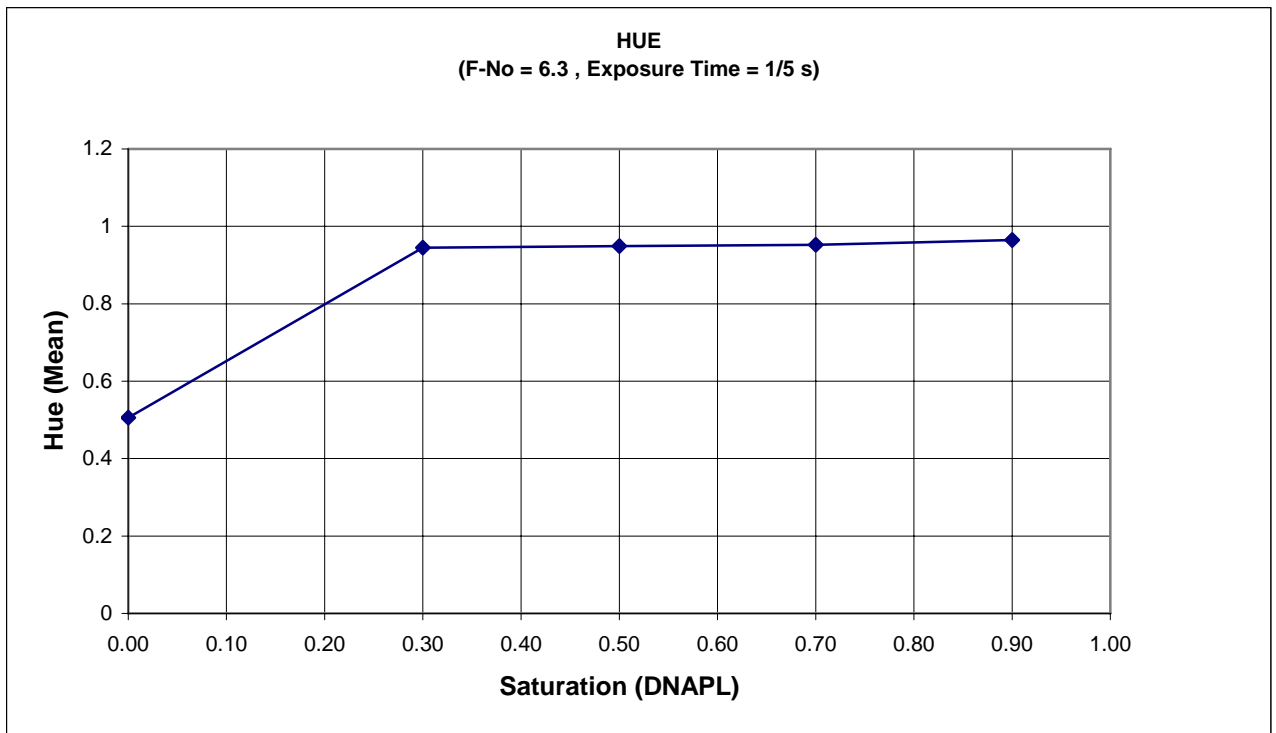


Figure 28: The variation of Hue with DNAPL saturation for a given F-Number and Exposure time

Remark: Due to its insensitivity to saturation the *hue* is not considered in comparison with other color attributes and will not be plotted from now in order to avoid overloading.

5.5. Saturation Color Attribute

In this chapter the *saturation* color attribute is analyzed with regard to its variation with the F-number and the DNAPL saturation.

Saturation color attribute can be used for calibration of the light transmission method but only for specific camera settings. In the following it will be shown that *saturation* is not a good color attribute to be used for building a calibration curve.

5.5.1. Variation of Saturation color attribute as a function of F-number for a given DNAPL saturation and different exposure times

Important remark: When reading the graphics it is not important to compare the values pointwise but to see the graphic's sensitivity (how the curves succeed by the variation of exposure time or the liquid saturation)

The main idea of this subchapter is that *saturation* color attribute strongly depends on the *WB Mode* and besides this it has a strong non-linear behavior depending on the different DNAPL saturations which make *saturation* not an appropriate color attribute to be used for LTM calibration.

From Figure 29 to Figure 33 it can be learned that the general behavior of the *Saturation* color attribute is that it increases with the increase of the F-number. On the other hand, the same color attribute value can be obtained for different F-numbers and exposure times.

Looking at the order of the curves in Figure 29 the curve corresponding to an exposure time of 1/6 seconds and a white balance WB4500k has the steepest slope and covers the widest range of saturation values followed by the curves with the white balance WB4500k. Only after WB4500 curves come the ones with WB4000k.

The order of the curves remains not the same so for the other DNAPL saturations the 1/6 seconds exposure time and WB4500k curve is not anymore the steepest.

Also the shape of the *Saturation* color attribute – F-number curves is changing for different DNAPL saturations and it is influenced by the white balance mode and sometimes they overlap.

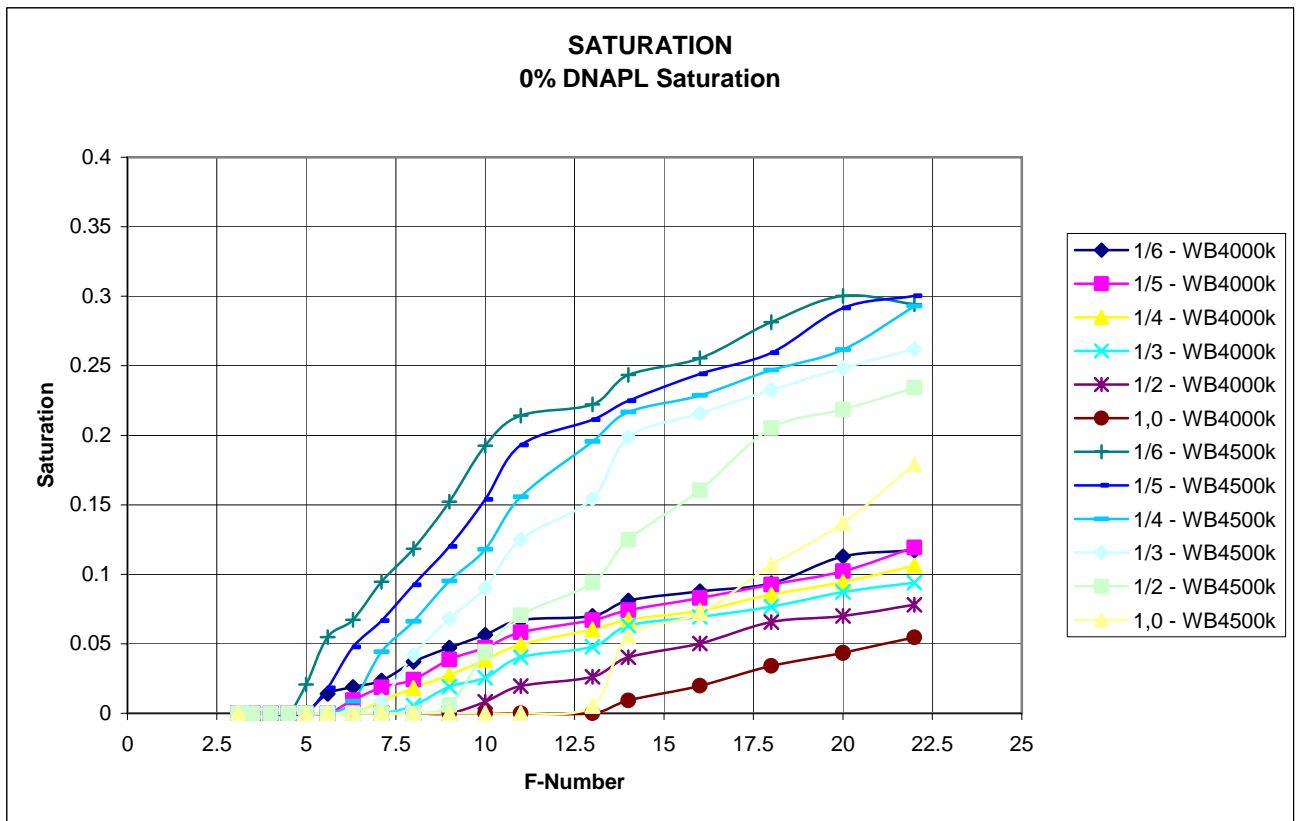


Figure 29: Variation of Saturation color attribute – F-Number curves for 0 % DNAPL saturation and different exposure times

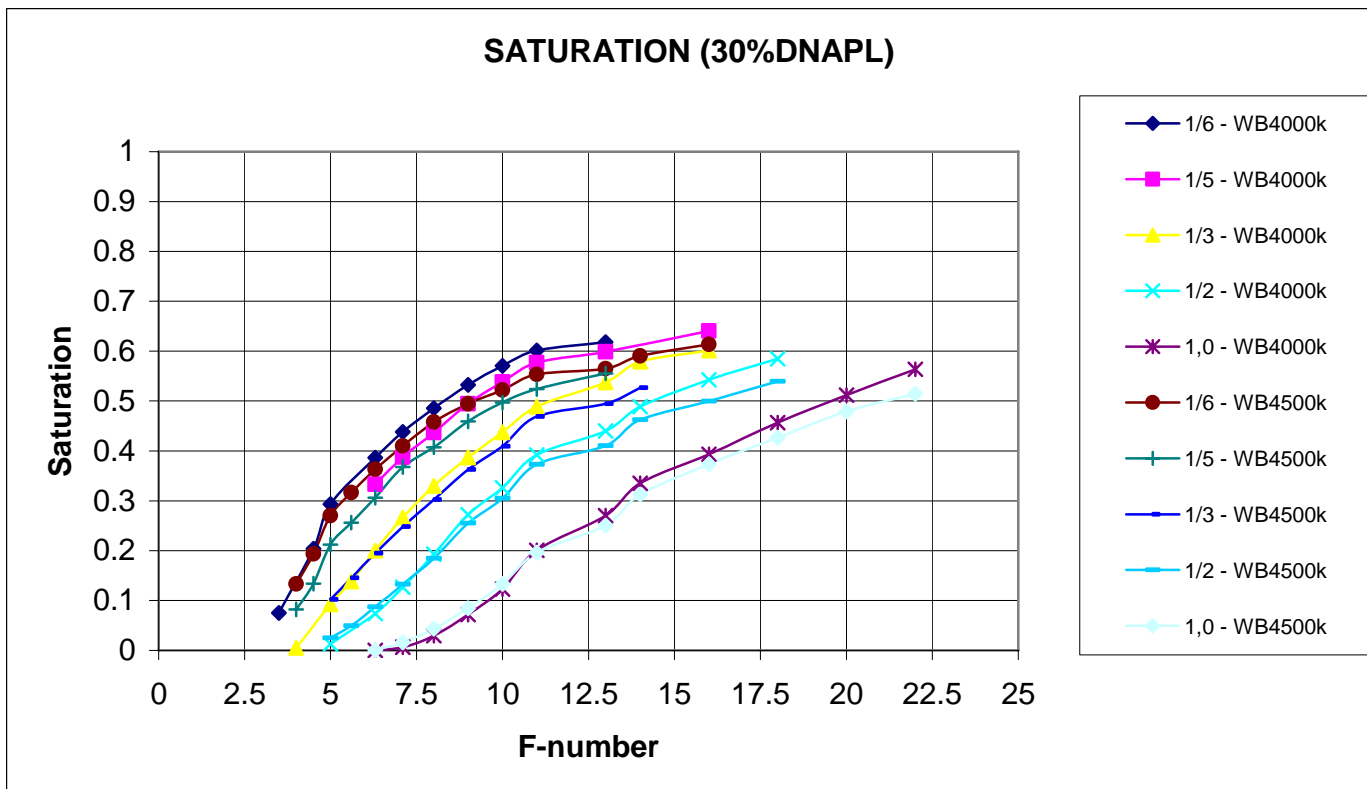


Figure 30: Variation of Saturation color attribute – F-Number for 30 % DNAPL saturation and different exposure times

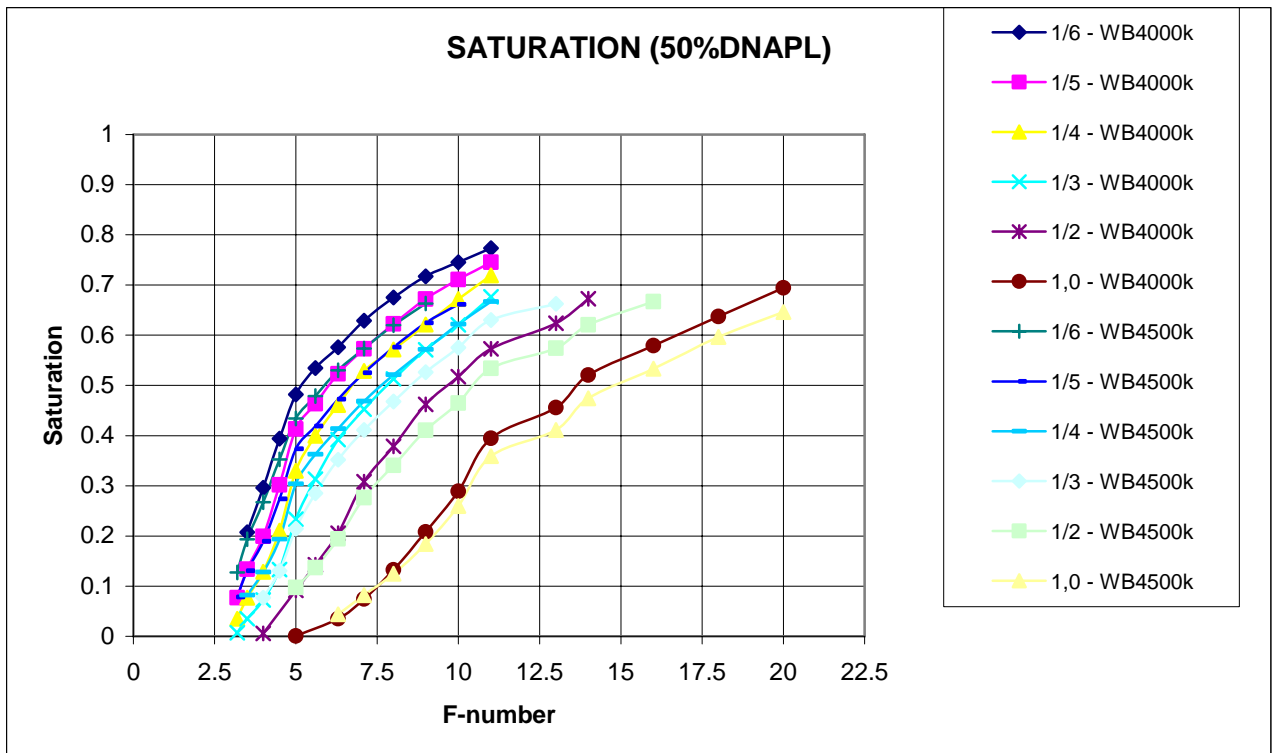


Figure 31: Variation of Saturation color attribute – F-Number for 50 % DNAPL saturation and different exposure times

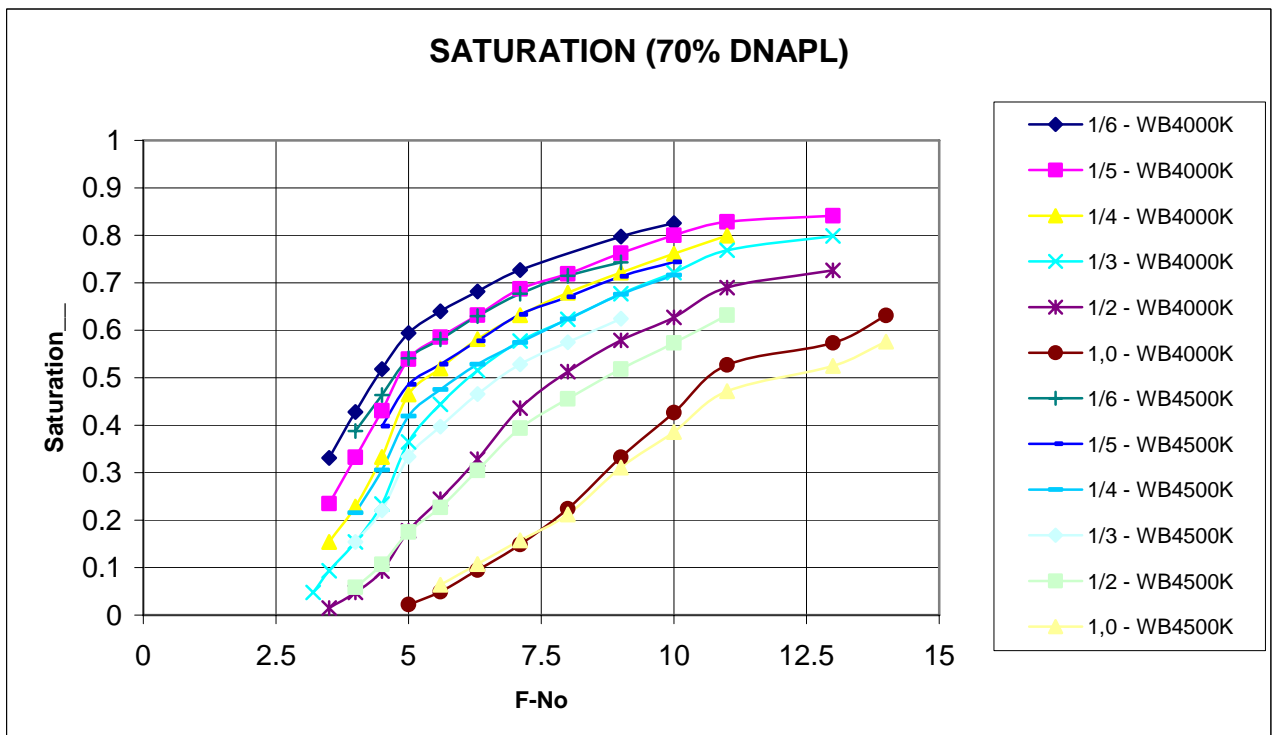


Figure 32: Variation of Saturation color attribute – F-Number for 70 % DNAPL saturation and different exposure times

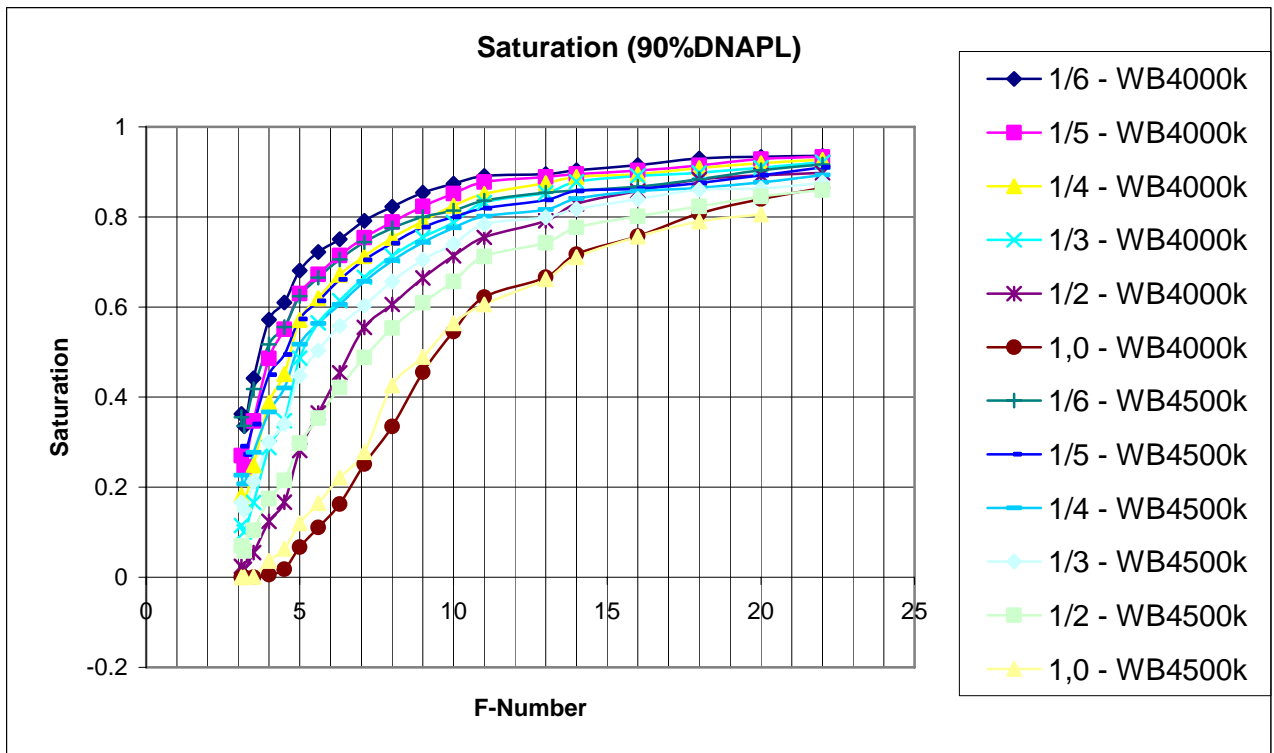


Figure 33: Variation of Saturation color attribute – F-Number for 90 % DNAPL saturation and different exposure times

5.5.2. Variation of Saturation color attribute with DNAPL saturation

Figure 34 depicts the *Saturation* color attribute curve plotted with DNAPL saturation for a given exposure time and F-number. The shape of the curve looks good and can be used for calibration. Still when using different combinations of F-numbers, exposure times and white balances we can get misleading results (Figure 35)

Considering constant exposure time 1/6seconds and white value WB=4000k the “Color Saturation – F-Number” curves plotted for different DNAPL saturations have a strong increase in slope for DNAPL saturations smaller than 50% but then they tend to overlap. The 70% and 90% DNAPL saturation curves are almost coinciding. This leads to difficulties in interpreting the pictures and in developing a calibration curve based on color *saturation*.

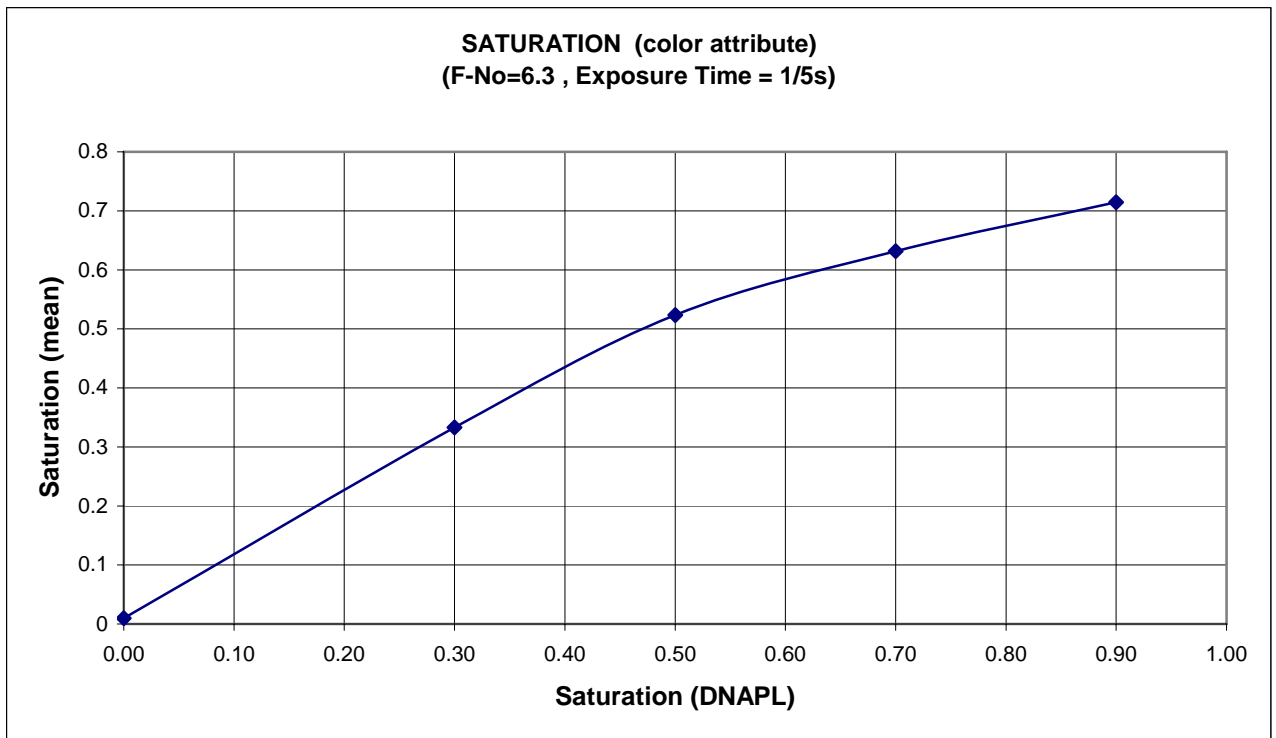


Figure 34: Variation of Saturation color attribute with DNAPL saturation for given F-No 8.3 and exposure time – 1/6 seconds

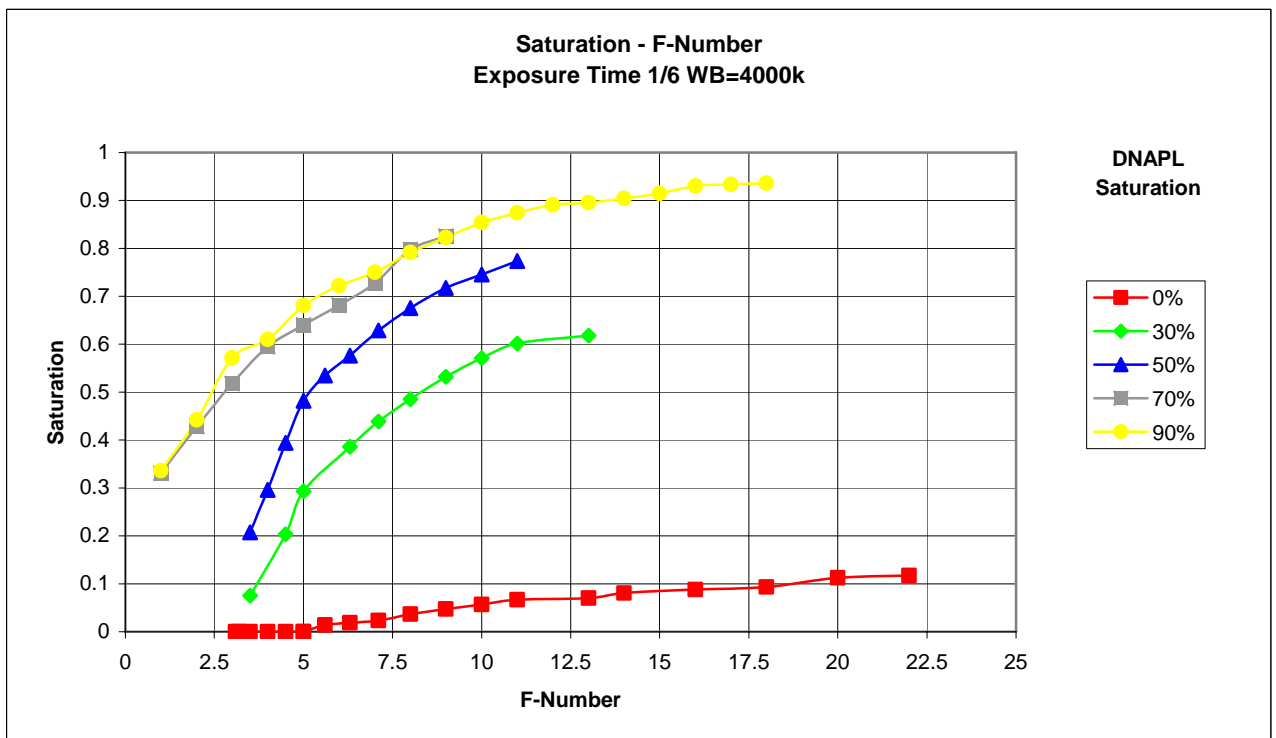


Figure 35: Variation of Saturation color attribute with F-number for different DNAPL saturations

5.6. RED Color Attribute

In this chapter shows that from the remaining color attributes *Red* has the smallest range of color units (when talking about the values resulted from 0%DNAPL saturation to 90% DNAPL saturation, while the color range itself is from 0 to 255) and therefore is not worth to be used for deriving a calibration curve.

5.6.1. Variation of RED color attribute as a function of F-number for different DNAPL saturations

From Figure 36 it can be observed that between all curves corresponding to DNAPL saturations from 0 to 90 percent the average differences are very small and that the curves are almost parallel to each other without overlapping. The corresponding curve for 90% DNAPL saturation is located beneath the others and the one corresponding to 0% is at the top. With the increase in the DNAPL saturation the curves succeed one under the other.

For different time exposures and white balance values the profile of the curves remains similar to the one in Figure 36 and the order in which they succeed is the same. Other examples are given in the Appendix.

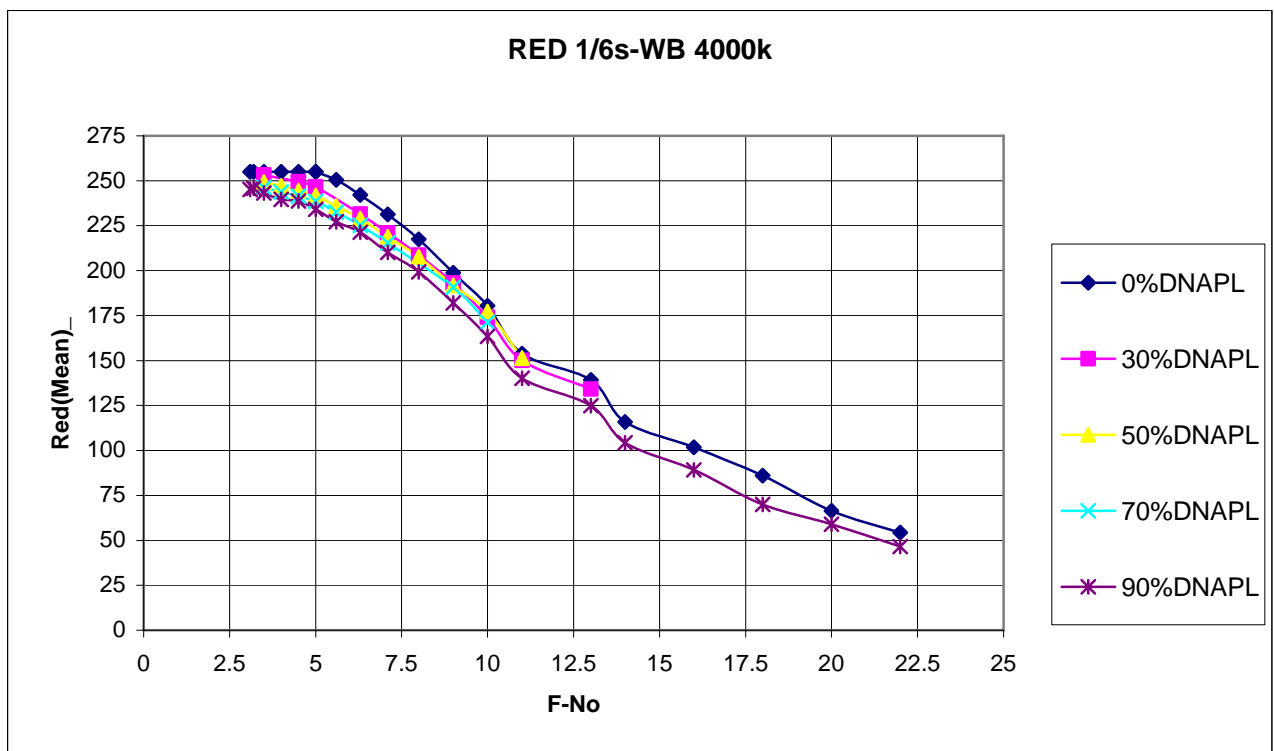


Figure 36: Red – F-No curves for 0, 30, 50, 70, 90% DNAPL saturation, for 1/6 seconds exposure time and white balance WB4000k

5.6.2. Comparison between RED color attribute as a function of F-number and the other color attributes

From Figure 37 it can be concluded that *Red* color attribute curve can be used as calibration factor for determination of the saturation in the porous media, nevertheless, when compared to the other color attributes it is not a good indicator because the difference between the red values corresponding to 0% and 100% DNAPL saturation (or the red color contrast) are the smallest.

The values of *red* color attributes are the highest for all range of F-numbers at the same exposure times and white balances and all the range of DNAPL saturations (Figure 37, Figure 38). From equation (2.12) *value* color attribute is defined as the maximum between *red*, *blue* and *green* color attributes. Due to this the *Red* color attribute and the *Value* color attribute curves are exactly the same.

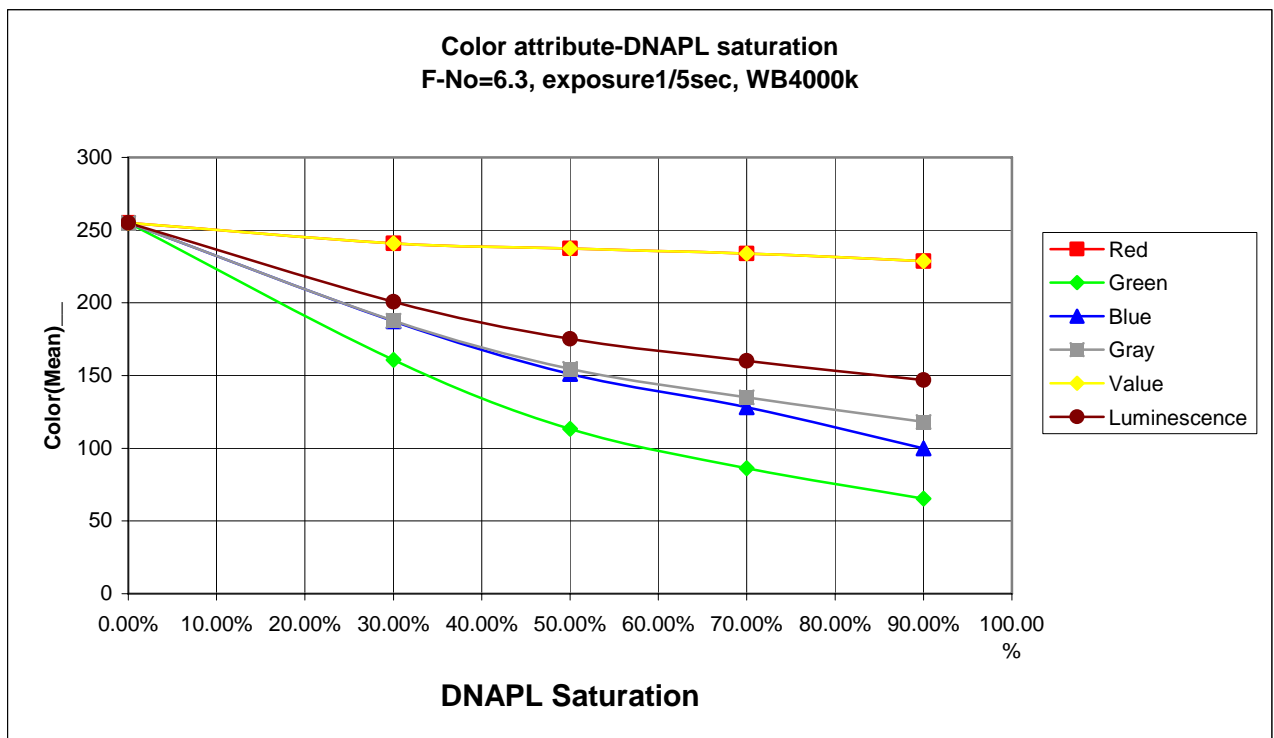


Figure 37: Comparison of the variation of the different color attributes with DNAPL saturation for F-number 6.3, 1/5 seconds exposure time and white balance WB4000k

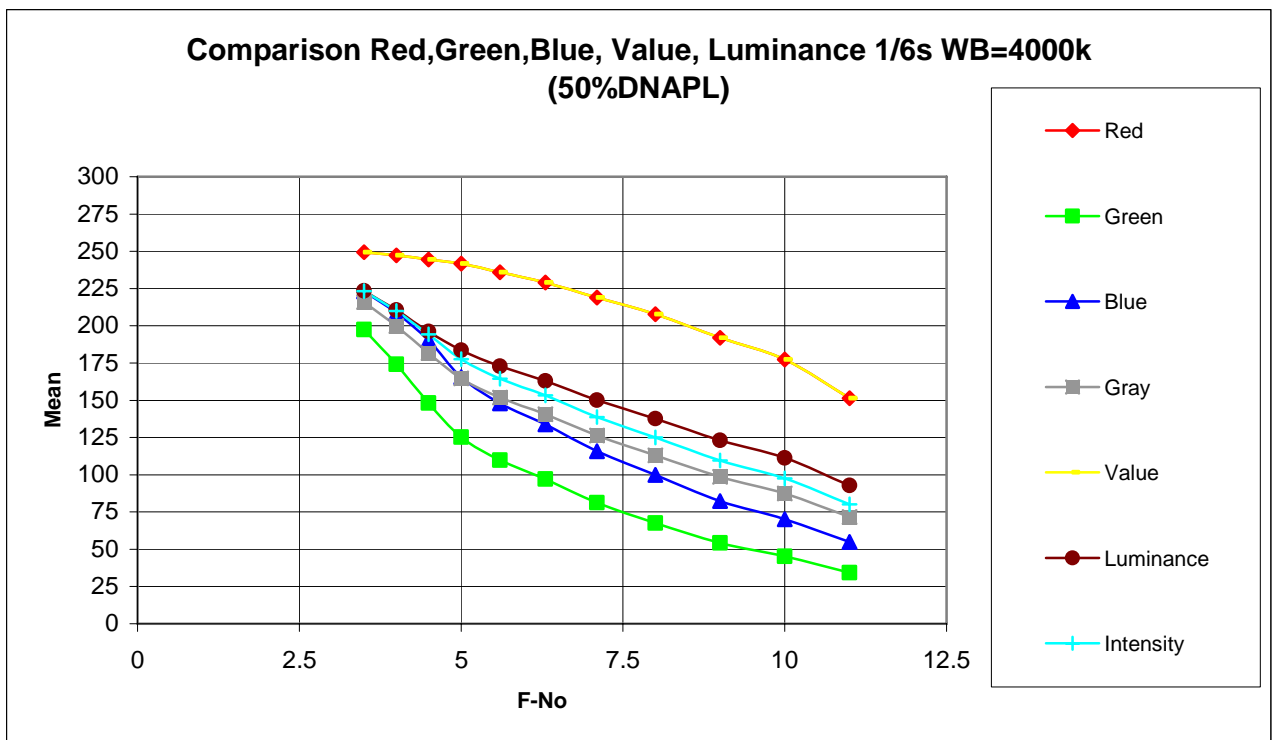


Figure 38: “Color attributes – F-No” curves plotted for 50%DNAPL saturation, 1/6 seconds exposure time and white balance WB4000k

Having the narrowest range of values for the *Red* and *Value* color attributes determines not to be further discussed. For other dyestuff color this conclusions should be reevaluated as *red* color attribute can have a totally different behavior in that situation.

5.7. Comparison of the different color attributes as function of F-number and white balance mode

Red, Green, Blue, Gray, Luminance, Value and *Intensity* color attributes have the same range of values, from 0 to 255 and can be compared on the same scale using the same graphics.

For different F-numbers we can get the same value of color attribute which means that the camera parameters have a strong influence on light transmission method calibration.

Important remark: When reading the graphics it is not important to compare the values pointwise but to see the graphic's sensitivity and what the order of succession for the curves is.

A comparison between all color attribute curves is shown in Figure 39 to Figure 43 for a fixed exposure time of 1/6 seconds, a white balance mode WB4000k for all DNAPL saturations.

Here we will present only the figures for white balance value of WB4000k.

For 0% DNAPL Saturation all the curves have only little deviation from each other. On the other hand, for 30, 50, 70, 90 and 100 percent DNAPL saturation we obtain the same sequence of the curve as depicted in Table 8; starting with *Green* the lower and following going upwards: *Blue, Gray, Intensity, Luminance, Value* and *Red*.

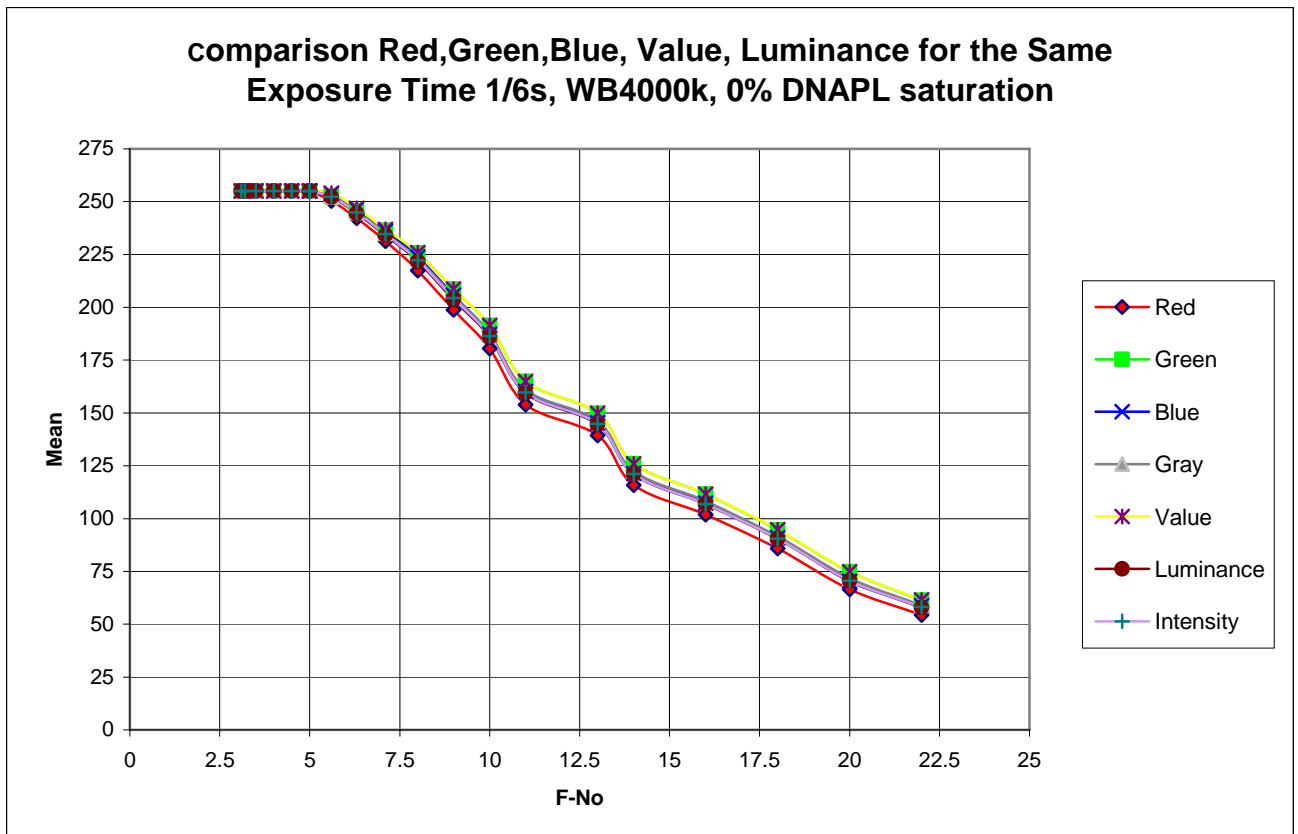


Figure 39: Comparison of the Color attribute – F-number curves for a 1/6 seconds exposure time, WB4000k plotted for 0% DNAPL saturation

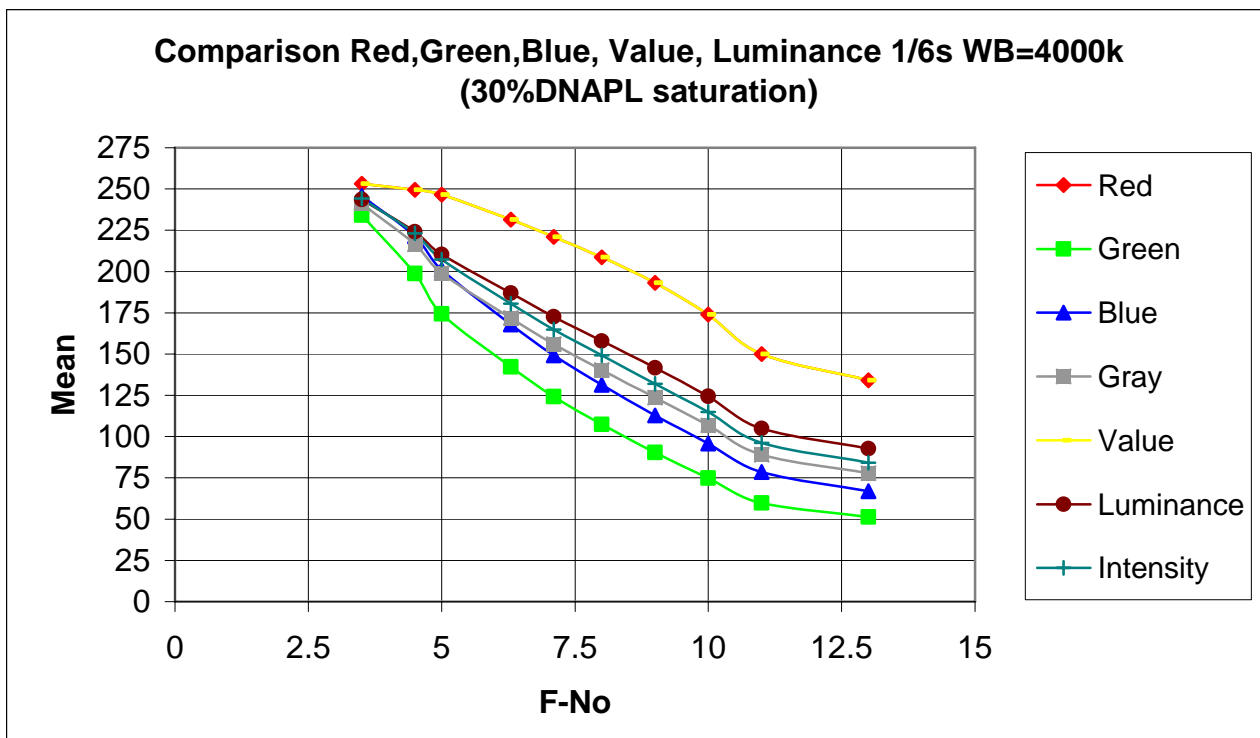


Figure 40: Comparison of the Color attribute – F-number curves for a 1/6 seconds exposure time, WB4000k plotted for 30% DNAPL saturation

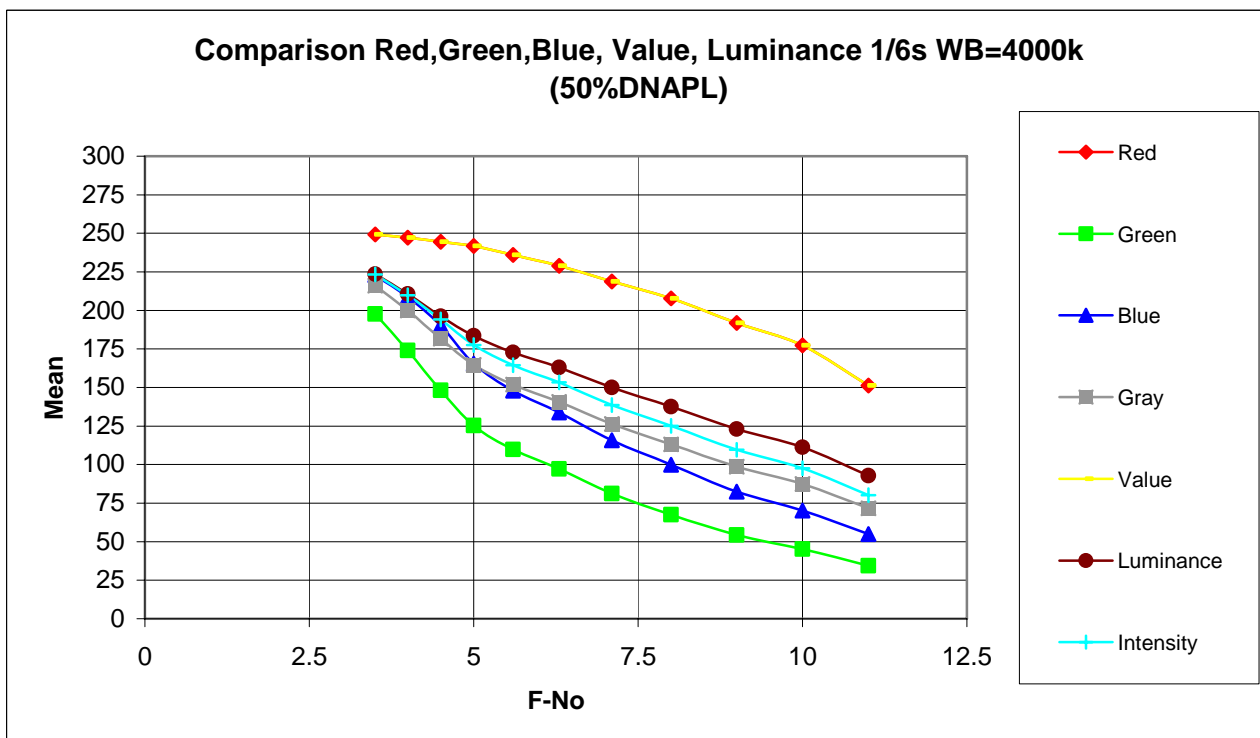


Figure 41: Comparison of the Color attribute – F-number curves for a 1/6 seconds exposure time, WB4000k plotted for 50% DNAPL saturation

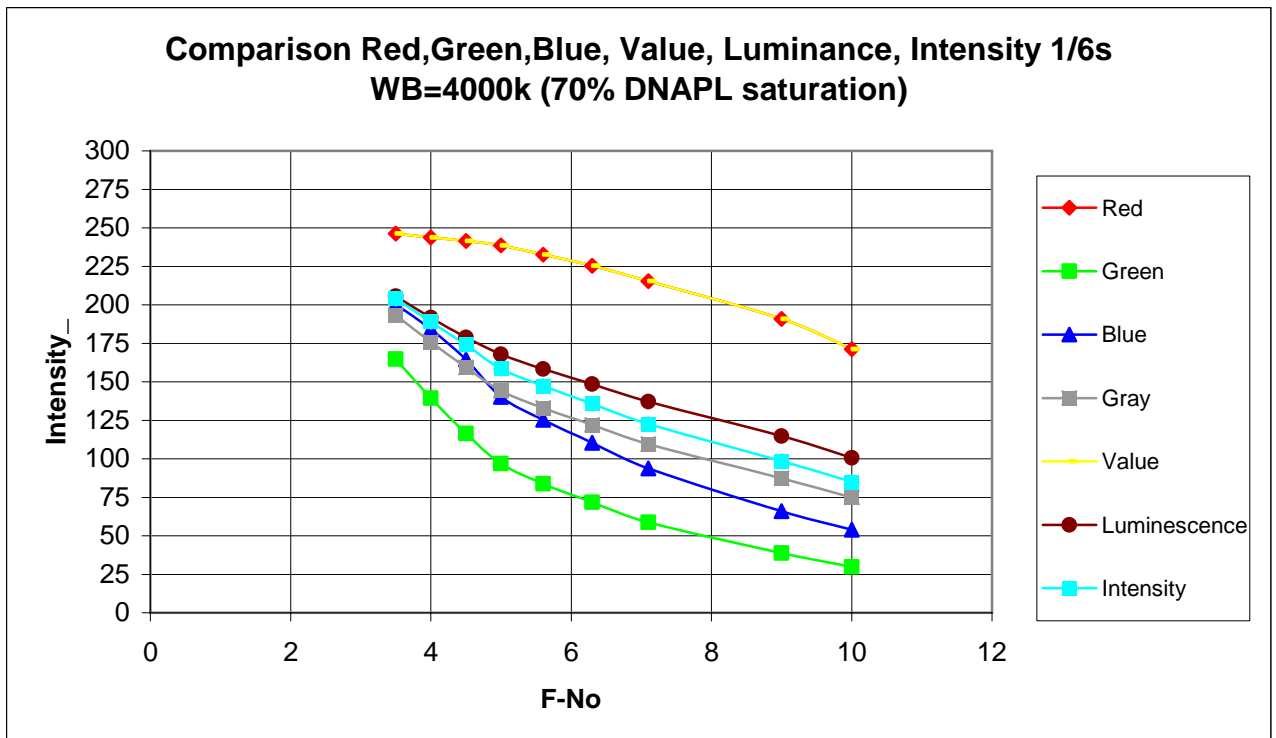


Figure 42: Comparison of the Color attribute – F-number curves for a 1/6 seconds exposure time, WB4000k plotted for 70% DNAPL saturation

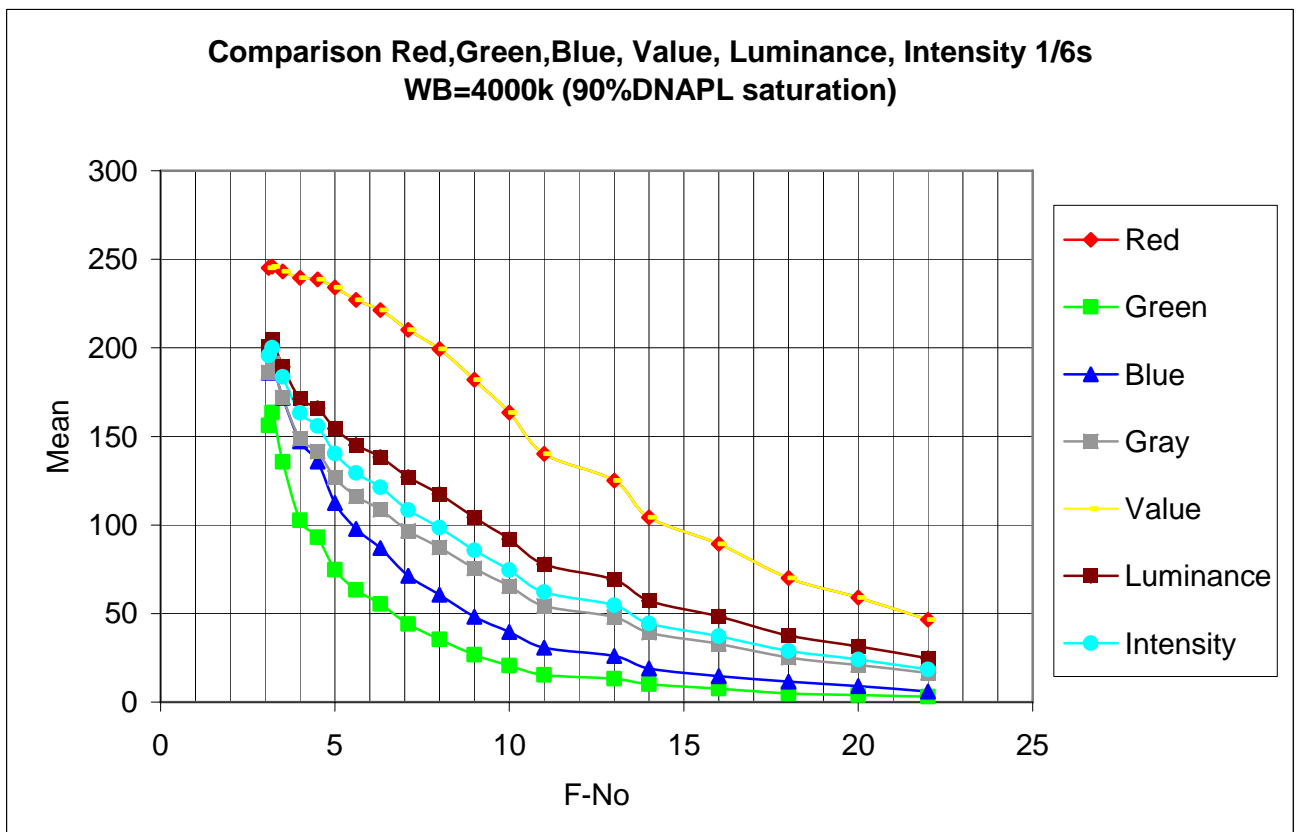


Figure 43: Comparison of the Color attribute – F-number curves for a 1/6 seconds exposure time, WB4000k plotted for 90% DNAPL saturation

For both WB modes tested in our experiments Fluorescent 1 (WB = 4000k) and Fluorescent 2 (WB = 4500k) we obtained as **best curves for interpretation green, blue and gray**.

Table 8 Curve order in the graphic “Color Attribute (Mean) – F-No”

0% DNAPL	30% DNAPL	50% DNAPL	70% DNAPL	90% DNAPL	100% DNAPL
1 Red	1=2 Green	Green	Green	Green	Green
2 Blue	1=2 Blue	Blue	Blue	Blue	Blue
3 Luminance	3=4=5 Gray	Gray	Gray	Gray	Gray
4 Intensity	3=4=5 Intensity	Intensity	Intensity	Intensity	Intensity
5 Gray	3=4=5 Luminance	Luminance	Luminance	Luminance	Luminance
6 Green	6=7 Value	6=7 Value	6=7 Value	6=7 Value	6=7 Value
7 Value	6=7 Red	6=7 Red	6=7 Red	6=7 Red	6=7 Red

(Obs: in the intermediate columns noted i.e. 1=2 means that the curve 1 is the same as 2 or 3=4=5 curve number 3 is the same as 4 and 5. On the first column for 0% DNAPL Red is the same as Blue curve and Luminance the same as Intensity and Gray. The curves are arranged starting with the steepest one and going decreasingly till the less steep)

The exposure time has an influence over the position of the curves relative to each other and over their slopes but it doesn't change the order they succeed for all our six selected intervals (1/6, 1/5, 1/4, 1/3, 1/2, 1).

The table with the color attribute-F-number curve succession plotted for each DNAPL saturation is given in the Appendix.

5.8. Variation of the color attributes (Green, Blue, Gray, Luminance, Intensity) averaged for all DNAPL saturations with the F-number and exposure time

Until now we have eliminated *hue, saturation, red* and *value* color attributes as they are not good for building a calibration curve. The remaining color attributes have to be analyzed further on in greater detail.

Because some curves behave good for a certain range of DNAPL saturations and bad for other ranges the overall behavior has to be somehow quantified and they have to be compared in only one graphic.

We have seen from the comparison of the different *color attributes* when plotted with the *F-No* (see section 5.7) that the curves keep the same order in the graphic for all the saturations. It is much easier to see the order of the curves if we could express it in only one graphic.

For this we chose an exposure time 1/6s and a white balance of 4000k and we plotted the averaged color attribute values with F-number averaged for all six saturations (0%, 30%, 50%, 70%, 90%). The result can be seen in Figure 44.

For each F-number a color attribute value corresponds (i.e. F=6.3, Green (0%DNAPL)= 245.87, Green (30%DNAPL)= 142.22, Green (50%DNAPL)= 97.09, Green (70%DNAPL)= 71.80, Green (90%DNAPL)= 55.36) . Averaging these values for each F-number and each color attribute and plotting them results in Figure 44.

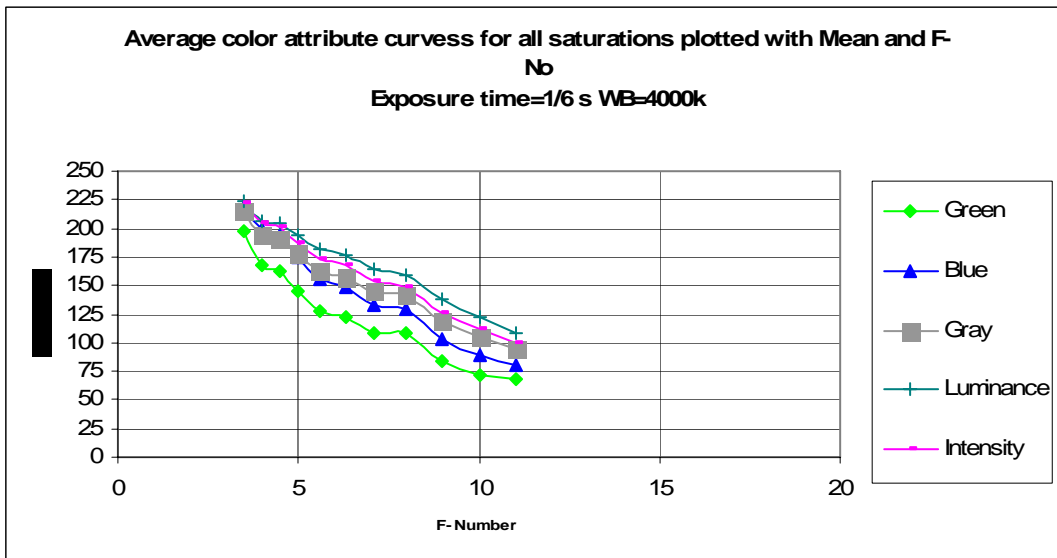


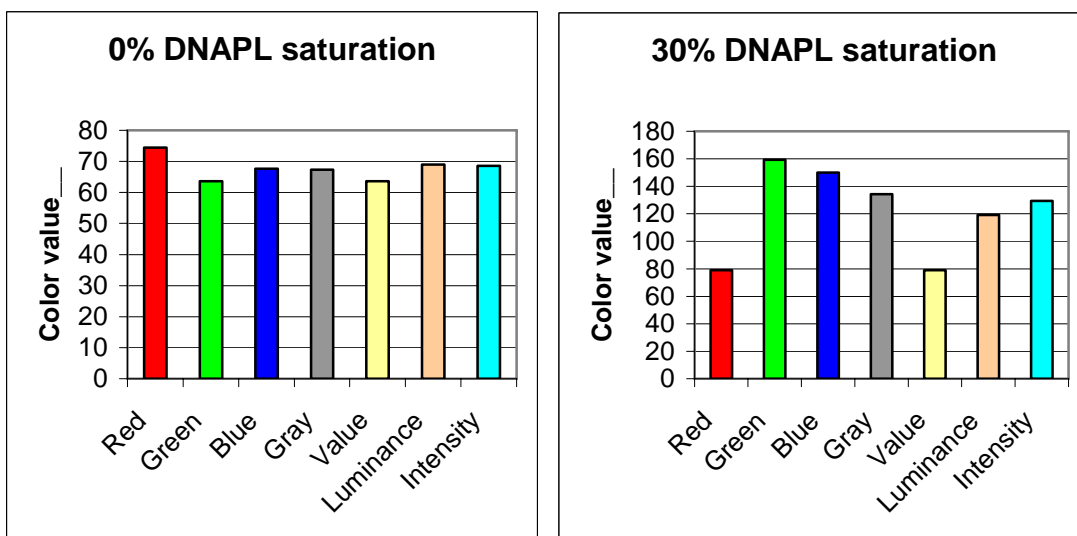
Figure 44: Color attributes averaged for all DNAPL saturation range plotted with F-number

All curves have a linear aspect and have almost the same slope. We only eliminated *Red* and *Value* color attributes which were the only ones that had a different slope and a smaller range of values for color.

5.9. Widest Color Attribute for a given range of F-Numbers

The color attribute with widest distribution for the same range of F-numbers has to be determined. The *red* and *value* color attributes are plotted just for comparison even it has been already shown that they are not going to be used (Figure 45).

Simply calculating the difference between the color attribute value for F-number 3.5 and 10 will give the F-number range.



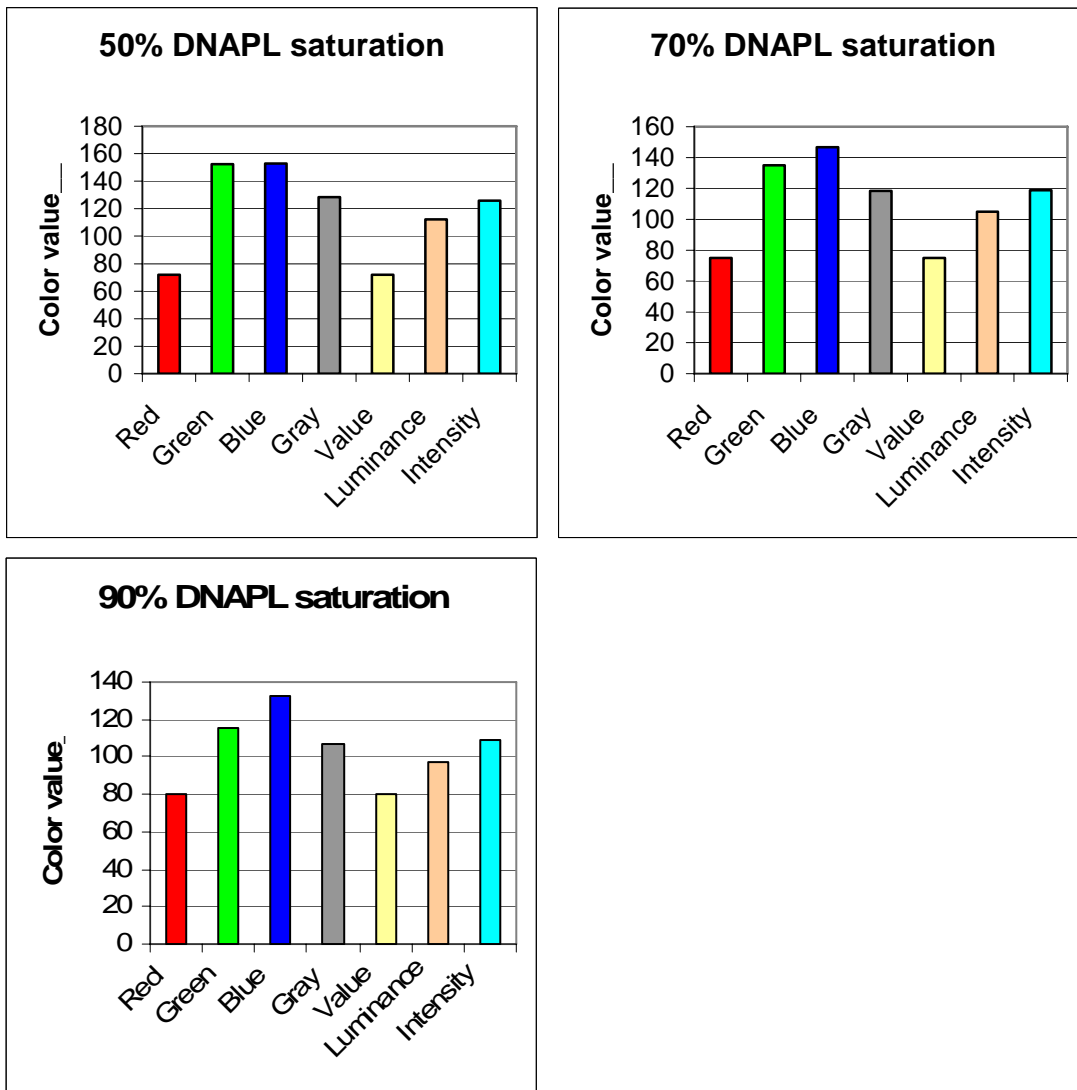


Figure 45: Variation of the color Contrast with the changing in the DNAPL saturation

From Figure 45 it is seen that the range of the different color attributes varies with the change in DNAPL saturation. By averaging the color ranges for all the saturation an overall range is being obtained. (Figure 46) In this case *blue* appears to be the best followed by *green*, *intensity*, *gray* and *luminance*.

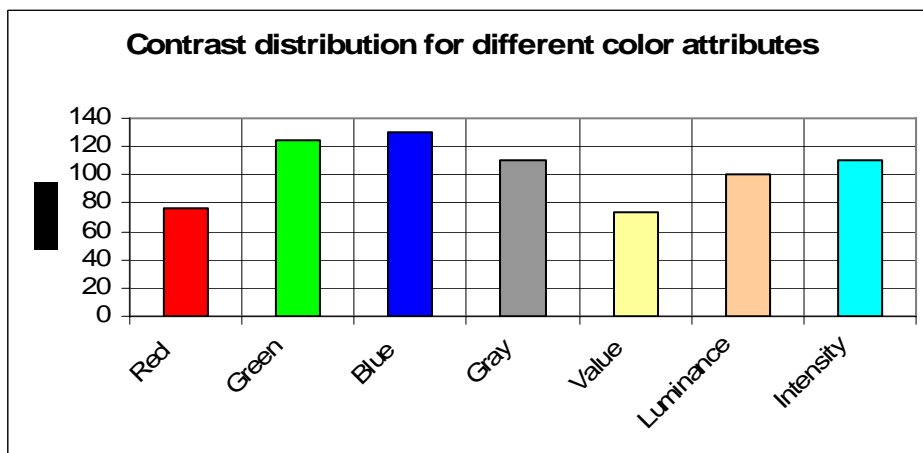


Figure 46 Comparison between averaged colors attribute ranges

5.10. Image contrast distribution for different color attributes

The measurement of saturation with either color attribute curve requires the achievement of a suitable image contrast. Contrast is defined as the difference between the color field transmitted through fully water saturated test media to that transmitted through the fully DNAPL saturated.

The previous statement is not completely correct because as we have seen in chapter 5.3 the 100% DNAPL saturation has a different behavior due to the lack of water-DNAPL interfaces. The threshold used as minimum color value was the one corresponding to 90% DNAPL saturation.

$$Contrast = CA(0\%) - CA(90\%) \quad (5.4)$$

CA(0%) – Color attribute value averaged at 0% DNAPL saturation

CA(90%) – Color attribute value averaged at 90% DNAPL saturation

Obs: The color attribute value averaged (i.e. green) is the color attribute obtained after averaging all of the pointwise values of the respective color attribute (from each pixel) in the representative area taken from the picture.

In Figure 47 the variation of the color contrast with F-number is plotted for an exposure time of 1/6 seconds and a white balance WB4000k. The maximum values of contrast are obtained for all contrast curves for a F-number value between 6.3 and 8.

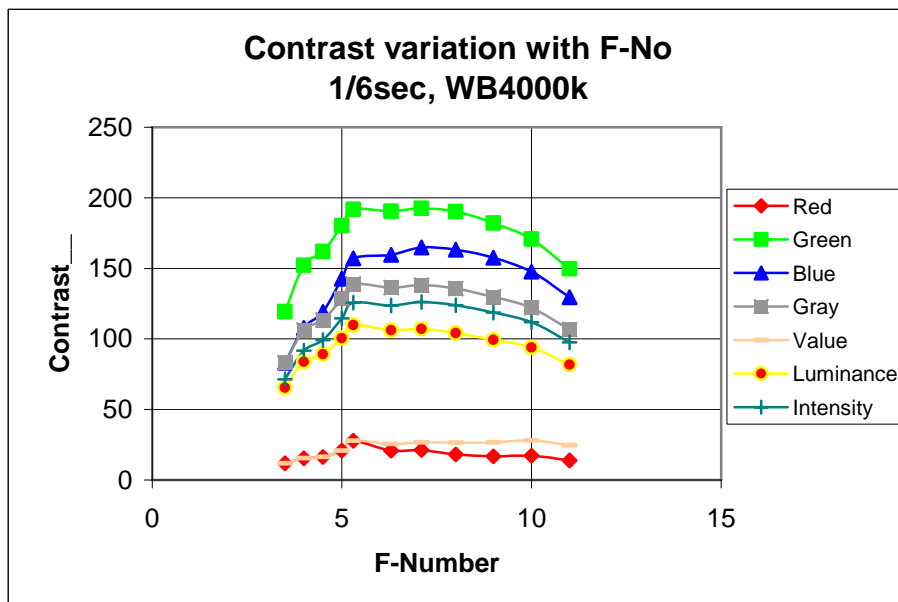


Figure 47: Variation of contrast with F-numbers for given exposure time 1/6 seconds and white balance 4000k

The color contrast is decreasing with the increase in the exposure time. (Figure 48)

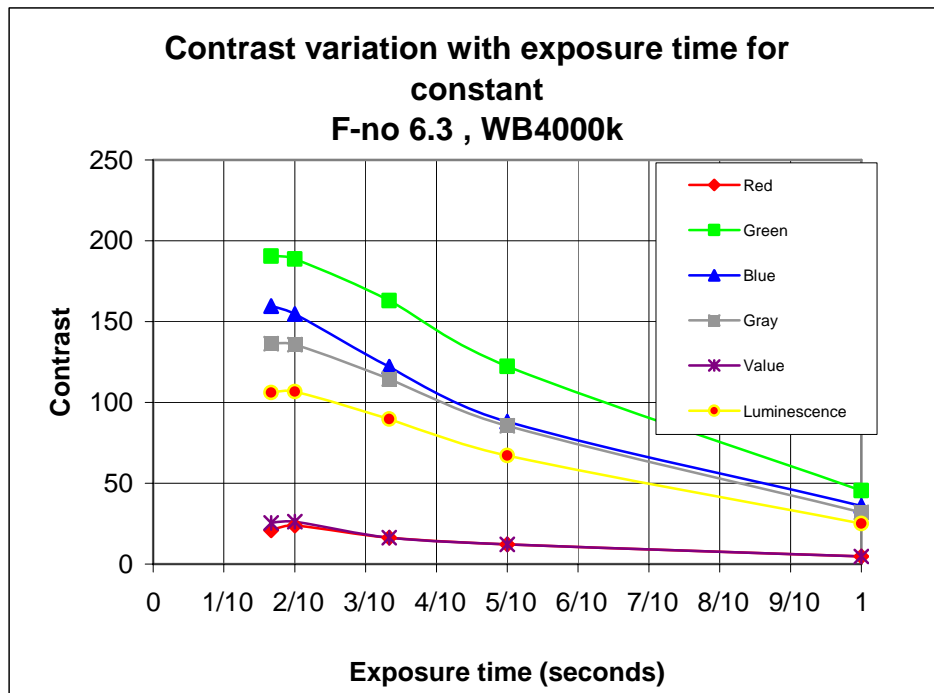


Figure 48 Variation of contrast with exposure time for given F-number 6.3 and white balance WB4000k

From both Figure 47 and Figure 48 results that the *green* color attribute is the best followed by *blue*, *gray*, *intensity* and *luminance*.

Important observation:

Until now, we determined that *green* and *blue* color attributes give the best image contrasts and have the **widest range of color units**.

We can say that the *green*, *blue*, *gray*, *intensity* and *luminance* are the best color attributes for developing a liquid saturation calibration curve.

Further we will discuss more in detail these color attributes.

Obs: Due to the limited space of this work the *gray*, *luminance* and *intensity* color attributes will not be discussed in detail.

5.11. Green Color Attribute

Green color attribute is one of the best color attributes to be used for building a calibration curve. What has to be determined is the best combination of F-numbers – exposure times – white balances for calibrating the light transmission method; so, to determine the camera parameters for the given color attribute.

Two analyses will be performed: the first is the variation of the *green* color attribute with regard to DNAPL saturation and the second is the variation of the *green* color attribute with regard to F-number.

5.11.1. Variation Green color attribute - DNAPL saturation curves with F-numbers and exposure times

In Figure 49 is plotted the variation of the *green* color attribute with DNAPL saturation for more combinations of F-numbers and exposure times (in this case in order not to overload the graphic the white balance is limited to WB4000k). All the curves in the figure are examples of calibration curves. We could theoretically chose any of them but then some will behave good for only a small range of DNAPL saturations and extremely bad for the whole rest.

Again, when reading the graphic it is not important to read the pointwise values but to see the succession of the curves.

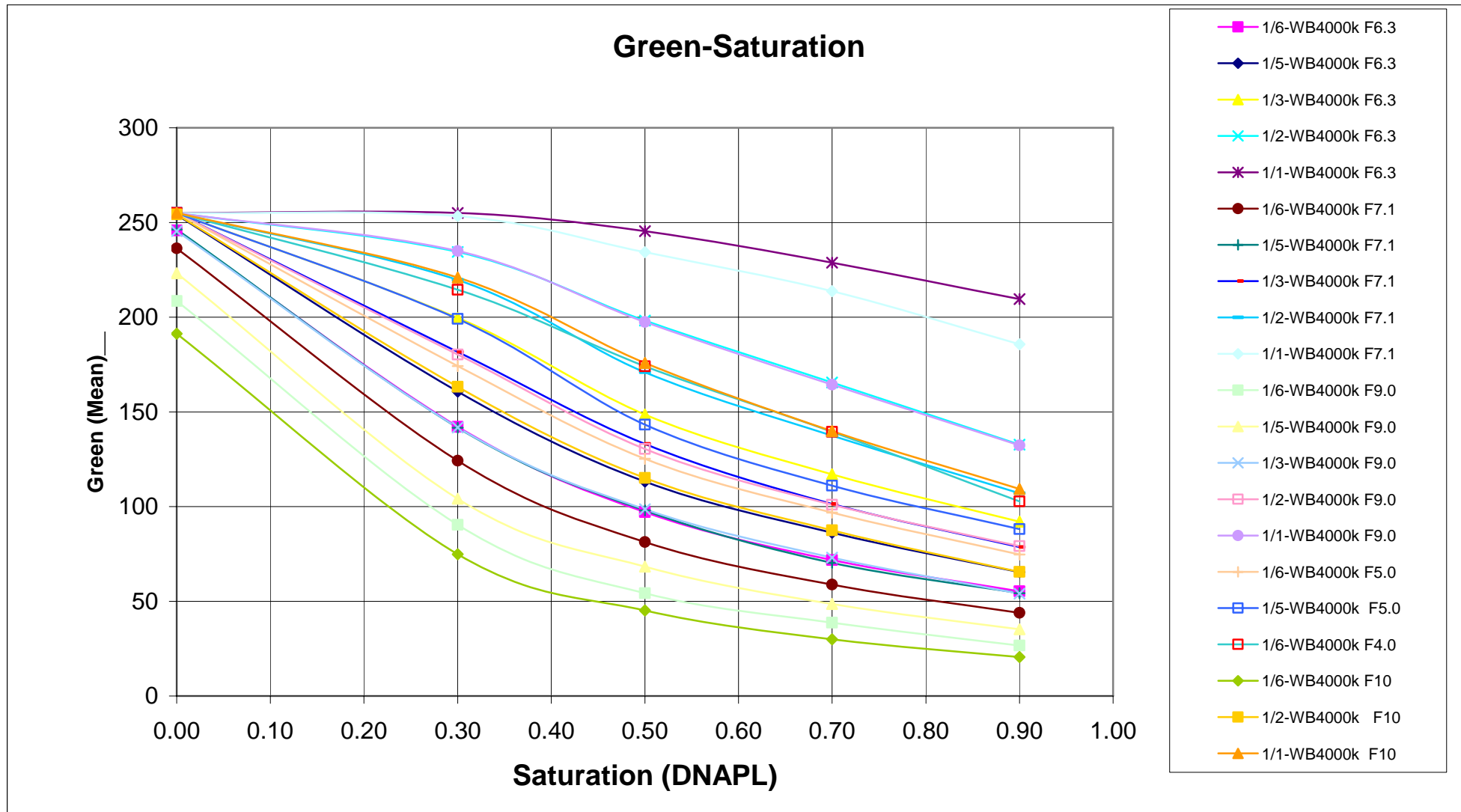


Figure 49: Variation Green (Mean) value – DNAPL saturation curves for different F-numbers and exposure times

There are two principal observations:

1. **F-Number variation:** we see that for increasing F-Numbers the curves tend to become steeper in the first part of the graphic, the one corresponding to small DNAPL saturation values, and less steep at the end, for big saturation values. (Figure 50)

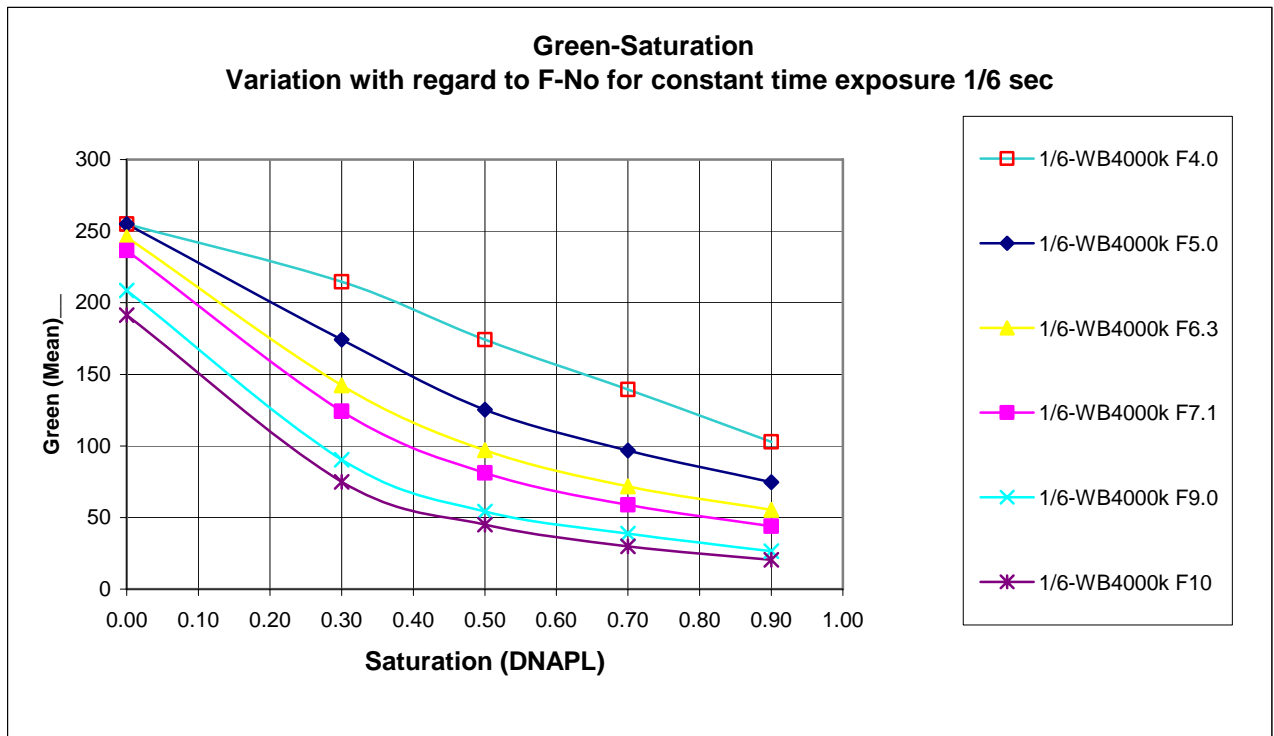


Figure 50: Variation of Green-DNAPL Saturation curves with F-numbers for 1/6 seconds exposure time

At the same time, the curves succeed one under the other with the increase of F-numbers.

2. **Exposure time variation:** When keeping the F-Number constant and for changing exposure time values we see the same behavior as when changing F-Number: for small exposure time the curves tend to have steeper slopes in the zone of small saturation and decrease by increasing the exposure time; for big exposure time values, the first part of the slope is flat and as the DNAPL saturation increases it becomes steeper. (Figure 51)

Like for the variation of the F-numbers, the curves succeed one under the other with the decrease of the exposure time.

From these two conclusions it is understandable that the best F-Number curve should be one that gives good results both for small and big saturations values. The big F-Numbers and the small exposure times give bad results for big saturations and the small F-Numbers and the big exposure times give bad results for small saturation values. The consequence is that the best curve would be the one that is the closest to a straight line. This would give good results for the whole domain.

One alternative would be to chose two curves: one for the small saturations and one for the bigger saturations. This, anyhow, requires more effort since one has to take the pictures with two camera settings.

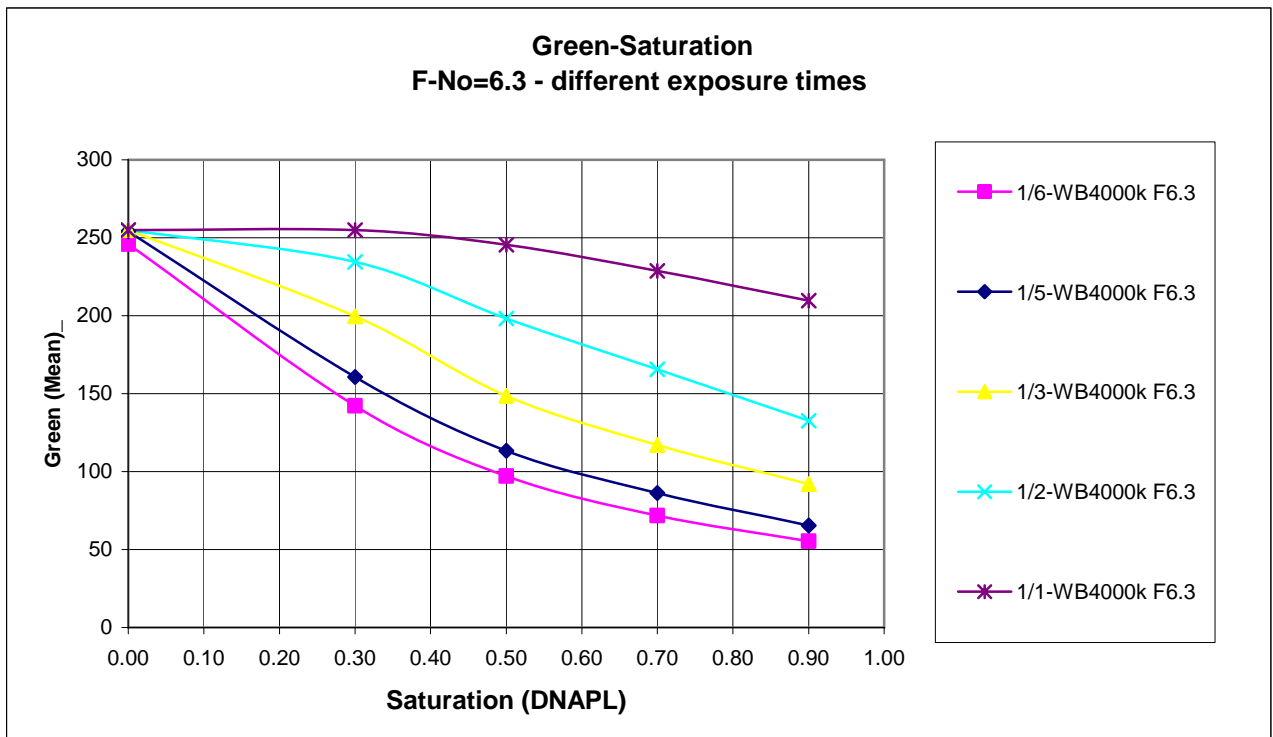


Figure 51 Variation of Green – DNAPL saturation with exposure time for F-No=6.3

From Figure 49 results that there is not only one curve that can be used but a combination of F-number and exposure time ranges.

5.11.2. Variation of Green color attribute with F-number plotted for different DNAPL saturations

The interpretation was performed for more exposure times and white balance values but here there will only be presented the results for 1/6 seconds exposure time and white balance WB4000k.

The curves decrease gradually with the increase of the F-number. The slope steepness increases with the DNAPL saturation, 90% saturation being the steepest, for F-numbers smaller than 5 (Figure 52:). The lowest curve is the 90% DNAPL saturation.

The three dimensional graphic is more suggestive in understanding the influence of the exposure time in the choice of the F-number (Figure 53). In this case the best curves for calibration would be the one corresponding to exposure times of 1/5 or 1/6 seconds because they give the widest range of values and they are close to a straight line.

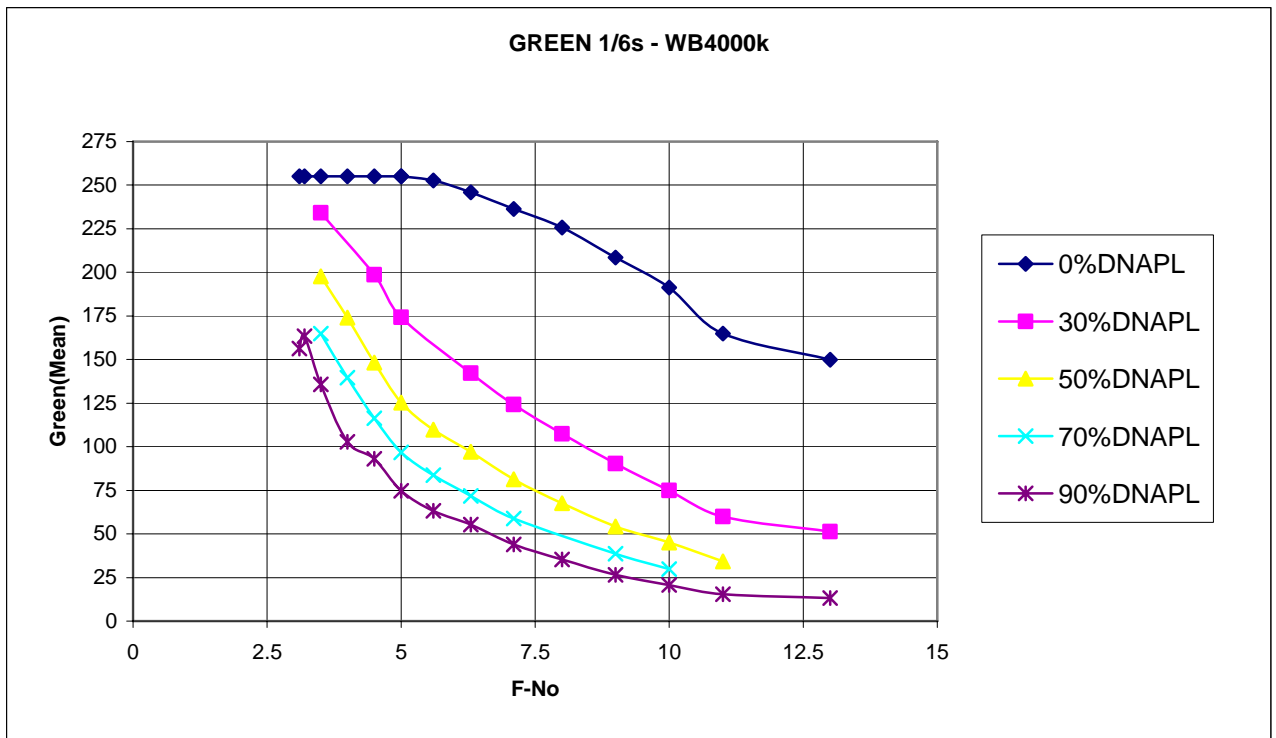


Figure 52: DNAPL Saturation curves in Green-F-No representation for 1/6 s exposure time and WB=4000k

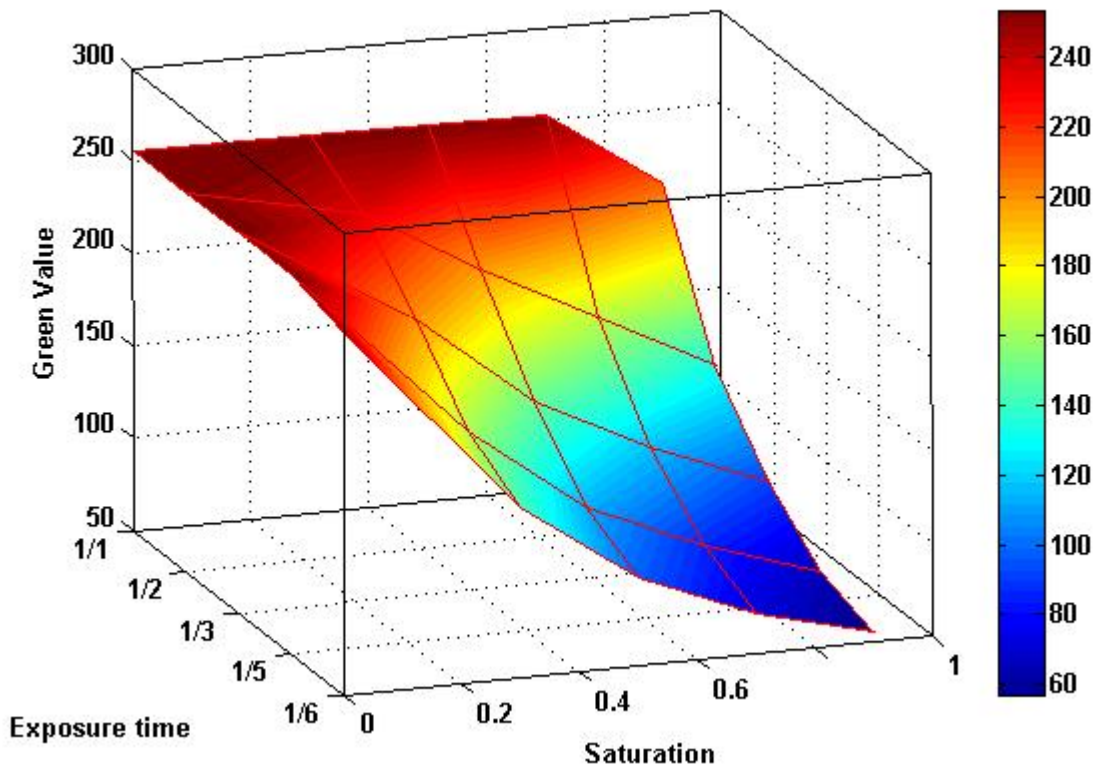


Figure 53 3D Plot of Green color attribute, Saturation and Exposure time for the same F-number 6.3 and WB=4000k

5.12. Blue Color Attribute

Blue is the color attribute with the widest color range (see section 5.9) and has the second color contrast value. For this reason in the following a similar analysis as in the case of *green* will be made.

5.12.1. Variation of BLUE color attribute with F-number plotted for different DNAPL saturation

As it has been discussed in the case of *green* color attribute the curves decrease gradually with the increase of the F-number and the slope steepness increase with the DNAPL saturation, 90% saturation being the steepest. (Figure 54)

We performed the interpretation for more exposure times and white balance values but here we will only present the results for exposure time 1/6 seconds and WB = 4000k also to see the differences and compare it with *green* in Figure 52 .

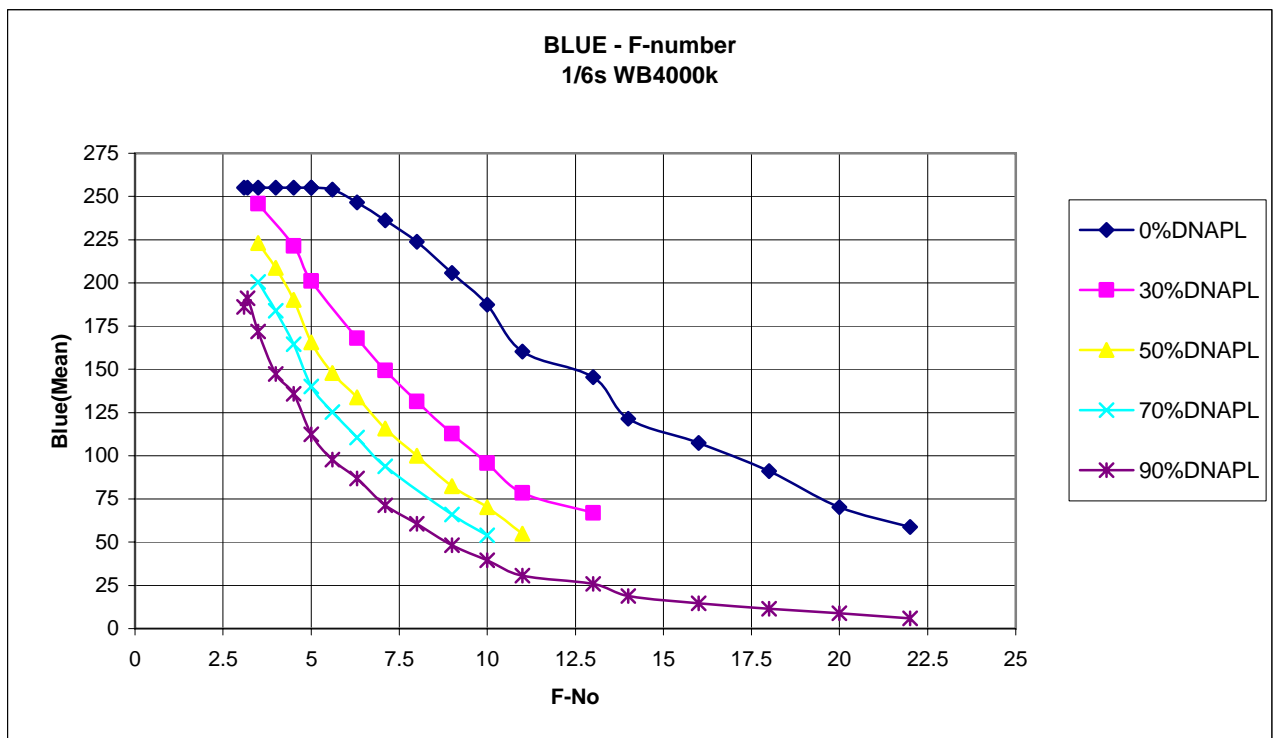


Figure 54: Blue color attribute – F-number curves for 1/6 seconds exposure time, WB4000k plotted for different DNAPL saturations

5.12.2. Variation of “Blue color attribute - DNAPL saturation” curves with F-numbers and exposure times

In Figure 55 it is plotted the variation of the *blue* color attribute with DNAPL saturation for more combinations of F-numbers and exposure times for white balance WB4000k.

Compared with Figure 49 we get curves with the same profile as the *green* color attribute. From the two graphics five calibration curves have been extracted that have the widest color range and are a very linear behavior. (See Figure 56 and Figure 57).

For the rest of the color attributes: *Gray, Luminance, Intensity* we have applied the same interpretations as for the first two previously discussed (*Green* and *Blue*) and won't be shown in this study since they produce similar results. The widest range of values belongs to *Green* and *Blue* and this two color attributes should be used for further interpretations.

Nevertheless, it should be mentioned that the advantage of *Gray* color attribute is that it is the least white balance dependent.

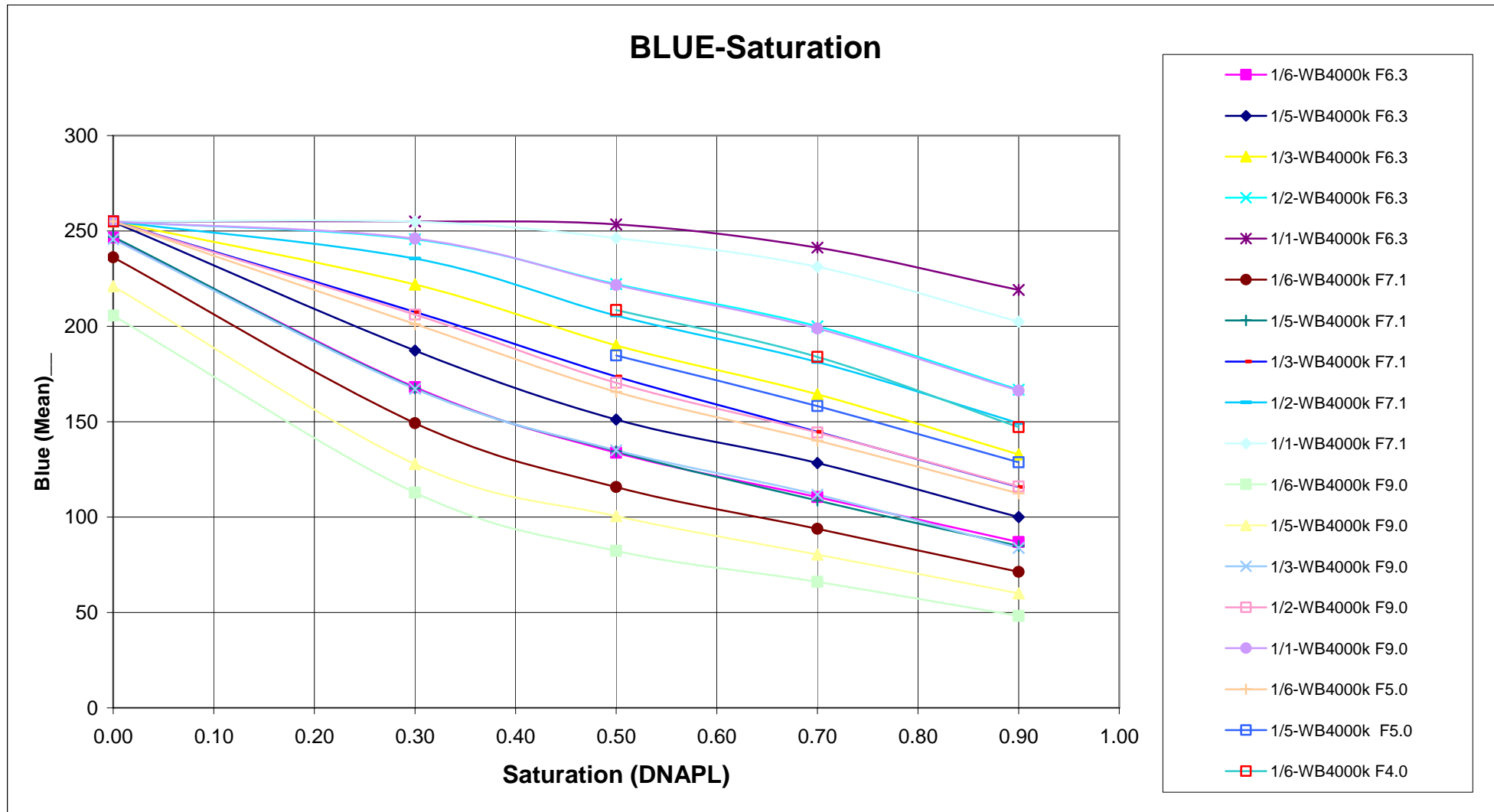


Figure 55: Variation Blue (Mean) value – DNAPL saturation curves for different F-numbers and exposure times

5.13. The Best Camera Settings (Ranges for F-number and Exposure times)

After plotting the “Color attribute – DNAPL Saturation” curves for all the color attributes (*Red, Green, Blue, Gray, Value, Luminance, Intensity*) we narrowed the range of useful values of F-numbers and exposure times determined initially in Table 7.

Very good values to be used in picture interpretation are presented below (the curves are almost linear):

Table 9: The best values of F-number and Exposure time

Exposure time	Green		Blue		Gray		Luminance		Intensity	
	F-No Min	F-No Max	F-No Min	F-No Max	F-No Min	F-No Max	F-No Min	F-No Max	F-No Min	F-No Max
1/6	4.5	6.3	5	6.3	4.5	6.3	4.5	6.3	4.5	6.3
1/5	5	6.3	5	6.3	5	7.1	5	7.1	5	7.1
1/4	5.6	7.1	5.6	7.1	5.6	7.1	5.6	7.1	5.6	7.1
1/3	6.3	7.1	7.1	9	6.3	9	6.3	9	6.3	9
1/2	8	10	9	10	8	11	8	11	8	11
1,0	11	13	11	13	11	13	11	13	11	13

5.14. Example of Calibration Curves

To clearly understand that for different camera settings the same behavior can be obtained, two curves with almost identical match are plotted in Figure 56 **Error! Reference source not found.** for *green* color attribute

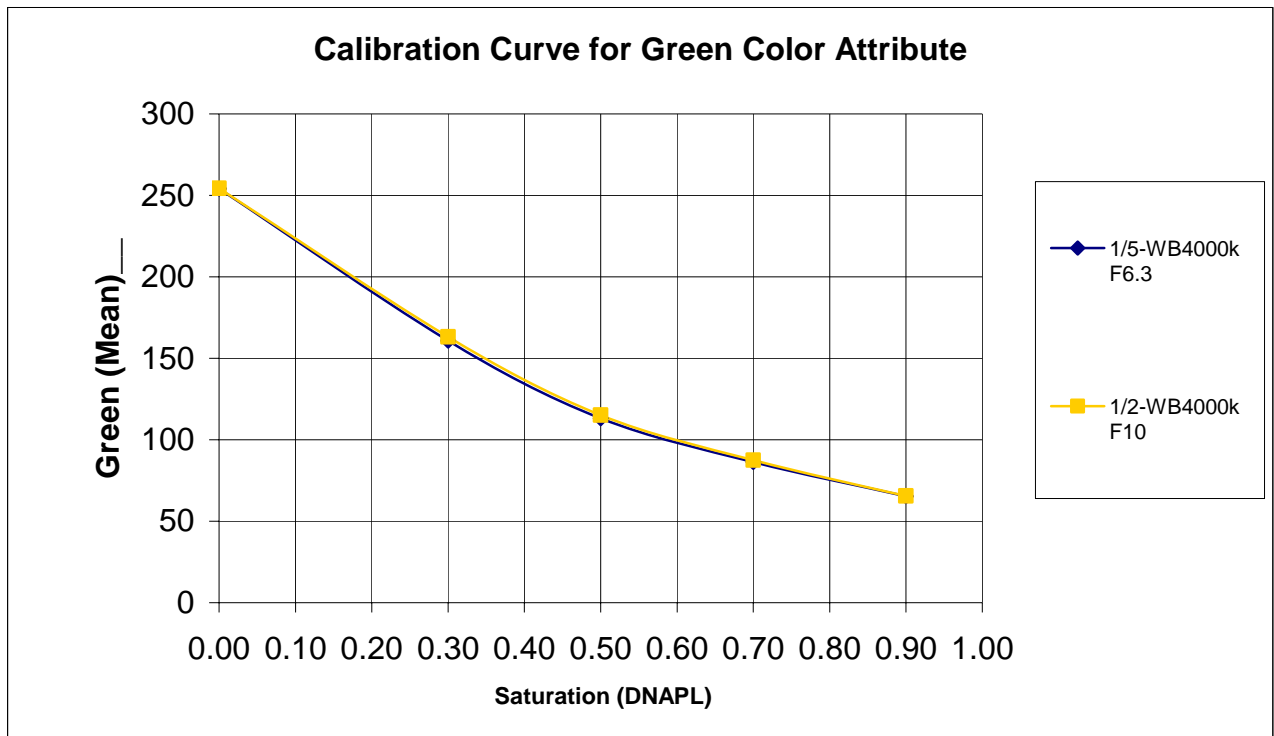


Figure 56: Green Color Calibration Curve; F-No6.3, 1/5 seconds exposure time, WB4000k

The best polygonal fit of the two *green* color attribute calibration curves is:

$$y = 162.45x^2 - 355.18x \quad (5.5)$$

For blue color attribute three distinct curves corresponding to the following different camera settings: 1/6 seconds exposure time, F6,3; 1/5 seconds exposure time, F7.1; 1/3 seconds exposure time, F9.0 have the same profile.

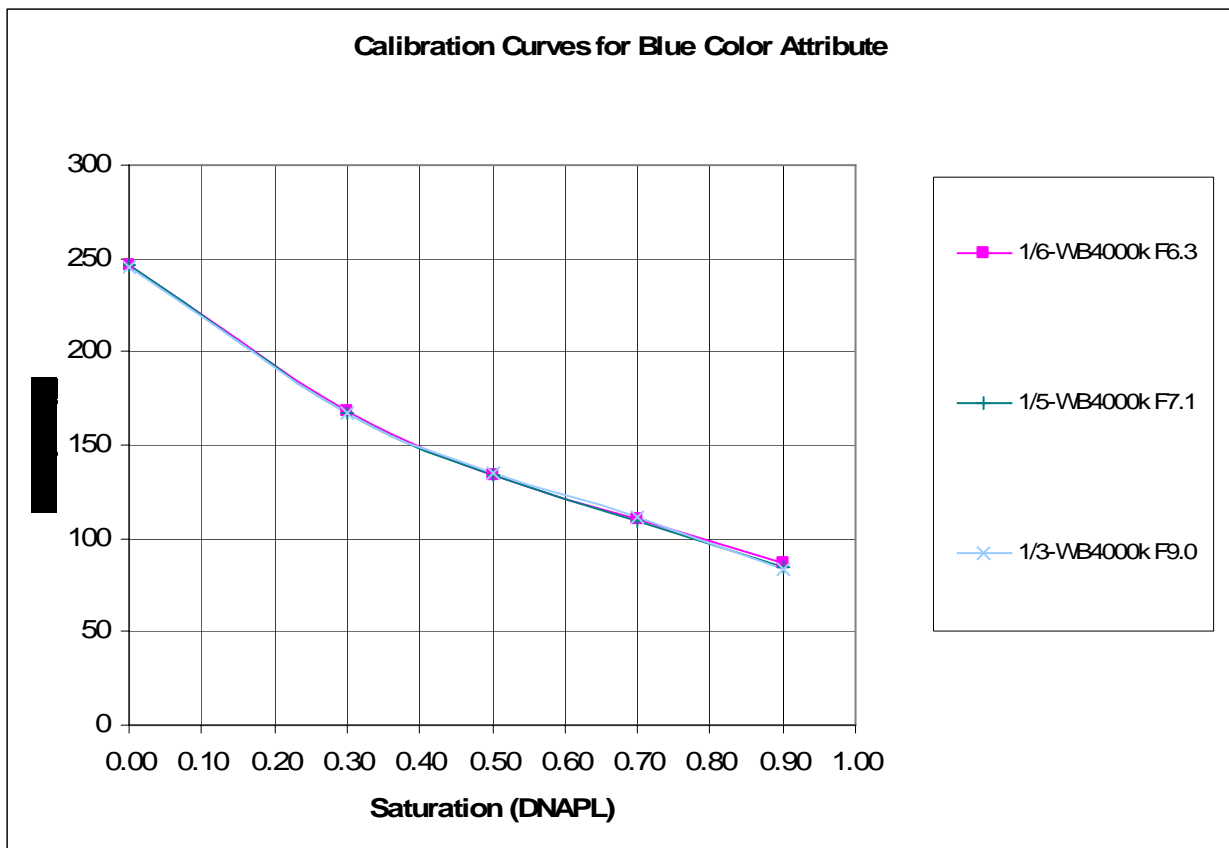


Figure 57: Blue Color Calibration Curves

The best polygonal fit for the *blue* color attribute calibration curves:

$$y = 123.31x^2 - 284.81x + 245.4 \quad (5.6)$$

These curves are the ones that are closest to a straight line and have the widest range of color value, so they are very good calibration curves to be used for a similar setup.

In other words, if we fix the camera parameters to F-No = 6.3, Exposure time = 1/6 and a WB4000k we get very good results for the whole spectrum of DNAPL saturations and we will have very similar results as when we would use F-No=7.1, Exposure time = 1/5 and WB4000k.

6. Discussion of Error

6.1. Experimental error

- **Air entrapment**

The main cause for error is due to entrapment of air. Entrapping of air cannot be avoided during the filling of the flume. It is therefore crucial to choose the most representative and most homogeneous area before making the image interpretation.

When mixing the DNAPL with water and sand a certain amount still remains at the surface forming small bubbles.

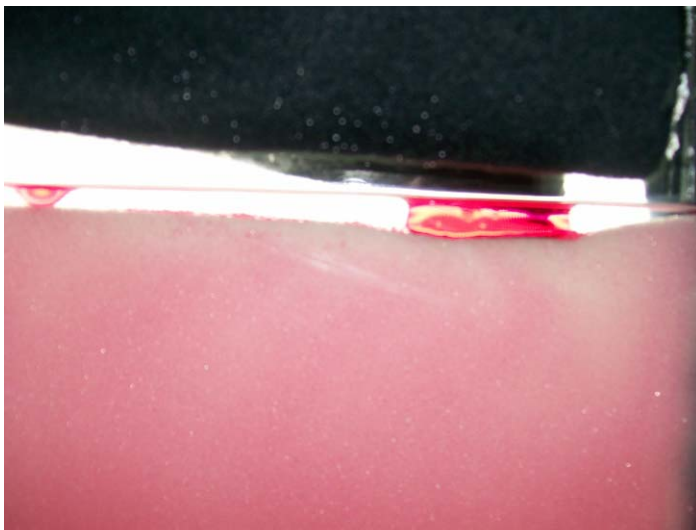


Figure 58 DNAPL bubble forming at the upper part of the sand media

The unknown amount of air leads to an uncertainty of the saturation in the system.

A syringe could be used to remove the bubbles. Anyhow, the operation is time consuming and not very helpful since it is almost impossible to quantify exactly how much DNAPL has been extracted and in the regions near the extraction will result in a saturation decreasing.

- **Video signal noise**

The noise from the video signal leads to an error of the interpretation

- **Slight variations in the source field:**

The light source is not uniformly distributed across the full imaging plane.

Variations in the light source occur each time the system is turned on and off. Also, the output of the bulbs is a function of temperature. For this reason the images were taken only after a stabilization period of 30 minutes when we assume the source has reached a constant temperature and the fluctuations are consequently very small.

- **Perfect alignment of the setup**

A perfect alignment of the flume perpendicular to the light source was impossible resulting in a small misalignment for each experiment. The misalignment can result in different distances between the camera and the slab chamber and result in different focal lengths.

The errors mentioned on the second, third and fourth point are relatively minor.

- **Dye absorbance error**

The refractive indices of the fluids are changed for different dye concentrations.

Increasing dye concentration causes accuracy error increase while precision error decreases.

Precision (or random) errors are due to the random variability of intensity measurements caused by random temporal and spatial variability in the CCD response.

Accuracy (or bias) errors are due to the absorbance and refractive characteristics of the fluid [Detwiller, 1999]

6.2. Errors Related to Assumptions in the Conceptual Model

In the case we would use an interpretation similar to the one used by Glass and Tidwell [1994] there are some other issues to be considered. However, this type of error does not apply for our experiments in this study.

- **Monochromatic light assumption**

In light transmission method in all the cases it is been neglected the polychromatic nature of the light source. The Beer Lambert law is assuming a monochromatic light.

- **Pore size distribution assumptions**

Niemet and Selker, 2001, discussed thoroughly five physically based models for predicting liquid saturation from light transmission in 2D laboratory systems containing translucent porous media. The basic assumptions concerning pore geometry, wettability and drainage were compared to each other. Their model considered a pore size distribution derived from Laplace equation and gave the smallest error.

In Glass 1994, the influence of the pore size distribution on saturation calculation in the light transmission technique (only for air-water system) has been studied.

6.3. Standard deviation

A good parameter for the quantification of the homogeneity of a domain and the averaging errors is the standard deviation the color attribute.

To exemplify we take a picture from the set of 90% DNAPL saturation with an exposure time of 1/6 seconds WB=4000k and F-number 4.5. After making the cut at the representative

homogenous area we obtain the image in Figure 59. The image has a rather homogeneous look for the naked eye.

Even after we plot the image with the color-bar showing the color value for each pixel the aspect is still homogeneous (Figure 60).

Further, we plotted the green color attribute of the same picture. The difference between maximum (121) and minimum (67) color values is 57 color units. The standard deviation calculated for all 300x1250 values is 5.433 which represents 5% of the mean .

$$STDEV = \sqrt{\frac{\sum (x - \bar{x})^2}{(n - 1)}}, \bar{x} - \text{the sample average, } n - \text{sample size} \quad (6.1)$$

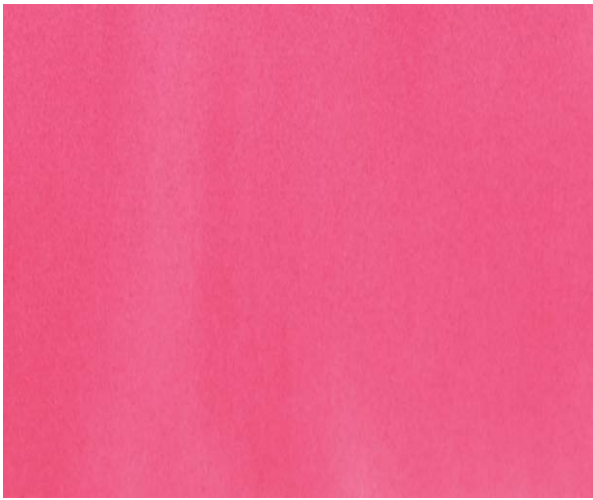


Figure 59 90% DNAPL saturation, exposure time 1/6 s, WB=4000k, F-No=4.5

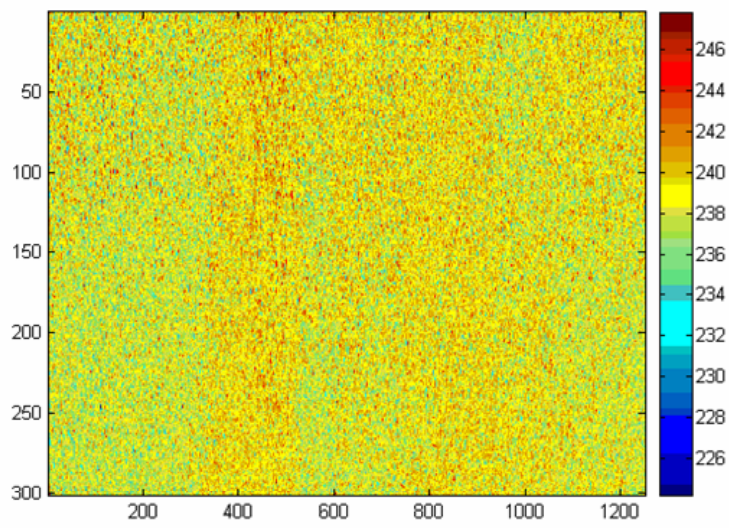


Figure 60 90% DNAPL saturation, exposure time 1/6 s, WB=4000k, F-No=4.5 plotted with RGB colorbar

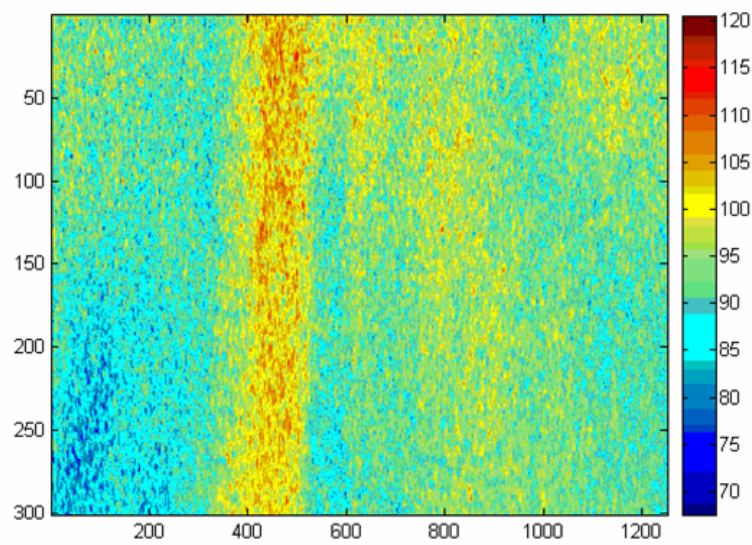


Figure 61: Green color attribute (90% DNAPL saturation, exposure time 1/6 s, WB=4000k, F-No=4.5) , visible heterogeneities

7. Summary of Conclusions

The main conclusions of this study could be summarized as follows:

1. The advantage of light transmission method (LTM) is that it records the fluid contents of the entire flow almost instantaneously (or the exposure time that it takes for a video camera to take an image)
2. LTM is a cheap, simple, efficient method to use for determining the liquid saturation in single and multiphase porous systems in laboratory; also it is able to provide data to validate one-dimensional and two-dimensional computer codes for transient multiphase flow
3. *F-number* and *exposure time* are important camera parameters for LTM
4. *Hue* color attribute cannot be used for building a calibration curve. (see chapter 5.4)
5. *Red* and *Value* color attributes have a small spectrum of color units (aprox. 50) which is more susceptible to error influence. (see chapter 5.6)
6. The best color attributes are: *Green, Blue, Gray, Luminance and Intensity*
7. *Green* is the color attribute that has the biggest contrast for all combinations of camera settings (see section 5.11)
8. *Blue* is the color attribute that have the biggest color range so it is less susceptible to errors. (see section 5.12)
9. *Gray* has the advantage that is less dependent on the white balance mode.
10. Still *Luminance* and *Intensity* are very good to use.
11. Similar results are obtained for different combinations of camera parameters (*Exposure Time, F-Number* and *White balance*).
12. The relation between the variables is non-linear and to derive general equation that could lead to a best solution is less probable, therefore for each experiment a calibration should be made.
13. There is no unique “BEST SOLUTION” for the camera settings. There are more possible combinations that give very good calibration curves. (See section 5.13)
14. The calibration curves exemplified in section 5.13 are the best that were obtained and can be used for transient flow experiments with similar features.
15. For dyestuff colors, tracer types, sand grain sizes and widths of the flume different than the ones mentioned in this study there have to be derived other calibration curves.

8. REFERENCES

1. James D. Foley, Andries Van Dam “Fundamentals of Interactive Computer Graphics”
2. Glass R., Steenhuis Tammo S., Parlange J.-Yves, “Mechanism for finger persistence in homogeneous unsaturated, porous media: theory and verification” *Soil Sci.* 148(1), 60-70
3. Glass R., Tidwell Vincent C., “X ray and visible light transmission for laboratory measurement of two-dimensional saturation fields in thin-slab systems” . *Water Resources Research*, Vol. 30, No.11, 2873-2882, Nov 1994
4. Darnault Christophe J.G, Throop James A., DiCarlo David A., Rimmer Alon, Steenhuis Tammo S., Parlange J.-Yves, “Visualization by light transmission of oil and water contents in transient two-phase flow fields”. *Journal of Contaminant Hydrology* 31 (1998), 337-348
5. Detwiler Russell L., Pringle Scott E., Glass Robert J. .“Measurement of fracture aperture fields using transmitted light: An evaluation of measurement errors and their influence on simulations of flow and transport through a single fracture”. *Water Resources Research*, Vol.35, No.9, 2605-2617, 1999
6. Darnault C.J.G, DiCarlo D.A., Buters T.W.J., Jacobson A.R., Throop J.A., Montemagno C.D., Parlange J.-Y., Steenhuis T.S. . “Measurement of fluid contents by light transmission in transient three-phase oil-water-air systems in sand”. *Water Resources Research*, Vol.37, No.7, 1859-1868, July 2001
7. Niemet R. Michael, Selker John. S . “A new method for quantification of liquid saturation in 2D translucent porous media systems using light transmission”, *Advances in Water Resources* 24 (2001), 651-666
8. Conrad H. Stephen, Glass J. Robert, Peplinski J. William . “Bench-scale visualization of DNAPL remediation processes in analog heterogeneous aquifers: surfactant floods and in situ oxidation using permanganate”. *Journal of Contaminant Hydrology* 58 (2002) 13-49
9. Schroth MH, Ahearn SJ, Selker JS, Istok JD. Characterization of miller-similar silica sands for laboratory hydrologic studies. *Soil Sci Soc Am J* 1996;60:1331-9